Exploring the innovation potential of single photon lidar for Ontario's eFRI

KTTD 5B-2018

Final Report to the Ontario Forestry Futures Trust

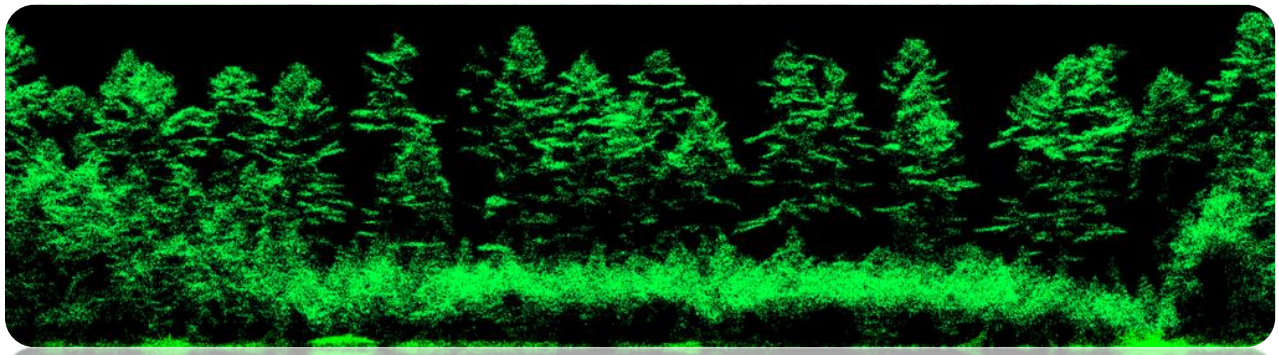

Joanne White[1], Murray Woods[2]

With contributions from:

Margaret Penner[3], Thomas Krahn[4], Craig Onafrychuk[4], Jean-François Prieur[5], Jili Li[6], David Bélanger[7], Charles Papasodoro[7]

[1]Canadian Forest Service, Natural Resources Canada
[2]Ontario Ministry of Natural Resources and Forestry (retired)
[3]Forest Analysis Ltd.
[4]Provincial Mapping Unit, Ontario Ministry of Natural Resources and Forestry
[5]Université de Sherbrooke
[6]FPInnovations
[7]Canada Centre for Mapping and Earth Observation, Natural Resources Canada

April 28, 2020

Executive Summary

Airborne Light Detection and Ranging (lidar) has been a transformative technology in forest inventory and terrain mapping. Lidar enables detailed characterization of trees and vegetation, as well as the terrain surface underneath vegetation. When combined with ground plot data, lidar can be used to build models to accurately estimate forest inventory attributes of interest, such as basal area and volume. Single Photon Lidar (SPL) is a form of lidar technology that enables large area data collection at a reduced cost. SPL data is however markedly different from that of the discrete return, small footprint lidar that is commonly used for enhanced forest inventory (EFI) projects in Canada (hereafter, linear mode lidar or LML). The objectives of this project were to investigate and quantify the capacity of SPL data for estimating forest attributes and characterizing the terrain surface, as well as identifying any incremental advantages of SPL data for Ontario's eFRI program. This study was conducted at the 10,000 ha Petawawa Research Forest (PRF) and adjacent 5,000 ha of lands of the Canadian Nuclear Laboratories (CNL) in southern Ontario, Canada. The PRF is the oldest research forest in Canada and combined with the CNL lands, represents a broad range of forest types and management histories.

To assess the performance of the SPL data in area-based models of forest inventory attributes, we used co-located ground plots and SPL data to develop models for a suite of forest inventory attributes. We then applied those models wall-to-wall and quantified the accuracy and precision of the modeled estimates using independent, stand-level validation data from 27 stands. In addition, we compared the performance of the SPL-derived EFI against that of a 2012 EFI for PRF that was derived using LML. Overall, we found that area-based models generated using the 2018 SPL data had small relative bias ($\leq$ 2%) and reasonable levels of error (RMSE ranging from 12–16%). Gross total volume for merchantable stems had an overall bias of 1 m^3/ha ± 7 m^3/ha (standard error), with a relative bias of 0% and a relative RMSE of 15%. Estimates of merchantable stem volume had similar levels of bias (2 m^3/ha ± 7 m^3/ha), and a similar relative bias (1%) and RMSE (16%). Basal area of merchantable stems was underestimated by 2% (0.5 m^2/ha ± 0.7 m^2/ha), with a relative RMSE of 14%. Estimates of quadratic mean diameter at breast height (DBH) had a relative bias of 1% (0.2 cm ± 0.6 cm) and a relative RMSE of 12%. As noted above, the study area represents a complex assemblage of forest types, silvicultural systems, and management histories, and this presents challenges for area-based models. We found that relative bias and RMSE varied markedly by forest type, with some forest types consistently overestimated (e.g. managed white pine), whereas other forest types were consistently underestimated (e.g. red pine plantations). The bias and error associated with the 2018 SPL area-based models were comparable to those generated using the 2012 LML. On average, the relative RMSE was 5% larger for the estimates generated using the 2018 SPL data, whereas the relative bias was typically larger for the estimates generated using the 2012 LML data, but on average, differed by less than 1% overall. Based on these results, we consider the quality of the SPL area-based estimates to be similar to those generated using the 2012 LML data.

To assess the accuracy of the SPL data for terrain characterization, we partnered with the Provincial Mapping Unit of the Ontario Ministry of Natural Resources and Forestry and the Canada Centre for Mapping and Earth Observation to design and conduct a Real Time Kinematic (RTK) GPS survey of a sample of checkpoints in different forest types within the PRF. RTK surveys accurately measure the elevation at a given location, and are used as reference data to assess the accuracy of elevations derived from other data sources, such as lidar. Following the Ontario Elevation Accuracy Guidelines, and targeting a 10 cm Vertical Accuracy Class, the checkpoint data acquired at PRF were used to assess the elevation accuracy of the 2018 SPL data, as well as the 2012 LML, and two additional leaf-off SPL acquisitions from 2019. Based on the results of the assessment, it was concluded that the four lidar datasets tested met the accuracy standards for Ontario Digital Geospatial Data for a 10 cm Vertical

Accuracy Class. Actual Non-vegetated Vertical Accuracy (NVA) was found to be +/- 19.6 cm at the 95th percentile. Actual Vegetated Vertical Accuracy (VVA) was found to be +/- 29.4 cm at the 95th percentile. For the majority of cover types, the leaf-on SPL data acquired in 2018 had slightly greater accuracies than the 2012 LML data, with the exception of the black spruce, mixedwood, and low vegetation categories. Although the 2018 SPL data had an aggregate nominal pulse density that was five times that of the 2012 LML data (32.4 points/m^2 for the 2018 SPL compared to 5.8 points/m^2 for the 2012 LML), the average ground point density of the 2018 SPL was only twice that of the 2012 LML. In other words, the 2018 SPL data is much denser than the 2012 LML, but that density is disproportionately concentrated in the overlying vegetation and does not result in an analogous increase in ground point density. This is further demonstrated in the higher ground point densities associated with the 2019 leaf-off SPL acquisitions. The low density of ground returns associated with the 2018 SPL data also influenced the derived digital terrain model, resulting in artifacts in areas with dense vegetation cover and complex terrain. Not surprisingly, the leaf-off SPL acquisitions resulted in digital terrain models that were superior to those of both the 2012 LML and 2018 SPL data.

For the final objective of this project, we explored the use of SPL data for tree species classification and the identification of small trees below the main canopy. In examining the utility of the 2018 SPL for species classification at the individual tree level, we found that the SPL data provided results that were inferior to those generated with the 2012 LML data. Specific characteristics of the SPL data, namely the dominance of first returns, the lack of returns distributed through the full vertical profile of the canopy, and unknown qualities of the intensity data, resulted in lower species classification accuracies when compared to the 2012 LML data. Similarly, the lack of returns distributed through the full vertical profile of the canopy precluded the detection of small trees below the main canopy. In some cases, the presence of a secondary layer under the main canopy could be readily identified, but the capacity to identify a second layer depended on the density and configuration of the overstorey canopy, which varied by forest type.

Overall, we conclude that the SPL data acquired to the specifications for the 2018 data used herein was suitable for both the area-based approach to estimating forest inventory attributes, and for characterizing terrain under a range of cover conditions, with acceptable levels of accuracy and overall quality for the derived digital terrain model. While leaf-off SPL acquisitions may be preferable for terrain characterization, the utility of these leaf-off acquisitions for area-based modelling was not investigated in this project. Lastly, the lack of returns in the 2018 SPL data through the full vertical profile of the canopy may limit these data for species identification at the individual tree level, and for the detection of secondary, small trees that exist below the main canopy, particularly if the main canopy is dense and/or has a uniform configuration

LIST OF FIGURES

LIST OF TABLES

1. Project scope and objectives

Airborne lidar (Light Detection and Ranging) has been a transformative technology, providing detailed characterizations of the earth's surface and three-dimensional measures of forest structure. The increase in spatial detail and precision afforded by lidar is critical for a broad range of natural resource management applications (Eitel et al. 2016), including forest inventory (Wulder et al. 2008, Hyyppä et al. 2012). In the last decade, the use of lidar for forest inventory has moved from the realm of research to operational implementation (Næsset et al. 2015), particularly for the area-based approach (White et al. 2013, 2016), with comprehensive demonstration of the efficacy of the technology in an Ontario context (Thomas et al. 2006, Woods et al. 2011, Treitz et al. 2012, Penner et al. 2013, 2015). These lidar data were derived from discrete return or full waveform sensors, which are referred to collectively as "linear-mode lidar" (hereafter LML; Stoker et al. 2016). Single photon lidar (SPL) represents a potential significant technological advance towards the rapid and cost-effective characterization of forest structure and terrain underneath canopy over large areas. At the time this project was proposed, the only large-area application of SPL (1700 km^2) reported in the literature compared metrics of forest structure and terrain, but did not apply an area-based approach or model any forest inventory attributes (Swatantran et al. 2016).

The objectives of this project were to address several gaps in current scientific and operational knowledge regarding the application of SPL for forest inventory. Specifically, the objectives of this project were as follows:

1. To quantify the comparative performance of SPL in an area-based approach to forest inventory attributes;
2. To quantify the comparative performance of SPL in characterizing terrain under varying forest types and canopy densities;
3. To identify and explore any incremental advantages or innovations for the eFRI program resulting from unique SPL data characteristics, particularly data density (e.g. to support individual tree approaches and the improved characterization of canopy vertical structure for applications such as habitat modelling).

The primary target audience for this work is the forest inventory community in Ontario and Canada. Forest practitioners want robust and transparent benchmarking of new technologies to be demonstrated and documented in an accessible manner. Ontario's Sustainable Forest Licence (SFL) managers in the Great Lakes and Boreal Forest regions require higher resolution inventory information with known accuracies to inform both their strategic and operational planning needs. A secondary target audience is the scientific community. Given the relatively recent commercial release of SPL technology, the performance of this technology for forest inventory and terrain characterization needs to quantified and documented and that was the ultimate goal of this project.

2. Deliverables

In addition to this report documenting the various investigations and analyses supporting the objectives of this project, technology transfer was an important project deliverable and included online lectures and in-person workshop presentations. All technology transfer activities associated with this project are summarized in Appendix A, including links to recorded online lectures and presentation materials that are available for download. Several supplementary reports were generated to address the specific information needs and objective of this project. Details on those reports, including means to access them, are provided in Appendices to this report.

3. Study Area

The Petawawa Research Forest (PRF) was established in 1918 and is the oldest, continuously operated research forest in Canada (Place 2002). Located approximately 200 km northwest of Ottawa, the PRF extends over 10,000 ha of forested land. An additional 5000 ha of adjacent land managed by the Canadian Nuclear Laboratory (CNL) was also included in this study (Figure 1). The forests of both the PRF and CNL sites are dominated by mature Great Lakes–St. Lawrence mixedwood stands (70% by area) with remaining stands being primarily hardwood (22%) and conifer (8%) dominated. Approximately 85% of the forest land within the PRF is considered productive and includes several long-term conifer plantation studies that are unique to Canadian forestry. With its combination of experimental plots, plantations, and non-research areas, the PRF represents a heterogeneous mixture of forest conditions.

The PRF and CNL forests are located on the southern edge of the Precambrian Shield with bedrock of granites and gneisses. The topography has been impacted by glaciation and post-glacial outwashing. The area contains extensive sand plains, imposing hills with shallow sandy soils, bedrock outcrops, and areas of gently rolling hills with moderately deep loamy sand containing numerous boulders. Elevation across the study area ranges from approximately 100 m to more than 310 m above sea level. Mean annual precipitation is approximately 800 mm with 230 mm in the form of snow. The mean annual temperature is 4.4°C. The minimum frost-free period is about 100 days and the average growing season is 136 days.

The PRF is also a designated remote sensing supersite (White et al. 2019)[1] and has been the focus of numerous data acquisition missions over the years, including airborne Light Detection and Ranging (lidar), as well as other airborne and satellite optical and radar data acquisitions. Likewise the PRF also has numerous ground plot data holdings, including permanent sample plots. The availability of reference data and the broad range of forest types and management regimes within the PRF make it an ideal location to benchmark new technologies such as SPL.

4. Objective 1: Quantify the performance of SPL in an area-based approach to generating an eFRI

4.1 Ground plot calibration data

Accurately measured ground plot data that is representative of the forest area of interest is critical for the implementation of the area-based approach (White et al. 2013). A total of 269 circular fixed-area plots of a nested (i.e. large and small tree plots; Figure 2) design were used for this project. A total of 249 plots were remeasured/established within the PRF in the summer of 2018, and an additional 20 plots were established within the CNL property in the summer of 2019. Ground plots within PRF were located to cover the full range of species and stand development. The 20 additional plots at CNL were acquired to capture the unique forest conditions found therein. The majority of plots measured within the PRF were initially established between 2012 and 2014 in support of a 2012 LML acquisition and subsequent development of an EFI. Locations for these plots were established following a structurally guided sampling approach, as detailed in White et al. (2013). As a result, an unbalanced sampling frame resulted when comparing plots by forest type. Additional plots were added to the 2013/2014 plot network to increase the number of observations and ensure representation of the main forest types within the PRF (Table 1; Appendix B).

[1] https://opendata.nfis.org/mapserver/PRF.html

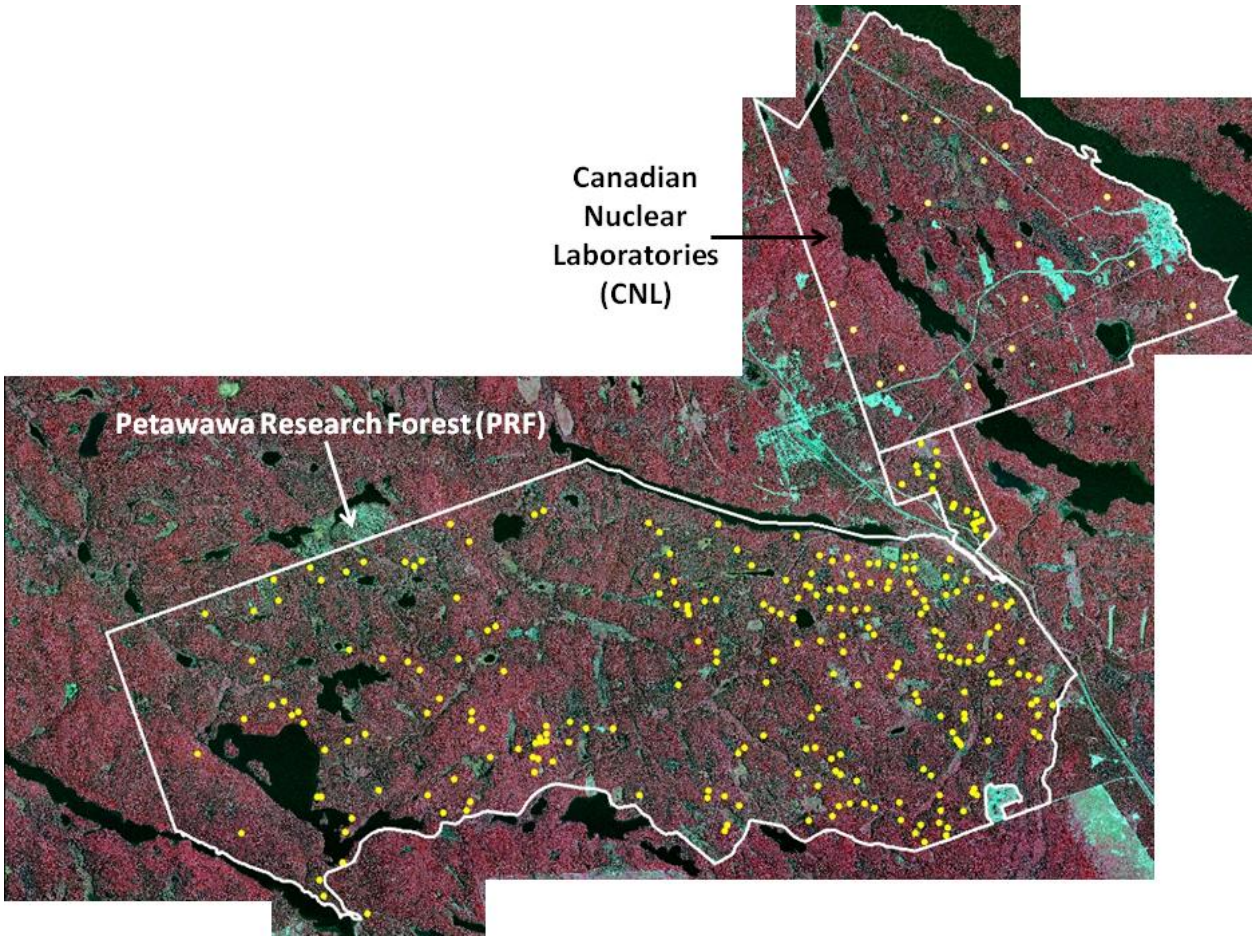

Figure 1. Map of established calibration plots (n = 269) within the Petawawa Research Forest (PRF) and Canadian Nuclear Laboratories (CNL) lands.

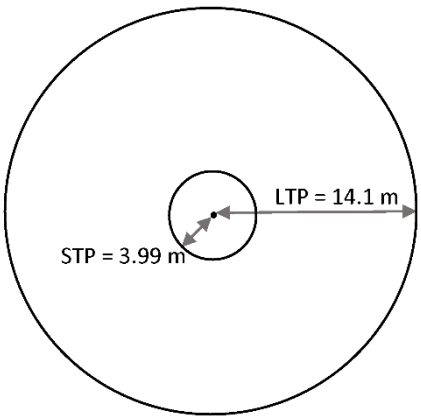

Figure 2. Configuration of small tree plot (STP) nested within large tree plot (LTP)

Live and dead trees with a diameter at breast height (DBH) ≥ 9.1 cm were measured on ground plots with an area of 625 m^2 (14.1 m radius; large tree plots). Trees with 2.5 < DBH < 9.1 cm were measured on 50 m^2 (3.99 m radius) ground plots (small tree plots), centered on the larger plot (Figure 2). DBH was measured on all trees, whereas only a subsample of trees was measured for height. The position of the plot centroid was recorded using a TopCon™ GPS unit, with a minimum 60 minute static collection for each plot centre. These positional data were later corrected using the NRCAN Precise Point Positioning tool to achieve sub-metre positioning. Ground plot photos were also acquired for each plot using the Ricoh Theta V 360 camera and following the protocol outlined in Woods et al. (2018; Appendix C). Attributes recorded within the large tree plots include tree status (live, dead, fallen down, harvested), species (using standard OMNRF numerical codes), origin (natural, planted, coppice, layering), DBH, crown class (codominant, dominant, emergent, intermediate, overtopped/suppressed, anomaly) and for dead trees, the decay class (for details refer to Woods et al. 2018; Appendix C). A height sample was measured at each plot throughout the range of diameters and species, with the six largest trees of the dominant plot species measured at each plot. Height measurements were made using a Vertex hypsometer.

Plot measurements were then compiled to provide a suite of plot-level attributes. Height-DBH curves were fit at the plot level, all species combined, and used to estimate heights of the trees without measured heights. The average dominant/codominant height was calculated as the average height of the live dominant/codominant/emergent trees with measured heights. Only the trees on the large tree plot had crown status recorded. The Sharma (2016) equation was used:

$$Ht = 1.3 + \alpha \cdot SHt^{\delta} \cdot \left(1 - e^{-\beta \cdot \left(TPH/BA\right) \cdot \varphi_{DBH}}\right)^{\gamma} \quad \text{(Eq. 1)}$$

Where:

Ht is total tree height (m)
DBH is Diameter at breast height (cm)
BA is stand basal area (m^2/ha)
TPH is stand density (trees/ha)
SHt is stand height (dominant/codominant height of the plot)
α, β. γ, δ and ϕ are parameters to be estimated.

Stem volumes were estimated using the Zakrzewski & Penner (2013) and Sharma & Parton (2009) models. Biomass was estimated using the equations of Lambert et al (2005) using height and DBH. The ground plots covered a range of forest types, and the mean values and range (in brackets) for each of these attributes are provided in Table 1.

Table 1. Summary of calibration plot data, which cover a range of forest conditions within PRF. Attributes are for all stems. N = number of plots for each forest type.

Forest Type	N	Gross total volume (m^3/ha)	Basal area (m^2/ha)	Trees/ha	Dominant/ co-dominant height (m)	Quadratic mean DBH (cm)
Black Spruce	14	152.5 (37.8 – 249.1)	21 (10.6 – 34.0)	1738 (592 - 2848)	16.3 (9.7 - 19.2)	13.2 (6.9 - 20.5)
Jack Pine	10	179.2 (114.4 – 261.1)	20.4 (15.8 - 26.3)	1377 (480 - 2976)	19.8 (16.3 - 22.9)	15.1 (9.7 - 21.5)
Lowland Conifer	4	232.6 (79.2 – 369.9)	33.2 (14 - 46.7)	2902 (1312 - 6224)	16.9 (12.6 - 20.4)	13.3 (9.2 - 17.4)
Mixedwood (Deciduous)	13	205.5 (35.3 – 350.1)	25.2 (9.2 - 38.2)	2171 (552 - 5656)	19.2 (11.8 – 24.8)	13.6 (4.6 – 21.5)
Mixedwood (Conifer)	13	160.6 (58.1- 310.4)	22.5 (8.5 – 39.3)	2014 (272 - 5512)	19.7 (13.8 - 27)	14.3 (7.2 – 20.0)
Mid-tolerant Hardwood	28	172.7 (2.8 – 299.4)	20.6 (0.5 – 32.0)	1726 (16 - 6280)	16.7 (11.1 – 21.2)	16.1 (4.9 – 34.3)
Intolerant Hardwood	15	401.3 (142.7 – 802.1)	36.6 (15.8 - 56.9)	1908 (392 - 4200)	25.3 (14.8 - 33.1)	17.2 (8.1 - 23.7)
Red Pine Plantation	23	430.3 (116.5 – 999.5)	40.5 (24.4 - 70.7)	1697 (408 - 3312)	22.5 (9.2 - 33.9)	19.0 (10.5 - 28.6)
White Pine Managed	14	210.0 (31.0 – 347.4)	27.1 (5.7 - 39.2)	1643 (48 - 2824)	18 (11.5 - 24.5)	16.3 (5.7 - 38.8)
White Pine Plantation	7	195.3 (13.8 – 434.7)	23.5 (6.7 - 44.4)	1239 (256 - 2456)	19.8 (5.6 - 37.2)	17.4 (8.9 - 34.3)
White Pine Natural	93	368.5 (19.9 – 949.0)	33.8 (2.9 - 68.4)	2082 (96 - 15392)	26 (8.2 – 43.0)	17.9 (6.0 - 39.9)
Tolerant Hardwood	23	272.7 (45.2 – 493.0)	29.0 (7.8 - 44)	1507 (360 - 4400)	23.9 (12.3 - 32.2)	16.9 (8.3 - 30.4)
Spruce Plantation	12	235.8 (110.2 – 457.8)	29.8 (12.3 - 52.5)	1705 (424 - 2968)	19 (13.8 - 26.5)	16.1 (10.7 - 26.4)
All	**269**	**291.99 (2.8 – 999.5)**	**30.1 (0.5 - 70.7)**	**1885 (16 - 15392)**	**22.2 (5.6 – 43.0)**	**16.6 (4.6 - 39.9)**

4.2 Stand-level validation data

Ten forest-types were identified for validation (Table 2; Appendix B) using a circa 2000 polygon-based forest inventory provided by PRF staff. Three mature stands of each forest type were selected for a total of 27 validation stands (Figure 3). A 50 m x 50 m sampling grid was superimposed over each of the stands and sampling station locations were identified (Figure 4). A maximum stand size of 15 ha was selected to maintain approximately 50 stations per stand. In many cases, far fewer stations were identified within the selected stands (due to stand size and shape). However, for some forest-types (i.e. tolerant hardwood, red oak, mixedwood), original photo-interpreted stand boundaries were modified as possible to enable 50 stations to be located within the stand. Stations along the 50 m x 50 m grid were adjusted as necessary to maintain a minimum distance of 20 m from clearly marked trails and roads. Each sampled stand was also buffered-inside by 12.5 m to ensure that sampling would be contained to the target stand condition (Figure 3). A recreational grade GPS unit was used to navigate to the identified stand-station waypoint (Figure 4), with a target accuracy of within 5 m the target station location. At each station, a BAF-2 prism was used to measure each tree determined to be "in" (i.e. DBH > 9.0 cm). Each "in" tree was recorded for species, DBH, and quality, as detailed in Appendix C. In addition, the tree with the

largest DBH for each prism sweep was measured for height. Crown class was not recorded. Borderline trees were checked with a limiting distance table.

After the cruise data was collected, a quality assurance process was used to examine each of the sampling stations relative to the stand boundary. As noted, stand boundaries were taken from a circa 2000 forest inventory, and when overlaid on the 2018 imagery, it was evident that the stand boundaries required some modification and update. Validation stand boundaries were manually edited to ensure roads were not included within the stand. Then, any station that was found within 12.5 m of the revised stand boundary was excluded. After the quality assurance process, a total of 1001 BAF-2 prism plots were used to derive validation summary information on 27 stands (Table 2).

Table 2. Stand-level validation data. Appendix B provides a cross-walk between forest types used in the calibration and validation data. A list of common species codes are also provided in Appendix B. N indicates the final number of stations within the stand after the quality assurance process was applied.

StandID	Forest Type	Species Composition (Species code and proportion within the stand)	N
28	White Pine Managed	Pw74Or10Pr8Mr4Po2Sb1Sw1Bf0Bw0	48
45	White Pine Natural	Pw42Or31Mr8Pr6Po5Bf3Ms2Sw2Sb1La0Iw0Bd0Be0Pj0	60
73	White Pine Natural	Pr41Pw28Bf15Sw5Po4Or3Bw2Mr2Iw0	30
74	Black Spruce	Sb37Pw22Ce12Bf9Mr5Pr5La4Or2Sw2Ab1Bw1By0He0Po0	22
77	Mixedwood	Or22Mr18Bf16Po14Pw7Sw6Bw6Bd3Ms2Ab2Iw2Pr2Cb0Sb0	48
85	White Pine Natural	Pw30Ce25Pr17Ab7Sw5Mr4Bf4Po3Bw2Be1Or1Pj1By0Sb0	24
92	Oak	Or45Po27Pw15Mr4Ms4Sw2Bf1Bw1Iw1Pr0Be0	55
161	Poplar	Po31Bf18Mr18Pw14Sw6Bw4Pr3Sb2By1Ce1La1Ms1Ab0Or0	24
186	Red Pine Plantation	Pr94Pw6	16
191	Jack Pine	Pj95Pw3Mr1Po1Bw0	20
192	Red Pine Plantation	Pr84Pw14Pj2	12
194	Red Pine Plantation	Pr61Pw19Pj9Mr4Po3Bf3Bw1Or0Sw0	25
198	Poplar	Po71Pj18Mr10Pr1	11
200	Jack Pine	Pj82Po14Pw2Bw1Pr1Mr0	36
442	White Pine Managed	Pw71Pr16Po5Sw4Mr1Or1Be1Bw1	34
455	Red Pine Plantation	Pr99Pw1Bw0	12
465	White Pine Managed	Pw73Pr22Be2By1Or1Po1Bf0Bw0He0Mr0Sw0	26
478	Black Spruce	Sb30Pw21Bf15Mr14Sw11Po6Bw1By1Ab1	21
518	Tolerant Hardwood	Mr26Ms14Bw12Bf12By9Iw7Pw4Bd4Sw4Or3Po2Ab1Be1Ea1	43
536	Mixedwood	Mr28Bf22Sw12Pw9Ms7Bw6Ab5Po3Bd3Pr2By1Iw1Or1Be0	50
547	Oak	Or40Pw39Mr4Bf4Pr3Sw3Ms2Bw1Iw1Po1He1La1Ab0Sb0	55
548	Mixedwood	Mr29Bf20Po18Sw13Pw10Bw4Or3Pr2Ab1Ms0Cb0La0Pb0	52
572	Tolerant Hardwood	Ms26Bf24Or14Mr10Sw10Pw7Iw3Bd2By2Be1Bw1Ab0Po0Pr0	61
588	White Pine Natural	Pw49Bf12Po11Mr10Pr8Sw7Bw1Sb1La1Ms0Or0Pj0	46
590	Mixedwood	Bf29Mr26Sw11Po7Or7Bw7Pw7Pr2Ms2Iw1Be1Ab0Bd0He0	60
619	Tolerant Hardwood	Pw21Ms15Mr11Bf10He9Or8Bw7Sw6Po5Bd4Pr1Ce1Be1Iw1	63
978	Lowland Conifer	Ce42Sb32La9Bf7Mr5Pw2Ab2By1Bw0Sw0	47

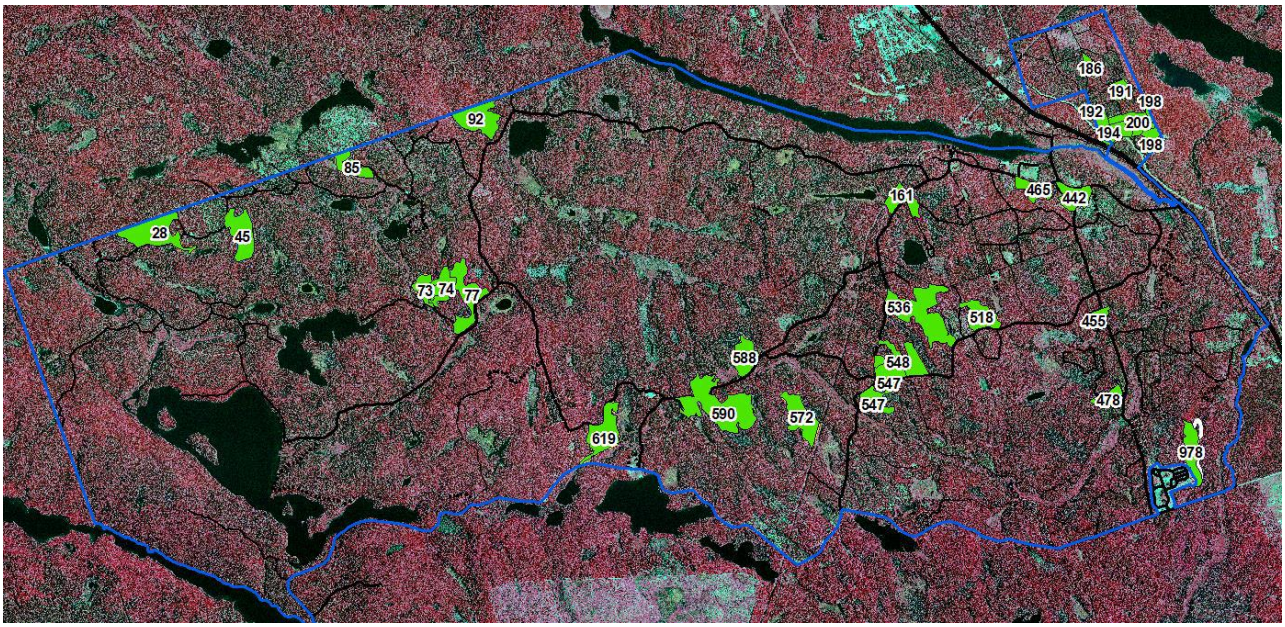

Figure 3. Map of selected validation stands at Petawawa Research Forest.

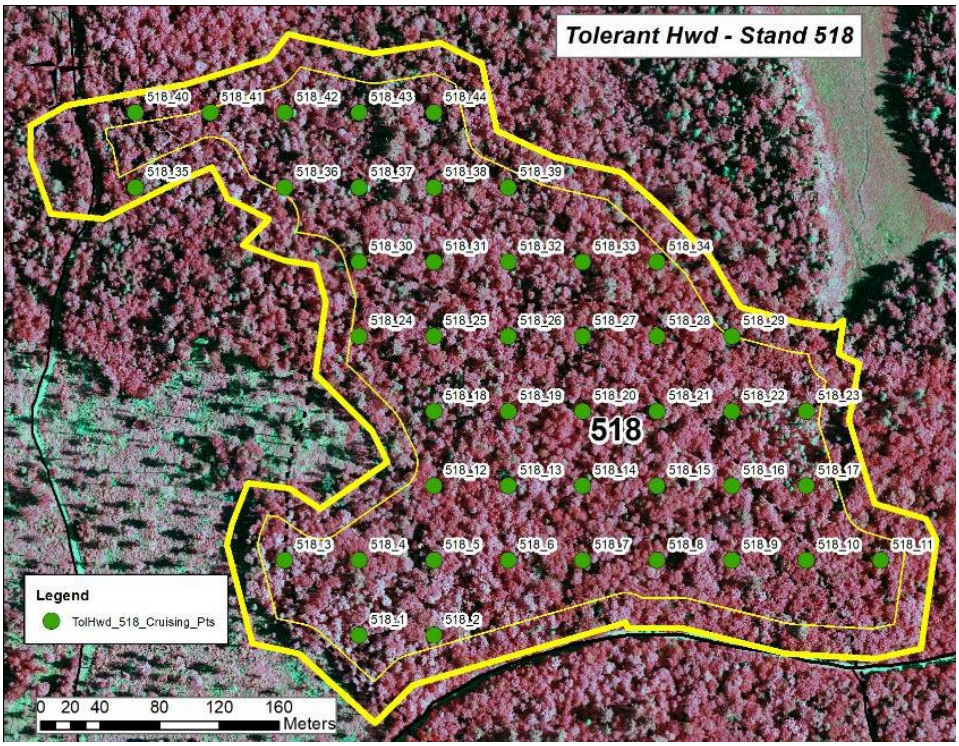

Figure 4. Example of a 50 m grid of stations super-imposed on validation stand 518 (tolerant hardwood). An internal buffer of 12.5 m was used to remove stations from the stand edge.

The following attributes were validated at the stand level: merchantable basal area, gross total volume for merchantable stems, merchantable stem volume, dominant/codominant height, quadratic mean diameter, top height, and Lorey's height. Details on the estimation of dominant/codominant height, top height, and Lorey's height from the cruise data are provided in Penner and Woods (2020; Appendix D). Validation stand summary statistics are provided in Table 3.

Table 3. Summary of stand-level validation data for the PRF. The mean value is followed by the range (in parentheses).

Forest Type	**Number of stands**	**Area (ha)**	**Average number of stations per stand**	**Top height (m)**	**Gross total volume, merchantable stems (m^3/ha) TVOL_merch**	**Merchantable stem volume (m^3/ha) MVOL**	**Basal area, merchantable stems (m^2/ha) BA_merch**	**Quadratic mean diameter (cm) DQ_merch**
Black Spruce	2	7 (7–8)	22 (21–22)	19.6 (19.0–20.1)	185.3 (178.3–192.3)	152.0 (145.3–158.8)	22.4 (22.3–22.5)	19.7 (18.9–20.4)
Jack Pine	2	9 (6–12)	28 (20–36)	20.3 (19.6–21.0)	206 (197.9–213.6)	183.0 (178.0–188.0)	22.3 (21.3–23.2)	19.4 (18.5–20.2)
Lowland Conifer	1	15 (15–15)	47 (47–47)	15.5 (15.5–15.5)	150.1 (150.1–150.1)	124.6 (124.6–124.6)	23.4 (23.4–23.4)	19.2 (19.2–19.2)
Mixedwood	4	18 (16–19)	53 (48–60)	19.9 (18.8–20.5)	220.9 (204.6–229.3)	168.0 (151.3–176.3)	26.8 (24.0–28.6)	20.3 (19.3–21.0)
Oak	2	19 (19–20)	55 (55–55)	21.5 (21.2–21.9)	278.6 (246.7–310.4)	228.6 (201.5–255.7)	29.6 (27.4–31.8)	24.7 (24.3–25.0)
Poplar	2	7 (4–9)	18 (11–24)	23.1 (22.5–23.6)	254.5 (222.7–286.4)	209.7 (187.5–231.9)	24.7 (21.9–27.5)	20.5 (19.0–21.9)
Red Pine Plantation	4	5 (4–9)	16 (12–25)	22.9 (20.5–25.5)	330.1 (230.6–429.3)	294.6 (216.4–395.6)	31.6 (21.4–38.5)	26.3 (21.2–32.6)
Managed White Pine	3	12 (9–16)	36 (26–48)	29.3 (25.8–33.8)	173.5 (102.6–212.5)	161.0 (94.6–201.0)	15.0 (9.0–19.7)	35.7 (31.9–41.4)
Natural White Pine	4	13 (10–19)	40 (24–60)	23.5 (21.9–25.2)	308.2 (292.0–315.6)	266.5 (248.8–285.1)	31.5 (30.1–32.9)	24.2 (23.2–25.5)
Tolerant Hardwood	3	18 (14–21)	56 (43–63)	20.7 (20.2–21.7)	232.8 (206.3–248.6)	177.6 (148.5–195.1)	27.5 (25.1–29.7)	21.0 (20.4–21.5)
All	**27**	**13 (4–21)**	**37 (11–63)**	**22.2 (15.5–33.8)**	**246.5 (102.6–429.3)**	**207.5 (94.6–395.9)**	**26.2 (9.0–38.5)**	**23.7 (18.5–41.4)**

4.3 Single-photon lidar (SPL) data

Leaf-on single photon lidar data were acquired for the Petawawa Research Forest and the adjoining Canadian Nuclear Laboratory property on July 2, 2018. The Leica SPL100 sensor was flown aboard a Piper-PA-31-350 at an average altitude of 3800 m, with the acquisition specifications detailed in Table 4.

Table 4. SPL data acquisition parameters.

Parameter	**2018 SPL**
Sensor	Leica SPL100
Laser wavelength (nm)	532
Laser beam divergence (mrad)	0.08
Average flying altitude (m AGL)	3800
Average flying speed (knots)	<180
Pulse repetition rate (pulses/sec)	60,000
Frequency	21 Hz
Scan Angle (degrees)	±15
Field of View (degrees)	30
Swath Width (m)	2000
Aggregate nominal point density (first returns only)	32.4

To support area-based modelling, lidar metrics were calculated from the SPL point clouds (Table 5). These lidar metrics are used as predictors to develop models for forest inventory attributes of interest following the approach outlines in White et al. (2013, 2017). SPL lidar metrics were generated with LAStools (Isenburg, 2020) using the full SPL point cloud (all returns), without the application of a height threshold.

Table 5. SPL predictors used for area-based modelling of forest inventory attributes (n = 65).

Predictor	Threshold	Description
a_std_95	0m	STD_Trimmed @95%
a_ske_95	0m	Skewness_Trimmed @95%
a_kur_95	0m	Kurtosis_Trimmed @95%
a_avg	0m	avgHt
a_qav	0m	average_Square_Ht
a_p01	0m	1st Percentile Height
a_p05	0m	5th Percentile Height
a_p10	0m	10th Percentile Height
a_p20	0m	20th Percentile Height
⋮		
a_p90	0m	90th Percentile Height
a_p95	0m	95th Percentile Height
a_p99	0m	99th Percentile Height
a_d0_2	0m	Number of returns from 0-2m/All returns
a_d2_4	0m	Number of returns from 2-4m/All returns
⋮		
a_d44_46	0m	Number of returns from 44-46m/All returns
a_d46_48	0m	Number of returns from 46-48m/All returns
a_b10	0m	decile 10% of points between 0 and 99% height
a_b20	0m	decile 20% of points between 0 and 99% height
⋮		
a_b80	0m	decile 80% of points between 0 and 99% height
a_b90	0m	decile 90% of points between 0 and 99% height
a_dns_2m	2m	Density_Percentage of All Returns 2m-49m/All Returns
a_dns_4m	4m	Density_Percentage of All Returns 4m-49m/All Returns
a_dns_5m	5m	Density_Percentage of All Returns 5m-49m/All Returns
a_dns_6m	6m	Density_Percentage of All Returns 6m-49m/All Returns
a_dns_10m	10m	Density_Percentage of All Returns 10m-49m/All Returns
a_dns_12m	12m	Density_Percentage of All Returns 12m-49m/All Returns
a_dns_14m	14m	Density_Percentage of All Returns 14m-49m/All Returns
a_dns_15m	15m	Density_Percentage of All Returns 15m-49m/All Returns
a_dns_16m	16m	Density_Percentage of All Returns 16m-49m/All Returns
a_dns_18m	18m	Density_Percentage of All Returns 18m-49m/All Returns
a_dns_20m	20m	Density_Percentage of All Returns 20m-49m/All Returns
a_dns_25m	25m	Density_Percentage of All Returns 25m-49m/All Returns
a_vci_1mbin	0m	Vertical Complexity Index with a 1 m bin
a_vci_0.5bin	0m	Vertical Complexity Index with a 0.5 m bin

4.4 Area-based modelling approach

Attributes were modelled using random forests (Breiman, 2001), as implemented in the *R* package *randomForest* (Liaw and Weiner, 2002). No stratification was used for model development. Ground attributes that were predicted directly are defined in Table 6. Merchantable attributes were only predicted when p99 > 5 m. The ground attributes that were not predicted directly, but rather derived from other predicted attributes (Table 6), are defined in Table 7. Area-based models were developed using the full set of lidar metrics as predictors (Table 5). The *mtry* parameter in *randomForest*, which determines the number of predictors used for splitting at each tree node, was set to $p/3$, where p is the total number of predictors used. 2018 area-based models for merchantable basal area, merchantable stem volume, and gross total volume (merchantable stems), used predictions of volume-to-basal area ratios (VBAR) to constrain the final predictions to ensure they were logical (e.g. gross total volume for merchantable stems

is always equal or greater than predictions of merchantable stem volume). VBAR ratios (VBAR_TVOL ratio, VBAR_MVOL_ratio, and BA_merch_ratio) were calculated as indicated in Table 6. Using these ratios, TVOL_merch, MVOL, and BA_merch were calculated as indicated in Table 7. Management size classes for basal area, volume, and biomass were defined by the DBH class range (Table 8). The attributes for each size class were calculated accordingly (Table 9 and Table 10).

Table 6. Ground plot attributes directly predicted in area-based models. Note that merchantable attributes are only predicted when the 99th percentile of lidar point cloud heights (p99) is greater than 5m.

Attribute	Definition	Size
TOPHT	top height (average height of thickest 6 trees/plot) (m)	All
HL_all	Lorey's height (average height weighted by BA) (m)	All
CD_ht	average height of dominant/codominant trees (m)	All
DQ_all	quadratic mean DBH, all stems (cm)	All
BA_all	basal area, all stems (m^2/ha)	All
TVOL_all	gross total volume, all stems (m^3/ha)	All
BIO_all	aboveground biomass, all stems (kg/ha)	All
DQ_merch	quadratic mean DBH, merchantable stems (cm)	DBH ≥ 9.1 cm
VBAR_TVOL_ratio	VBAR_TVOL_merch/VBAR_TVOL	DBH ≥ 9.1 cm
VBAR_MVOL_ratio	VBAR_MVOL/VBAR_TVOL_merch	DBH ≥ 9.1 cm
BA_merch_ratio	BA_merch/BA_all	DBH ≥ 9.1 cm
HL_merch_ratio	HL_merch/HL_all	DBH ≥ 9.1 cm
BIO_merch_ratio	BIO_merch/ BIO _all	DBH ≥ 9.1 cm

Table 7. Ground plot attributes that are not predicted directly from SPL data, but rather derived from other attributes (i.e. those listed in Table 6).

Attribute	Definition	Size	Calculation
TPH_all	stems/ha, all stems	All	BA_all/ (DQ_all*DQ_all*0.00007854)
HL_merch	Lorey's height, merchantable stems (m)	DBH ≥ 9.1 cm	HL_all*HL_merch_ratio
BA_merch	basal area, merchantable stems (m^2/ha)	DBH ≥ 9.1 cm	BA_all* BA_merch_ratio
TPH_merch	stems/ha, merchantable stems	DBH ≥ 9.1 cm	BA_merch/ (DQ_merch*DQ_merch*0.00007854)
TVOL_merch	gross total volume, merchantable stems (m^3/ha)	DBH ≥ 9.1 cm	TVOL_all*VBAR_TVOL_ratio*BA_merch_ratio
BIO_merch	aboveground biomass, merchantable stems (kg/ha)	DBH ≥ 9.1 cm	BIO_all*BIO_merch_ratio
MVOL	merchantable stem volume (m^3/ha)	DBH ≥ 9.1 cm	TVOL_merch*VBAR_MVOL_ratio

Table 8. Management size class as defined by DBH range.

Size	Size class	DBH range (cm)
Large	Large sawlog	DBH > 49
Medium	Medium sawlog	37 < DBH ≤ 49
Small	Small sawlog	25 < DBH ≤ 37
Poles	Polewood	9 < DBH ≤ 25

Table 9. Predicted size class attributes and their mode of calculation.

Attribute	Definition	Size	Calculation
BALarge_frac	Fraction of BA in large sawlogs	large	BALarge/BA_merch
BAMedium_frac	Fraction of BA in medium sawlogs	medium	BAMedium/(BA_merch – BALarge)
BASmall_frac	Fraction of BA in small sawlogs	small	BASmall/(BA_merch – BALarge – BAMedium)
MVOL_Large_frac	Fraction of merchantable stem volume in large sawlogs	large	MVOL_Large/MVOL
MVOL_Medium_frac	Fraction of merchantable stem volume in medium sawlogs	medium	MVOL_Medium/(MVOL – MVOL_Large)
MVOL_Small_frac	Fraction of merchantable stem volume in small sawlogs	small	MVOL_Small/(MVOL – MVOL_Large – MVOL_Medium)
TVOL_Large_frac	Fraction of gross total volume of merchantable stems in large sawlogs	large	TVOL_Large /TVOL_merch
TVOL_Medium_frac	Fraction of gross total volume of merchantable stems in medium sawlogs	medium	TVOL_Medium/(TVOL_merch – TVOL_Large)
TVOL_Small_frac	Fraction of gross total volume of merchantable stems in small sawlogs	small	TVOL_Small/(TVOL_merch – TVOL_Large – TVOL_Medium)
BIOLarge_frac	Fraction of aboveground biomass for merchantable stems in large sawlogs	large	BIOLarge/BIO_merch
BIOMedium_frac	Fraction of aboveground biomass for merchantable stems in medium sawlogs	medium	BIOMedium/(BIO_merch – BIOLarge)
BIOSmall_frac	Fraction of aboveground biomass for merchantable stems in small sawlogs	small	BIOSmall/ (BIO_merch – BIOLarge – BIOMedium)
DQ_Poles	Quadratic mean DBH of merchantable stems for poles	poles	
DQ_Large	Quadratic mean DBH of merchantable stems for large sawlogs	large	
DQ_Medium	Quadratic mean DBH of merchantable stems for medium sawlogs	medium	
DQ_Small	Quadratic mean DBH of merchantable stems for small sawlogs	small	

Table 10. Mode of calculation for size class attributes for BA and TPH. Calculations for MVOL, TVOL, and biomass (Table 9) are similar.

Attribute	Definition	Size	Calculation
BA_Large	basal area	large	BA_merch * BALarge_frac
BA_Medium	basal area	medium	(BA_merch – BALarge) * BAMedium_frac
BA_Small	basal area	small	(BA_merch – BALarge – BAMedium) * BASmal _frac
BA_Poles	basal area	poles	BA_merch - BALarge - BAMedium - BASmall
TPH_Poles	stems/ha	poles	BAPoles/(DQ_Poles DQ_Poles * 0.00007854)
TPH_Large	stems/ha	large	BALarge/(DQ_Large * DQ_Large * 0.00007854)
TPH_Medium	stems/ha	medium	BAMedium/(DQ_Medium * DQ_Medium * 0.00007854)
TPH_Small	stems/ha	small	BASmall/(DQ_Small * DQ_Small * 0.00007854)

4.5 Measures of model performance

Measures of model performance included bias, the standard error (SE) of the bias, and the root mean squared error. Relative bias and RMSE were also calculated, using the mean of the observed values for each forest type.

Bias is the difference between the observed Y_{obs} and predicted Y_{pred} attribute and the average bias was calculated as follows:

$$Bias = \frac{\sum(Y_{obs} - Y_{pred})}{n} = \frac{\sum bias_i}{n} \quad \text{(Eq. 2)}$$

The SE of the bias is a measure of how consistent the bias is. When the bias is reported SE of the bias is also reported. The SE of the bias was calculated as follows:

$$SE_{bias} = \sqrt{\frac{\sum(bias_i - \overline{bias})^2}{n}} \Big/ n = {\sigma_{bias}}/{\sqrt{n}} \quad \text{(Eq. 3)}$$

The root mean squared error (RMSE) is another measure of the goodness of the predictions and was calculated as follows:

$$RMSE = \sqrt{\frac{\sum(Y_{obs} - Y_{pred})^2}{n}} \quad \text{(Eq. 4)}$$

The relative bias and RMSE were calculated relative to the mean of the observed values as follows:

$$Bias\% = \frac{\overline{bias}}{mean(Y_{obs})} \times 100 \quad \text{(Eq. 5)}$$

$$RMSE\% = \frac{RMSE}{mean(Y_{obs})} \times 100 \quad \text{(Eq. 6)}$$

4.6 Results

4.6.1 Calibration data results

The *predict* function in the *randomForest R* package was used to obtain out-of-bag (OOB) errors. The OOB is a form of internal cross validation generated using hold-out sets of the calibration data (White et al. 2017). While OOB error provides an indication of model performance for the calibration plots, independent validation data at the management unit level (i.e. the stand) is always preferable for an area-based inventory (see Section 4.6.2). Results for dominant/codominant height (Table 11) indicate that although overall estimation bias was minimal, model performance varied by forest type, with mixed deciduous stands having the largest relative bias (-6%), and white pine-red pine stands and white pine plantations having the largest relative RMSE (19% and 15%, respectively)

Table 11. Calibration results for dominant/codominant height.

Forest Type	N	Observed (m)	Predicted (m)	Bias + SE (m)	Bias%	RMSE (m)	RMSE%
Black Spruce	14	16.3	16.6	-0.3 ± 0.2	-2%	0.8	5%
Jack Pine	10	19.8	19.2	0.6 ± 0.3	3%	1.2	6%
Lowland Conifer	4	16.9	17.2	-0.3 ± 0.4	-2%	0.7	4%
Mixedwood (Deciduous)	13	16.7	17.7	-0.9 ± 0.7	-6%	2.7	16%
Mixedwood (Conifer)	13	19.7	19.4	0.3 ± 0.5	2%	1.7	9%
Mid-tolerant Hardwood	28	19.2	19.5	-0.4 ± 0.5	-2%	2.6	14%
Intolerant Hardwood	15	25.3	24.4	0.8 ± 0.6	3%	2.5	10%
Red Pine Plantation	23	22.5	22.3	0.2 ± 0.2	1%	0.9	4%
White Pine Plantation	7	19.8	19.1	0.7 ± 1.2	4%	2.9	15%
White Pine Managed	14	18	18.2	-0.2 ± 0.6	-1%	2.1	12%
White Pine Natural	93	26	25.7	0.3 ± 0.5	1%	5	19%
Tolerant Hardwood	23	23.9	24.1	-0.2 ± 0.4	-1%	1.9	8%
Spruce Plantation	12	19	18.3	0.7 ± 0.4	4%	1.5	8%
All	**269**	**22.2**	**22.1**	**0.1 ± 0.2**	**0%**	**3.3**	**15%**

Overall, bias was minimal for estimates of gross total volume of merchantable stems, but varied by forest type, ranging from -43% for mixed conifer to 22% for red pine plantation (Table 12). Relative RMSE likewise varied, ranging from a low of 16% for intolerant hardwoods to a high of 49% for mixed conifers. Note that there was one calibration plot in a white pine plantation where p99 < 5 m and no merchantable attributes could be predicted.

Table 12. Calibration results for gross total volume (merchantable stems).

Forest type	N	Observed (m^3/ha)	Predicted (m^3/ha)	Bias + SE (m^2/ha)	Bias%	RMSE (m^3/ha)	RMSE%
Black Spruce	14	149	129	20 ± 7	13%	32	22%
Jack Pine	10	177	187	-9 ± 10	-5%	31	18%
Lowland Conifer	4	219	183	36 ± 29	16%	62	28%
Mixedwood (Deciduous)	13	152	170	-18 ± 10	-12%	39	26%
Mixedwood (Conifer)	13	166	237	-71 ± 12	-43%	81	49%
Mid-tolerant Hardwood	28	196	212	-16 ± 8	-8%	44	22%
Intolerant Hardwood	15	391	406	-15 ± 16	-4%	63	16%
Red Pine Plantation	23	426	332	94 ± 24	22%	145	34%
White Pine Plantation	6	222	231	-10 ± 16	-4%	38	17%
White Pine Managed	14	203	212	-9 ± 15	-4%	54	26%
White Pine Natural	93	360	350	10 ± 11	3%	102	28%
Tolerant Hardwood	23	266	335	-69 ± 16	-26%	101	38%
Spruce Plantation	12	230	196	34 ± 18	15%	67	29%
All	**268**	**286**	**285**	**1 ± 5**	**0%**	**87**	**31%**

Merchantable basal area was overestimated by approximately 1% overall (Table 13), but was greatest for mixed conifer stands (-38%). Relative RMSE ranged from 17% for intolerant hardwoods to 42% for mid-tolerant hardwoods.

Table 13. Calibration results for merchantable basal area.

Forest Type	N	Observed (m^2/ha)	Predicted (m^2/ha)	Bias + SE (m^2/ha)	Bias%	RMSE (m^2/ha)	RMSE%
Black Spruce	14	19.3	17	2.3 ± 1	12%	4.3	22%
Jack Pine	10	19.6	21.7	-2.2 ± 1.2	-11%	4.2	21%
Lowland Conifer	4	29	22.5	6.5 ± 4.1	23%	9.7	33%
Mixedwood (Deciduous)	13	20.1	20.9	-0.8 ± 1	-4%	3.5	17%
Mixedwood (Conifer)	13	18.6	25.6	-7 ± 1	-38%	7.9	42%
Mid-tolerant Hardwood	28	22.4	24.1	-1.8 ± 0.9	-8%	5.1	23%
Intolerant Hardwood	15	33.9	35.1	-1.1 ± 1.5	-3%	5.8	17%
Red Pine Plantation	23	39.2	31.2	7.9 ± 1.4	20%	10.4	27%
White Pine Managed	14	25	25.8	-0.9 ± 1.5	-3%	5.4	22%
White Pine Plantation	6	25.2	22.1	1.3 ± 2.8	5%	6.4	25%
White Pine Natural	93	31	29.9	1.1 ± 0.8	3%	8.2	26%
Tolerant Hardwood	23	27.3	31.7	-4.5 ± 1.6	-16%	8.7	32%
Spruce Plantation	12	28.3	25.2	3.2 ± 1.6	11%	6.1	21%
All	**268**	**27.9**	**27.5**	**0.3 ± 0.5**	**1%**	**7.4**	**26%**

4.6.2 Stand-level validation data results

Stand-level validation data, as described in Section 4.2, was used to assess the stand-level predictions of forest inventory attributes. These validation data are completely independent, and were not used for model development or calibration. In the comparison between observed and predicted stand-level attributes, the observed attribute for each stand is the arithmetic average of the field samples (i.e. cruise stations) found within that stand. The predicted attribute is the arithmetic average of the SPL-derived grid cell estimates within the stands. For some attributes, measurement approaches for the calibration and validation data were not identical and these differences undoubtedly contribute some uncertainty to the comparisons. Where relevant, these are highlighted below and should be considered when interpreting the results presented. Overall, the area-based models generated with data had minimal bias and a reasonable level of error. Results did vary by forest types however, with managed white pine typically having the largest relative bias and RMSE. Conversely, jack pine stands tended to have low relative bias and RMSE.

4.6.2.1 Top height

By definition, top height represents the average height of the thickest 100 trees/ha. For the calibration data, top height was the average of the six tallest trees in the plot (equalling 100 trees/ha). However, for the validation data, only the largest tree at each prism station was measured for height. These differences in field protocols resulted in large biases for top height shown in Table 14. Managed white pine stands had the largest relative bias at 21% and largest relative RMSE at 22% (Table 14; Figure 5; Appendix E, Figure E1), reflecting the common scenario whereby the few large trees left in the stand following harvesting are combined with shorter trees to enable the calculation of top height, thereby lowering top height for the calibration data in these forest types. Of note, a key challenge for the top height attribute is having an adequate sample of trees to enable top height calculation at the plot level; the degree to which the sample used for the calculation of top height at the plot-level is also representative of stand-level height distributions varies considerably.

Table 14. Validation results for top height.

Forest Type	N	Observed (m)	Predicted (m)	Bias + SE (m)	Bias%	RMSE (m)	RMSE%
Black Spruce	2	25.6	22	3.6 ± 0.1	14%	3.6	14%
Jack Pine	2	22.2	22.7	-0.4 ± 0.3	-2%	0.5	2%
Lowland Conifer	1	19.1	18.2	0.9 ± NA	4%	NA	NA
Mixedwood	4	25	22.3	2.7 ± 0.4	11%	2.8	11%
Oak	2	26.3	24.7	1.7 ± 1.2	6%	2.1	8%
Poplar	2	27.8	25.2	2.7 ± 2.4	10%	3.6	13%
Red Pine Plantation	4	25.3	24.6	0.7 ± 1	3%	1.9	8%
Managed White Pine	3	32	25.2	6.8 ± 1.6	21%	7.2	22%
Natural White Pine	4	28.7	25.4	3.3 ± 0.1	12%	3.3	12%
Tolerant Hardwood	3	26.9	23.3	3.6 ± 0.6	14%	3.7	14%
All	**27**	**26.5**	**23.8**	**2.7 ± 0.5**	**10%**	**3.6**	**14%**

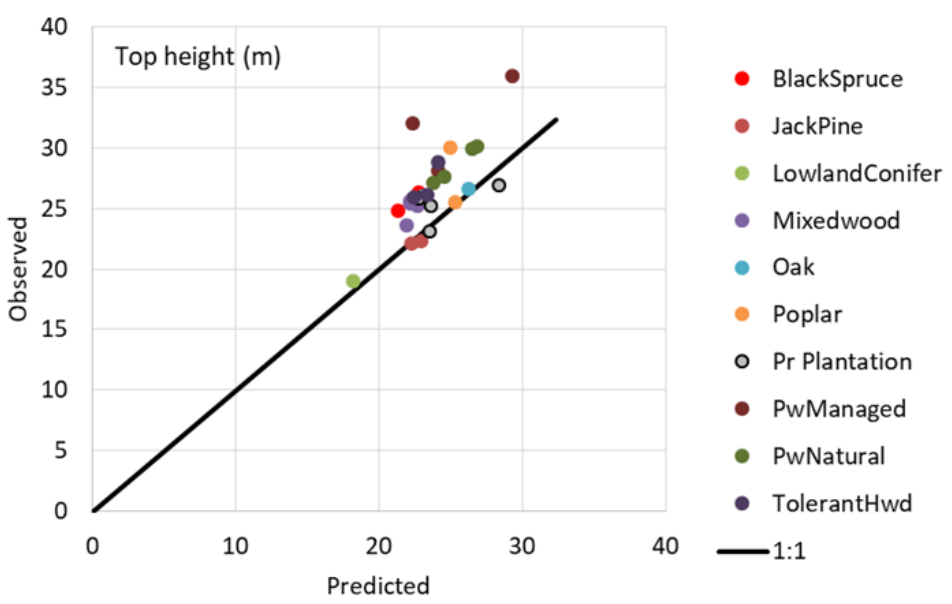

Figure 5. Stand-level assessment of observed versus predicted values for top height.

4.6.2.2 Gross total volume, merchantable stems

It is worth noting that the non-parametric approach used to generate the predictive models (random forests) used approximately 63% of the calibration data to generate predictions for each regression tree and is unable to extrapolate beyond the range of that calibration data. As a result, these random forest models are known to under predict high values and over predict low values (White et al. 2017). In this study however, the calibration data used in model development (Table 1) covered a much broader range of volumes than the validation data (Table 3), so extrapolation should not theoretically be an issue for volume predictions in the validation stands.

Predictions of gross total volume for merchantable stems were relatively unbiased, but bias varied by forest type (Table 15; Figure 6; Appendix E, Figure E2). In particular, volume was underestimated for white pine managed stands, which are tall, but have had some of the overstorey trees removed to encourage growth of residual stems and establish regeneration. These stands have a relatively low volume to height ratio compared to the other forest types, leading to an overestimation of volume (relative bias = -24%). Poplar stands also had a high relative negative bias (-13%), which may be a function of data compilation: ground estimates of volume use individual tree taper models, which work well for single straight tree stems; however hardwood tree species often have significant branching that confounds the definition and measurement of the main stem volume. Field crews also noted overstorey mortality in the poplar validation stands. Red pine plantations had the largest underestimation for merchantable volume (relative bias = 18%). As noted above, the calibration data for red pine plantation forest type covers a broader range of gross total merchantable volumes than the validation data; however, there are fewer calibration plots at the upper end of the distribution (i.e. with large volumes), so that may have influenced the results.

Table 15. Validation results for gross total volume, merchantable stems (DBH > 9 cm).

Forest Type	N	Observed (m^3/ha)	Predicted (m^3/ha)	Bias + SE (m^3/ha)	Bias%	RMSE (m^3/ha)	RMSE%
Black Spruce	2	185	199	-14 ± 10	-8%	17.2	9%
Jack Pine	2	206	217	-11 ± 3	-5%	11.5	6%
Lowland Conifer	1	150	125	25 ± NA	16%	NA	NA
Mixedwood	4	221	227	-6 ± 6	-3%	11.2	5%
Oak	2	279	287	-8 ± 1	-3%	8.2	3%
Poplar	2	255	288	-34 ± 1	-13%	33.8	13%
Red Pine Plantation	4	330	271	59 ± 21	18%	68.8	21%
Managed White Pine	3	174	215	-41 ± 19	-24%	49.6	28%
Natural White Pine	4	308	283	25 ± 4	8%	26.1	8%
Tolerant Hardwood	3	233	250	-17 ± 11	-7%	23.2	10%
All	**27**	**246**	**245**	**1 ± 7**	**0%**	**36**	**15%**

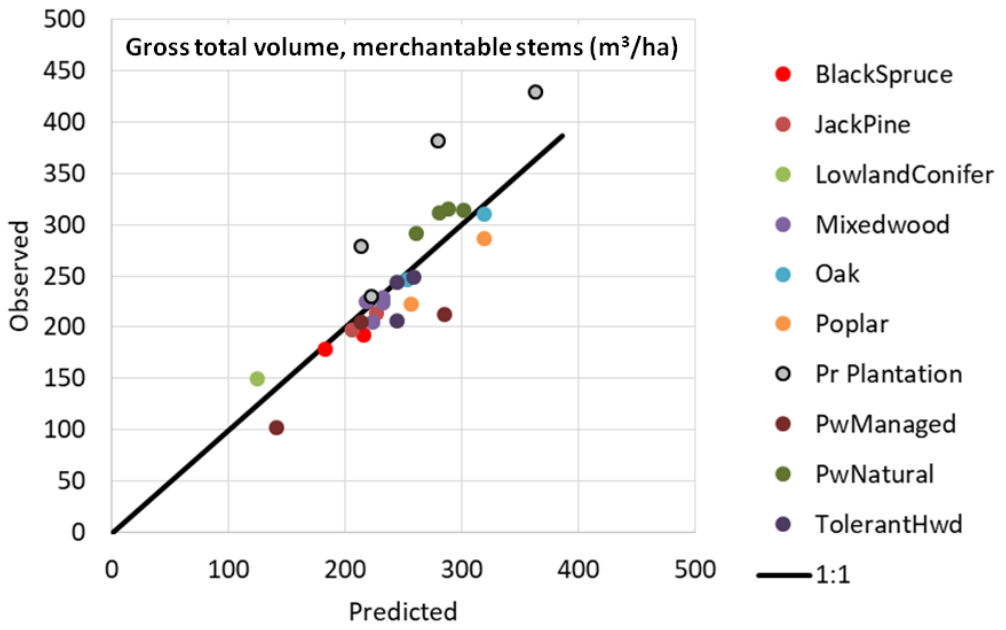

Figure 6. Observed versus predicted values of stand-level gross total volume of merchantable stems.

4.6.2.3 Merchantable stem volume

Overall, results for merchantable stem volume (Table 16; Figure 7; Appendix E, Figure E3) are similar to those of gross total volume of merchantable stems (Table 15), with minimal relative bias of 1% and relative RMSE of 16%. Merchantable stem volume was overestimated for poplar and managed white pine, and underestimated for lowland conifer (a lone cedar stand that was originally photointerpreted as a spruce stand).

Table 16. Validation results for merchantable stem volume.

Forest Type	N	Observed (m^3/ha)	Predicted (m^3/ha)	Bias + SE (m^3/ha)	Bias%	RMSE (m^3/ha)	RMSE%
Black Spruce	2	152	167	-15 ± 11	-10%	18.8	12%
Jack Pine	2	183	187	-4 ± 6	-2%	7.5	4%
Lowland Conifer	1	125	97	27 ± NA	22%	NA	NA
Mixedwood	4	168	175	-7 ± 6	-4%	13	8%
Oak	2	229	227	2 ± 5	1%	5.5	2%
Poplar	2	210	245	-36 ± 10	-17%	37.1	18%
Red Pine Plantation	4	295	239	56 ± 15	19%	61.3	21%
Managed White Pine	3	161	195	-34 ± 19	-21%	43.6	27%
Natural White Pine	4	266	241	26 ± 5	10%	27.3	10%
Tolerant Hardwood	3	178	194	-17 ± 14	-9%	25.3	14%
All	**27**	**208**	**205**	**2 ± 7**	**1%**	**33.7**	**16%**

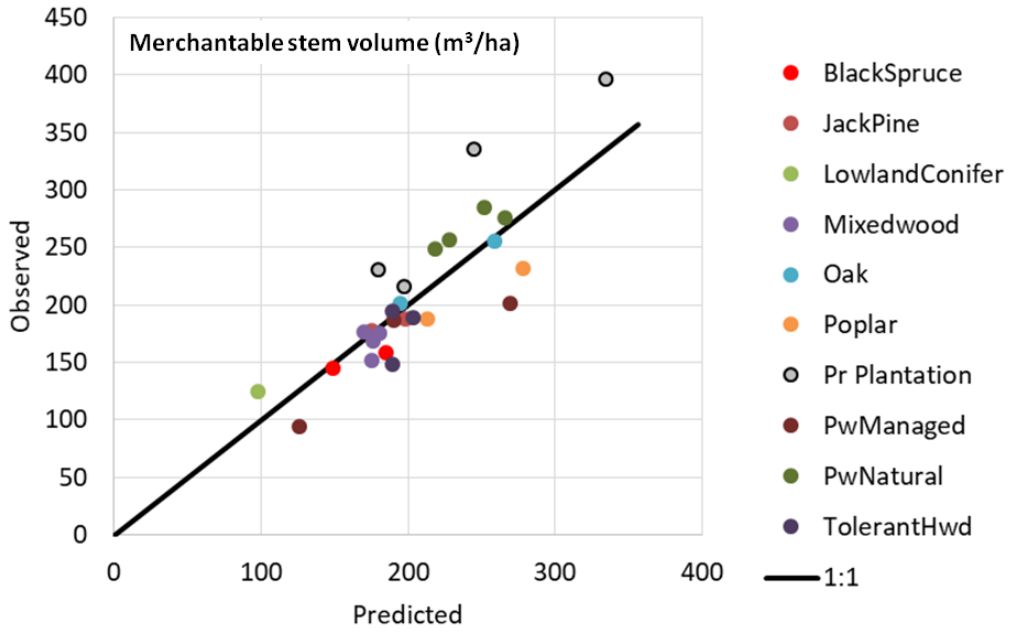

Figure 7. Observed versus predicted values for merchantable stem volume.

4.6.2.4 Basal area, merchantable stems

Results for merchantable basal area are shown in Table 17, Figure 8, and Appendix E (Figure E4). Overall, relative bias was small (2%) and relative RMSE was 14%. Similar to trends observed for gross total volume of merchantable stems, basal area for merchantable stems is overestimated in managed white pine and poplar stands, and underestimated in lowland conifer and mature red pine plantations. Once again, the largest relative RMSE is associated with managed white pine stands.

Table 17. Validation results for merchantable basal area.

Forest type	N	Observed (m^2/ha)	Predicted (m^2/ha)	Bias + SE (m^2/ha)	Bias%	RMSE (m^2/ha)	RMSE%
Black Spruce	2	22.4	23.5	-1.1 ± 0.8	-5%	1.4	6%
Jack Pine	2	22.3	22.8	-0.5 ± 0.5	-2%	0.7	3%
Lowland Conifer	1	23.4	16.5	6.9 ± NA	29%	NA	NA
Mixedwood	4	26.8	27.3	-0.5 ± 0.8	-2%	1.5	5%
Oak	2	29.6	30.5	-0.9 ± 1	-3%	1.3	4%
Poplar	2	24.7	29.1	-4.4 ± 0.6	-18%	4.4	18%
Red Pine Plantation	4	31.6	25.3	6.3 ± 1.9	20%	7.1	22%
Managed White Pine	3	15	18.4	-3.4 ± 1.2	-23%	3.8	25%
Natural White Pine	4	31.5	29.5	2 ± 1.1	6%	2.8	9%
Tolerant Hardwood	3	27.5	28.2	-0.7 ± 1.1	-3%	1.7	6%
All	**27**	**26.2**	**25.8**	**0.5 ± 0.7**	**2%**	**3.8**	**14%**

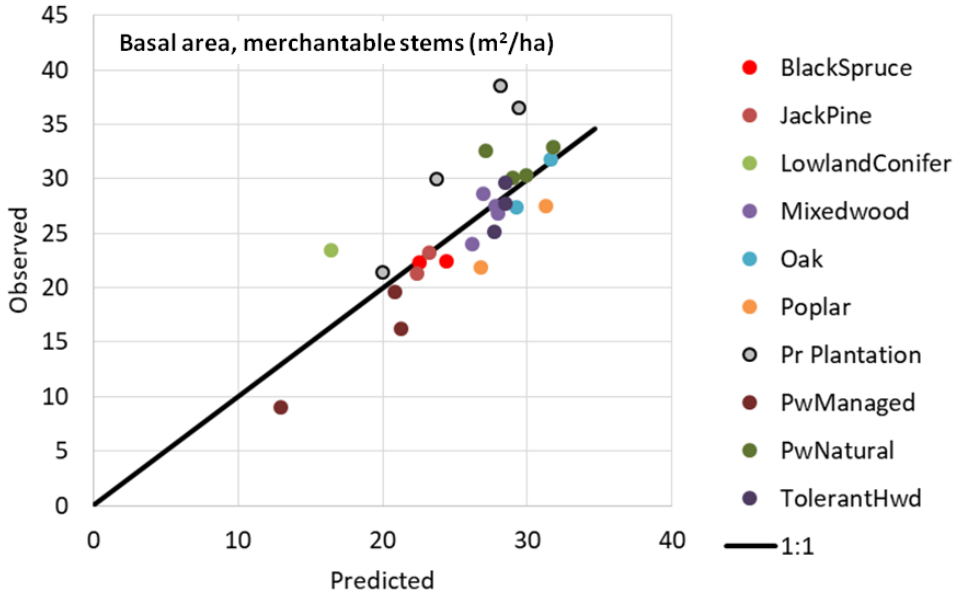

Figure 8. Observed versus predicted values for basal area, merchantable stems.

4.6.2.5 Quadratic mean DBH, merchantable stems

Overall, the predicted merchantable quadratic mean DBH for the validation stands had minimal bias (1%), with the highest negative bias for poplar stands and highest positive bias for managed white pine stands (Table 18; Figure 9; Appendix E, Figure E5).

Table 18. Validation results for quadratic mean DBH, merchantable stems.

Strata	N	Observed (cm)	Predicted (cm)	Bias + SE (cm)	Bias%	RMSE (cm)	RMSE%
Black Spruce	2	19.7	20.5	-0.8 ± 0.3	-4%	0.9	4%
Jack Pine	2	19.4	20.8	-1.4 ± 1.5	-7%	2	10%
Lowland Conifer	1	19.2	18.3	0.9 ± NA	5%	NA	NA
Mixedwood	4	20.3	20.8	-0.5 ± 0.3	-3%	0.7	4%
Oak	2	24.7	23.2	1.5 ± 1.1	6%	1.9	7%
Poplar	2	20.5	24.1	-3.6 ± 2.4	-17%	4.3	21%
Red Pine Plantation	4	26.3	25.5	0.7 ± 2.4	3%	4.3	16%
Managed White Pine	3	35.7	31	4.7 ± 1.8	13%	5.4	15%
Natural White Pine	4	24.2	23.9	0.4 ± 0.8	1%	1.4	6%
Tolerant Hardwood	3	21.0	21.8	-0.8 ± 0.6	-4%	1.1	5%
All	**27**	**23.7**	**23.5**	**0.2 ± 0.6**	**1%**	**2.9**	**12%**

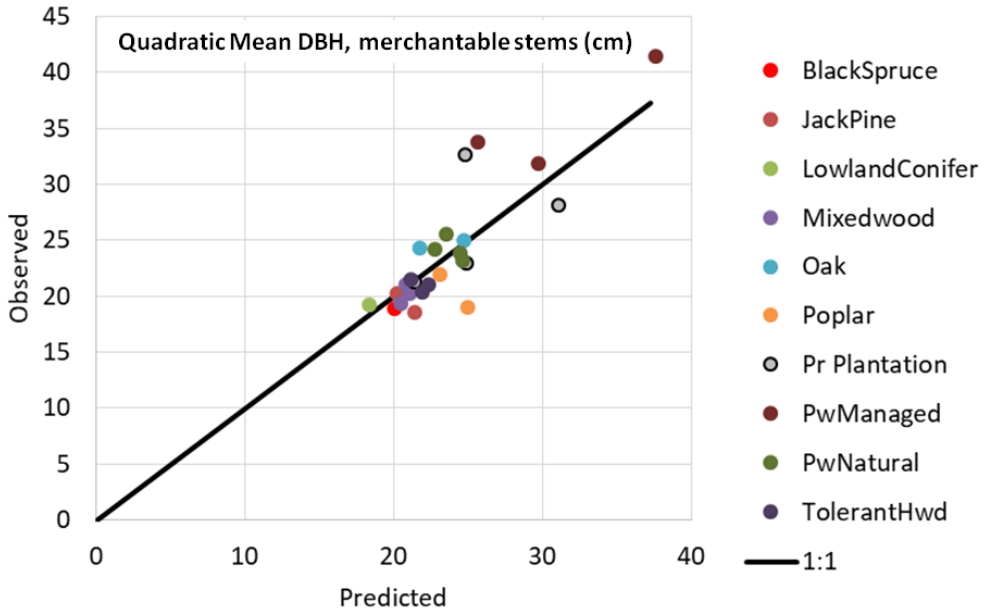

Figure 9. Observed versus predicted values for quadratic mean DBH, merchantable stems.

4.7 Comparison of 2012 LML and 2018 SPL area-based forest inventory attribute estimates

4.7.1 2012 data: lidar, calibration, and validation

In 2012, conventional, linear model lidar (LML) data were acquired for the PRF to support the generation of an EFI. The 2012 LML lidar data were collected over the PRF from August 17th to 20th, 2012. The Riegl 680i sensor was carried aboard a Cessna 172 aircraft flown at an average flying altitude of 725 m. Technical acquisition specifications are provided in Table 26. The average point density was approximately 15 points/m^2 (all returns) and ~6 points/m^2 (last returns). The data were originally collected as full waveform and written out as a discrete point file for use in subsequent applications.

A total of 223 ground plots were acquired between the fall of 2012 and the summer of 2014 to support area-based modelling. Plots had a radius of 14.1 m^2 and an area of 625 m^2 and measurement protocols were similar to those used in 2018 (Appendix C). In order to represent the full range of forest conditions within the PRF, plot selection was conducted using a structurally guided sampling approach, as detailed in White et al. (2013). Structurally guided sampling uses the lidar point cloud metrics (Appendix F) in a Principal Component Analysis. For the 2012 lidar metrics, the first principal component was strongly loaded to metrics of crown closure and vertical complexity, whereas the second principal component was more heavily weighted to lidar metrics of height and height distributions.

Live and dead trees with a DBH ≥ 9.1 cm were each assessed on the 625 m^2 plot for species and DBH, and had heights sampled across the range of diameter classes. Trees with a DBH less than 9.1 cm but taller than 1 m and that had a DBH > 2.5 cm were assessed by counting by species and 1 m height classes. An average DBH was measured and assigned to each species-height class assessed. Plots were summarized to per hectare values for all trees >2.5 cm (all) and ≥ 9.1 cm (merchantable).

Height-DBH curves were fit by species for all plots involved in this study. A variance of the Sharma and Parton (2009) ht-DBH model was used to predict heights. The variant of the prediction equation is the following:

$$\hat{ht} = 1.3 + \theta \cdot (TopHt)^{\delta} \cdot (1 - e^{-\beta \cdot Dbh})^{\gamma} \qquad \text{(Eq. 7)}$$

Where TopHt is defined as the average height of the 100 thickest trees per ha.

Zakrzewski's taper model (Zakrzewski 1999) was used to estimate total tree volumes and merchantable volumes using Crown Forest Sustainability Act (CFSA) upper stem diameter limits. The equation was refit in Zakzrewski and Penner (2013) and Equation 1 and the coefficients in Table 2 of that report were used. Soft maple taper equations were used for unknown hardwood species.

As per the 2018 SPL EFI described herein, validation data were acquired to provide an independent data source for validating the 2012 area-based estimates at the stand level. Intensive variable radius sampling (VAR) with a BAF 2 prism, on a 50 m grid interval was carried out in 19 stands of the PRF during the summer of 2015. Many of these stands corresponded with planned harvesting allocations scheduled for the winter of 2015 or subsequent years. As a result, some stands used for the validation of the 2012 EFI had previously been cruised at a lower intensity in 2014 or earlier in 2015. In these situations, previously collected stations were spatially included within the overlaid 50 m grid interval planned for this investigation. All stations that fell within the stand polygon were eligible. No internal buffering from the stand edge was implemented. The spatial distribution of the validation stands was constrained by planned operational blocks, and the range of conditions sampled for forest types was impacted. Two of the validation stands (472 and 509) were removed from any further analysis due to excessive windthrow that

occurred between the time of the lidar acquisition and validation sampling. The 17 stands used for validation of the 2012 EFI (Figure 10) ranged in size from 3.2 ha to 37.8 ha, resulting in a sampling intensity range of 13 to 145 sampling stations per stand. Live trees ≥ 10 cm that were deemed "in" were recorded by DBH and species. No heights were measured during the cruising. The same compilation methods were used for these data as for the 2018 calibration plot dataset. The species height-DBH relationships built from the 2012 LML calibration plots were used in the compilation of the validation data. Stand summaries for the 2012 LML validation data are provided in Table 19. Note that to permit later comparisons with the 2018 SPL results, a similar forest type classification was assigned to each stand. This post-sampling modification to the forest type assignment resulted in an uneven sampling matrix; however, the consistency in forest type enabled comparison between attribute estimates for the 2012 and 2018 EFIs.

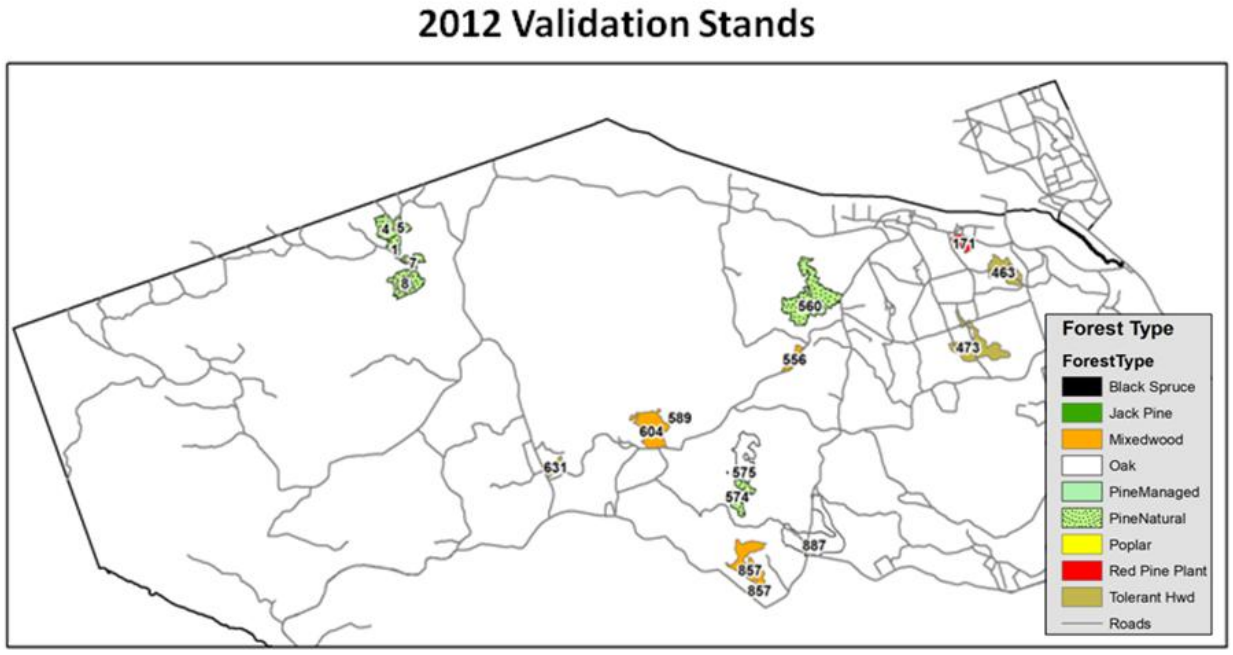

Figure 10. Location of independent validation stands used to assess 2012 area-based model estimates of forest inventory attributes.

Table 19. Summary of stand-level validation data for the 2012 EFI. Note that merchantable stem volume (mvol) and gross total volume for merchantable stems (TVOL_merch) were expressed per ha and by stand total. Species codes are provided in Appendix B.

Stand	Forest Type	Species Composition	N	Ha	BA_merch (m^2/ ha)	DQ_merch (cm)	MVOL (m^3/ha)	MVOL stand total (m^3)	TVOL_merch (m^3/ha)	TVOL_merch stand total (m^3)
MG1	PineNatural	Pr62Pw32Bf3Sw1La1Bw1	18	4.9	28.1	30.6	325.2	1585.4	348.9	1701.0
MG4	PineNatural	Pw40Or28Pr10Bw6BF6Mr3Sw3	37	8.9	26.3	24.1	204.2	1837.8	242.3	2180.3
MG5	PineNatural	Pr63Pw20Bf8Sw4Mr3Bw1Be1	19	4.4	23.9	24.9	245.3	1088.7	267.7	1188.0
MG7	PineNatural	Pr52Pw29Bf15Mr2Sw2	20	4.7	19.2	24.1	192.2	889.0	210.4	973.1
MG8	PineNatural	Pr39Pw36Bf10Mr7Po3Sw2Bw2	65	15.1	28.0	24.5	264.2	3996.6	301.1	4553.8
560	PineNatural	Pw41Mr15BF10Pr9Po8Sw5	141	37.8	23.8	22.8	191.2	7180.7	230.9	8671.6
574	PineNatural	Pw34Pr24Bf13Or11Mr9Sw4Sb2Po2	41	10.3	25.9	22.9	208.4	2122.6	242.28	2468.2
589	PineNatural	Pw44Bf28Po8Pr7Sw5Mr4Sb2Ab1Bw1	51	12.7	26.6	21.7	220.8	2760.0	252.4	3154.5
463	TolerantHwd	$Mh_{18}Be_{17}Pw_{13}PT_7By_4Bw_4Pl_3Bd_3Sw_2$	59	14.3	28.9	23.5	215.3	3122.1	277.4	4022.6
473	TolerantHwd	Mr27Pw12Mh12Bf10Sw8Or8Bw5	94	23.6	26.3	21.7	161.6	4777.9	218.5	6460.6
631	TolerantHwd	Or23Mh15Sw13Po12Be9Bw7Pw5By4Mr4Aw1	13	3.2	25.5	20.2	134.9	438.4	206.1	669.8
171	PrPlantation	Pr48Sw29Bf6By5Bw5Mr2Pw2Bd2Mh1	21	5.2	30.1	22.6	255.4	1341.1	295.5	1551.4
556	Mixedwood	Pw34Bf31Sw13Bw4Mr3	17	3.7	23.1	19.8	162.7	589.8	197.2	715.0
604	Mixedwood	Bf33Po20Pw14Sw10Mr10Sb6Bw5Pr1Or1	81	20.5	23.7	18.6	143.9	2967.7	186.1	3837.7
857	Mixedwood	Po25Pw20Or20Mr11BF9SW6Mh3Bw2Bd2Iw1Ab1	73	19.0	24.5	22.8	177.9	3379.3	225.3	4279.8
575	Oak	Or42Pw24Mr11Bf10Pr4Sw4	71	17.3	26.1	20.9	160.6	2840.8	209.1	3697.7
887	Oak	Or34Pw30Mr9Pr8Bf8Sw3Po3Bw2Sb1Mh1Ab1	145	34.6	25.9	22.0	174.4	6017.1	221.8	7650.4

4.7.2 2012 EFI: area-based modelling approach

Similar to the 2018 EFI, a non-parametric random forests modelling approach (Breiman, 2001) was implemented using the *randomForest* package in *R* (Liaw and Wiener 2002), with the *mtry* parameter set to the number of predictors divided by 3 (p/3), and the *ntree* parameter set to 500. Inventory attributes were predicted for a 25 m grid cell, with 145 predictors generated from the lidar point cloud. Thresholds for metric calculation included both 0 m and 2 m. Additional predictors for use in model development were generated using a canopy height model (CHM) with a 50 cm spatial resolution. These predictors included measures of canopy roughness, ruggedness, mean, variance, and standard deviations based on various window sizes. A full list of the predictors used in the development of the 2012 area-based models is provided in Appendix F.

Note that for the 2012 area-based models, all inventory attributes were predicted directly (and independently). In some cases, this approach can lead to predictions that may not conform to logical expectations, such as when gross total volume for merchantable stems exceeds gross total volume for all stems. To address this, some of the attributes in the 2018 EFI were derived from other predicted attributes, rather than being predicted directly, as described in the area-based modelling approach described in Section 4.4. A comparison of random forest OOB error indicates similar model performance between the 2012 LML and 2018 SPL area-based models (Table 20).

Table 20. Random forest out-of-bag (OOB) RMSE and bias of calibration plot data for inventory attributes. Note that one plot (PRF208, PwPlant) was removed as the 99th percentile of lidar heights was < 5m, which was the height threshold for predicting merchantable attributes.

	Basal Area, merchantable stems (m^2/ha)		Quadratic Mean DBH, merchantable stems (cm)		Merchantable Stem Volume (m^3/ha)		Gross Total Volume, merchantable stems (m^3/ha)	
	2012	**2018**	**2012**	**2018**	**2012**	**2018**	**2012**	**2018**
N	223	268	223	268	223	268	223	268
RMSE	7.6	7.4	5.6	5.3	85.3	83.5	86.1	87.2
RMSE%	27.9%	26.4%	22.9%	21.0%	38.8%	34.1%	31.3%	30.6%
Bias	0.0	0.3	0.0	0.0	-0.3	4.2	0.3	0.8
Bias%	0.0%	1.1%	-0.1%	0.1%	-0.1%	1.7%	0.1%	0.3%

4.7.3 Comparison of results for stand-level validation data: 2012 and 2018 EFIs

As noted previously, all forest inventory attributes for the 2012 area-based models were predicted directly, in contrast to the approach applied for the 2018 area-based models, whereby VBAR ratios were used to constrain estimates for merchantable basal area, merchantable stem volume, and gross total volume for merchantable stems (Table 6 and Table 7). The variable importance scores for the lidar metrics that were used in the area-based models are provided in Appendix G. An evaluation of overall results using absolute and relative RMSE and bias are presented in Table 21. Results by forest type are presented for 2012 (Table 22) and 2018 (Table 23). The equations used to calculate bias and relative bias are the same as those described in Section 4.5. Both merchantable stem volume and gross total volume for merchantable stems were expressed at the stand level (i.e. stand total in m^3), which was calculated as the mean per ha value (m^3ha^{-1}) multiplied by the total area of the validation stand (ha). Both the 2012 and 2018 attribute models were applied to generate wall-to-wall estimates for PRF with a grid cell resolution of 25 m.

Table 21. Overall validation results for 2012 LML and 2018 SPL area-based estimates. Absolute and relative RMSE and bias statistics are reported for validation stands. BA_merch = basal area, merchantable stems, DQ_merch = quadratic mean DBH, merchantable stems. Note that merchantable stem volume (MVOL) and gross total volume for merchantable stems (TVOL_merch) were expressed per ha and by stand total.

	BA_merch (m^2/ha)		DQ_merch (cm)		MVOL (m^3/ha)		MVOL Stand Total (m^3)		TVOL merch (m^3/ha)		TVOL merch Stand Total (m^3)	
	2012	**2018**	**2012**	**2018**	**2012**	**2018**	**2012**	**2018**	**2012**	**2018**	**2012**	**2018**
N	17	27	17	27	17	27	17	27	17	27	17	27
RMSE	1.5	3.8	2.6	2.9	20.6	33.7	219.7	295.7	17.3	36.0	207.8	312.1
%RMSE	5.8%	14.5%	11.6%	12.2%	10.2%	16.2%	8%	11.9%	6.8%	14.6%	6.1%	10.4%
Bias	0.3	0.5	-1.2	0.2	11.3	2.4	143.0	2.0	-9.7	1.0	-121.7	-22.0
%Bias	1.0%	1.7%	-5.3%	1.0%	5.6%	1.2%	5.2%	0.1%	-3.8%	0.4%	-3.6%	-0.7%

Overall, the validation results for the 2012 and 2018 estimates data are not markedly different. On average, the relative RMSE was 5% larger for the estimates generated from the 2018 SPL data. In contrast, the relative bias was typically larger for the 2012 estimates, but on average, differed by less than 1% overall. Of note, 2012 LML had larger bias for merchantable stem volume (underestimating by an average of 4.75%), and gross total volume of merchantable stems (overestimating by an average of 3.5%).

Table 22. 2012 Stand-level validation results by forest type. Note that merchantable stem volume (MVOL) and gross total volume for merchantable stems (TVOL_merch) were expressed per ha and by stand total. Absolute and relative RMSE and bias statistics are reported for validation stands. BA_merch = basal area, merchantable stems, DQ_merch = quadratic mean diameter, merchantable stems. Note that merchantable stem volume (MVOL) and gross total volume for merchantable stems (TVOL_merch) were expressed per ha and by stand total.

	Forest Type	BA_merch (m^2/ha)	DQ_merch (cm)	MVOL (m^3/ha)	MVOL Stand Total (m^3)	TVOL_merch (m^3/ha)	TVOL_merch Stand Total (m^3)
N	**Pine Natural**	8	8	8	8	8	8
RMSE		1.3	3.6	23.7	280.4	10.6	59.3
RMSE%		5.1%	14.8%	10.2%	10.5%	4.0%	1.9%
Bias		0.4	-2.1	21.2	240.8	-3.4	-17.6
Bias%		1.6%	-8.4%	9.2%	9.0%	-1.3%	-0.6%
N	**Red Pine Plantation**	1	1	1	1	1	1
RMSE		1.2	1.7	34.2	179.3	5.7	30.0
RMSE%		4.1%	7.5%	13.4%	13.4%	1.9%	1.9%
Bias		1.2	-1.7	34.2	179.3	5.7	30.0
Bias%		4.1%	-7.5%	13.4%	13.4%	1.9%	1.9%
N	**Tolerant Hardwood**	3	3	3	3	3	3
RMSE		1.9	1.0	21.1	107.9	31.8	271.4
RMSE%		7.0%	4.4%	12.4%	3.9%	13.6%	7.3%
Bias		-1.2	-0.4	-9.5	-17.1	-26.3	-254.1
Bias%		-4.6%	-2.1%	-5.6%	-0.6%	-11.2%	-6.8%
N	**Mixedwood**	3	3	3	3	3	3
RMSE		2.0	0.7	7.4	144.0	14.2	217.9
RMSE%		8.3%	3.6%	4.6%	6.2%	7.0%	7.4%
Bias		1.4	-1.1	2.4	33.2	-10.8	-129.4
Bias%		5.7%	-5.5%	1.5%	1.4%	-5.3%	-4.4%
N	**Oak**	2	2	2	2	2	2
RMSE		0.2	1.2	5.2	176.8	16.1	413.3
RMSE%		0.9%	5.7%	3.1%	4.0%	7.5%	7.3%
Bias		-0.2	1.2	4.4	138.7	-16.0	-403.6
Bias%		-0.7%	5.7%	2.6%	3.1%	-7.4%	-7.1%

Table 23. 2018 stand-level validation results, by forest type. Note that merchantable stem volume (MVOL) and gross total volume for merchantable stems (TVOL_merch) were expressed per ha and by stand total.

	Forest Type	Basal Area, merchantable stems (m^2/ha)	Quadratic Mean DBH, merchantable stems (cm)	MVOL (m^3/ha)	MVOL (m^3)	TVOL merch (m^3/ha)	TVOL merch (m^3)
N	**Black Spruce**	2	2	2	2	2	2
RMSE		1.4	0.9	18.9	124.1	17.2	113.1
RMSE%		6.3%	4.3%	12.4%	11.7%	9.3%	8.8%
Bias		-1.1	-0.8	-15.1	-100.3	-14.1	-94.5
Bias%		-5.1%	-4.1%	-9.9%	-9.5%	-7.6%	-7.3%
N	**Jack Pine**	2	2	2	2	2	2
RMSE		0.7	2.0	7.5	87.1	11.5	123.3
RMSE%		3.3%	10.4%	4.1%	5.1%	5.6%	6.4%
Bias		-0.5	-1.4	-3.9	-52.9	-11.2	-110.5
Bias%		-2.3%	-7.4%	-2.1%	-3.1%	-5.4%	-5.8%
N	**Lowland Conifer**	1	1	1	1	1	1
RMSE		7.0	0.9	27.1	418.6	24.7	381.5
RMSE%		29.8%	4.7%	21.8%	21.8%	16.5%	16.5%
Bias		7.0	0.9	27.1	418.6	24.7	381.5
Bias%		29.8%	4.7%	21.8%	21.8%	16.5%	16.5%
N	**Mixedwood**	4	4	4	4	4	4
RMSE		1.5	0.8	13.0	206.9	11.2	180.5
RMSE%		5.6%	3.7%	7.7%	6.9%	5.1%	4.6%
Bias		-0.5	-0.6	-7.3	-113.7	-5.8	-88.0
Bias%		-1.8%	-2.8%	-4.4%	-3.8%	-2.6%	-2.3%
N	**Oak**	2	2	2	2	2	2
RMSE		1.3	1.8	5.5	109.1	8.2	157.6
RMSE%		4.4%	7.4%	2.4%	2.5%	2.9%	2.9%
Bias		-0.8	1.4	1.9	39.8	-8.1	-156.5
Bias%		-2.8%	5.8%	0.8%	0.9%	-2.9%	-2.9%
N	**Poplar**	2	2	2	2	2	2
RMSE		4.4	4.3	37.1	221.1	33.8	258.4
RMSE%		17.7%	21.0%	17.7%	15.8%	13.3%	15.4%
Bias		-4.3	-3.6	-35.6	-219.7	-33.8	-238.1
N	**Red Pine Plantation**	4	4	4	4	4	4
RMSE		7.1	4.3	61.3	327.3	68.8	389.6
RMSE%		22.3%	16.3%	20.8%	21.5%	20.8%	22.5%
Bias		6.3	0.7	55.6	294.1	58.7	322.6
Bias%		19.8%	2.8%	18.9%	19.3%	17.8%	18.7%
N	**Managed White Pine**	3	3	3	3	3	3
RMSE		3.8	5.4	43.6	399.5	49.6	469.0
RMSE%		25.1%	15.0%	27.1%	20.5%	28.6%	22.2%
Bias		-3.4	4.7	-34.3	-333.5	-41.5	-419.6
Bias%		-22.7%	13.3%	-21.3%	-17.1%	-23.9%	-19.9%
N	**Pine Natural**	4	4	4	4	4	4
RMSE		2.8	1.4	27.3	362.3	26.1	361.8
RMSE%		9.0%	6.0%	10.2%	10.2%	8.5%	8.8%
Bias		2.0	0.4	25.6	332.3	25.0	330.9
Bias%		6.4%	1.5%	9.6%	9.4%	8.1%	8.0%
N	**Tolerant Hardwood**	3	3	3	3	3	3
RMSE		1.7	1.2	25.3	371.6	23.2	328.6
RMSE%		6.2%	5.5%	14.3%	11.4%	10.0%	7.7%
Bias		-0.7	-0.8	-16.6	-249.3	-17.0	-260.2
Bias%		-2.6%	-3.7%	-9.3%	-7.6%	-7.3%	-6.1%

It should be noted that a direct comparison of the validation results from 2012 and 2018 EFIs is challenging as a result of the following considerations;

1. Different stands were sampled for the 2012 and 2018 validation data;
2. The range and number of forest types included in the validation sample is not the same for both 2012 and 2018. Only a subset of forest types was common to both validation datasets (Table 24);
3. The number of plantation or silviculturally managed stands sampled in the 2012 and 2018 validation data is not consistent, with 2018 having more managed stands (with managed stands having conditions that make them more difficult to model, such as multiple distinctive layers);
4. Although many of the predictor variables derived from the lidar were similar, the 2012 models used more than twice as many input predictors (145) than 2018 (66);
5. Estimates for some attributes were not consistent between the 2012 and 2018 data. For the 2012 inventory, all attributes were modelled directly, but for 2018, some attributes were derived using ratio constraints to maintain consistency in estimation; and
6. Growth and mortality occurred between the acquisition of the 2012 LML data and the field plot measurement, whereas no growing season occurred between the acquisition of the 2018 SPL data and the acquisition of the validation data.

Overall, the accuracy of inventory attributes estimates derived from 2012 LML and 2018 SPL area-based models was similar (Table 24); however for all attributes considered, the relative RMSE was greater for the 2018 estimates and ranged from a low of 0.6% for merchantable quadratic mean diameter to a high of 8.7% for merchantable basal area. In contrast, relative bias was always larger for the 2012 estimates, with the exception of merchantable basal area. The largest positive bias was for per ha estimates of gross total volume for merchantable stems at 5.6%, and the largest negative bias was for 2012 estimates of quadratic mean diameter of merchantable stems at -5.3%. Stand-level merchantable stem volume and gross total volume for merchantable stems were the attributes estimated with the lowest RMSE% and bias%. For the 2012 EFI, merchantable basal area was the attribute estimated with the lowest RMSE% and bias%.

Table 24. Overall stand-level validation results for 2012 and 2018 EFIs.

	BA_merch (m^2/ha)		DQ_merch (cm)		MVOL (m^3/ha)		MVOL Total (m^3)		TVOL_merch (m^3/ha)		TVOL_merch Total (m^3)	
	2012	**2018**	**2012**	**2018**	**2012**	**2018**	**2012**	**2018**	**2012**	**2018**	**2012**	**2018**
RMSE	1.5	3.8	2.6	2.9	20.6	33.7	219.7	295.7	17.3	36.0	207.8	312.1
RMSE%	5.8%	14.5%	11.6%	12.2%	10.2%	16.2%	8%	11.9%	6.8%	14.6%	6.1%	10.4%
Bias	0.3	0.5	-1.2	0.2	11.3	2.4	143.0	2.0	-9.7	1.0	-121.7	-22.0
Bias%	1.0%	1.7%	-5.3%	1.0%	5.6%	1.2%	5.2%	0.1%	-3.8%	0.4%	-3.6%	-0.7%

Trends in estimation accuracy for 2012 and 2018 that were observed overall (Table 24) were not consistent for the forest types common to both EFIs: pine natural, tolerant hardwood, mixedwood (Table 25). Relative RMSE and bias varied by forest type and attribute, with no consistent trends observed between 2012 and 2018. Of note, estimation bias for tolerant hardwoods was always negative, regardless of year or attribute.

Table 25. Comparison of 2012 and 2018 validation results for forest types common to both EFIs.

		BA_merch (m^2/ha)		DQ_merch (cm)		MVOL (m^3/ha)		MVOL Total (m^3)		TVOL_merch (m^3/ha)		TVOL_merch Total (m^3)	
		2012	2018	2012	2018	2012	2018	2012	2018	2012	2018	2012	2018
N	**Pine Natural**	8	4	8	4	8	4	8	4	8	4	8	4
RMSE		1.3	2.8	3.6	1.4	23.7	27.3	280.4	362.3	10.6	26.1	59.3	361.8
RMSE%		5.1%	9.0%	14.8%	6.0%	10.2%	10.2%	10.5%	10.2%	4.0%	8.5%	1.9%	8.8%
Bias		0.4	2.0	-2.1	0.4	21.2	25.6	240.8	332.3	-3.4	25.0	-17.6	330.9
Bias%		1.6%	6.4%	-8.4%	1.5%	9.2%	9.6%	9.0%	9.4%	-1.3%	8.1%	-0.6%	8.0%
N	**Tolerant Hardwood**	3	3	3	3	3	3	3	3	3	3	3	3
RMSE		1.9	1.7	1.0	1.2	21.1	25.3	107.9	371.6	31.8	23.2	271.4	328.6
RMSE%		7.0%	6.2%	4.4%	5.5%	12.4%	14.3%	3.9%	11.4%	13.6%	10.0%	7.3%	7.7%
Bias		-1.2	-0.7	-0.4	-0.8	-9.5	-16.6	-17.1	-249.3	-26.3	-17.0	-254.1	-260.2
Bias%		-4.6%	-2.6%	-2.1%	-3.7%	-5.6%	-9.3%	-0.6%	-7.6%	-11.2%	-7.3%	-6.8%	-6.1%
N	**Mixedwood**	3	4	3	4	3	4	3	4	3	4	3	4
RMSE		2.0	1.5	0.7	0.8	7.4	13.0	144.0	206.9	14.2	11.2	217.9	180.5
RMSE%		8.3%	5.6%	3.6%	3.7%	4.6%	7.7%	6.2%	6.9%	7.0%	5.1%	7.4%	4.6%
Bias		1.4	-0.5	-1.1	-0.6	2.4	-7.3	33.2	-113.7	-10.8	-5.8	-129.4	-88.0
Bias%		5.7%	-1.8%	-5.5%	-2.8%	1.5%	-4.4%	1.4%	-3.8%	-5.3%	-2.6%	-4.4%	-2.3%

4.8 Summary

To quantify the performance of SPL data in an area-based approach to predicting forest inventory attributes, we developed area-based models for a suite of forest inventory attributes using SPL data acquired in July 2018, and co-located ground plot data. We quantified the accuracy of the resulting forest inventory attribute predictions using independent, stand-level validation data, and then compared the accuracy of the 2018 models to that of an earlier EFI that was generated using LML acquired in 2012. Overall, we found that the area-based models generated using the SPL data produced accurate predictions of our forest inventory attributes of interest, with minimal bias. Certain forest types were more challenging to model as a function of multiple layers or cohorts in the stands. The results achieved using the 2018 SPL data were comparable to those generated with the 2012 LML data. We therefore conclude that the SPL data provided a useful data source for generating reasonably accurate estimates of forest inventory attributes in an area-based approach.

5. Objective 2: Quantify the performance of SPL in characterizing terrain under varying forest types and canopy densities

One of the advantages associated with SPL technology is the capacity for large area coverage. The nature of the SPL instrument means that SPL data can be acquired at higher altitudes than is currently possible with linear mode lidar acquisitions. A key objective of this project was to assess the accuracy with which SPL technology could characterize terrain in different forest types and density of vegetation cover.

5.1 Lidar data

In addition to the leaf-on SPL data acquired in 2018 (Table 2), SPL data were also acquired for a portion of PRF in May 2019 (Figure 11), under predominantly leaf-off conditions. These data were acquired at two different altitudes, 3800 m and 2000 m, for the purposes of testing the impact of acquisition altitude on terrain characterization. The 2019 SPL data were not used in the forest inventory applications described in Section 4. In addition to the SPL data, the terrain assessment also considered a 2012 LML acquisition (leaf-on), which was used to generate an EFI for the PRF, as described in Section 4.7. Details for all four lidar datasets used in the terrain assessment are detailed in Table 26.

Table 26. Lidar acquisition parameters for all four lidar datasets used in the terrain assessment.

Parameter	2012 LML	2018 SPL	2019H SPL	2019L SPL
Acquisition date and conditions (leaf-on or leaf-off)	August 17–20 Leaf-on	July 1–2 Leaf-on	May 31 Leaf-off	May 31 Leaf-off
Sensor	Riegl 680i	Leica SPL100	Leica SPL100	Leica SPL100
Laser wavelength (nm)	1550	532	532	532
Laser beam divergence (mrad)	0.5	0.08	0.08	0.08
Average flying altitude (m AGL)	750	3760	3760	2000
Average flying speed (knots)	<100	<180	<180	<160
Pulse repetition rate (pulses/sec)	150,000	60,000	60,000	50,000
Frequency	76.67 Hz	21 Hz	23 Hz	23 Hz
Scan Angle (degrees)	±20	±15	±15	±15
Field of View (degrees)	40	30	30	30
Swath Width (m)	~600–700	2000	2000	1000
Aggregate Nominal Point Density (points/m^2)	5.8	32.4	28.6	51.4
Average ground point density (points/m^2)	1.3	2.8	3.8	5.5
Percentage of 25 m grid cells that have > 2 points classified as ground returns (%)[1]	17.2	37.2	81.5	94.7
Percentage of returns that are first returns	17.1	88.3	58.8	46.4
Ratio of first returns to second returns	0.6	8.8	1.7	1.1

[1]*Note that this is only calculated for the area common to all four lidar acquisitions, as shown in Figure 11.*

These lidar data vary in the degree to which they can penetrate through small openings in the canopy. A lidar sensor is capable of measuring multiple returns of energy for each laser pulse that it emits. The relative distribution of these returns provides an indication of whether or not the lidar pulse is intersecting features through the full vertical profile of the canopy. For example, the 2012 LML data records up to six returns for each laser pulse, with a relatively consistent distribution of returns for first returns to fourth

returns (Figure 12). Approximately 17% of 2012 LML returns are first returns. In contrast, the 2018 SPL data is dominated by first returns (> 88%), whereas leaf-off conditions for the 2019 SPL data increase the number of second and third returns (Table 25). The ratio of first to second returns is likewise insightful: the ratio for the 2012 LML is 0.6 compared to 8.8 for the 2018 SPL. Thus, although the aggregate nominal point density of the 2018 SPL data is almost 5.5 times greater than the 2012 LML data, the average ground point density of the 2018 SPL is, on average, only 2 times greater than that of the 2012 LML data. Leaf-off conditions and lower acquisition altitudes further increase the average ground point density to 5.5 points/m^2 for the SPL data acquired at 2000 m, and for these data 95% of 25 m grid cells have more than 2 points classified as ground returns (Table 26).

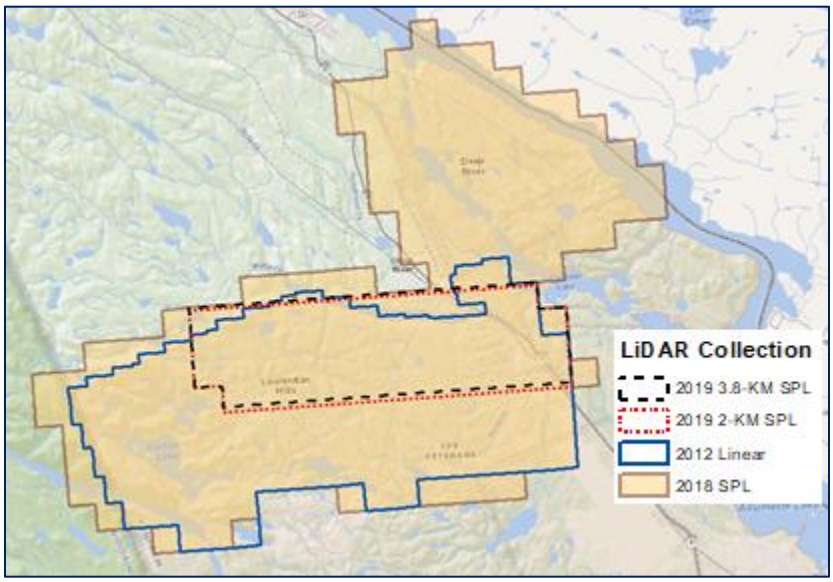

Figure 11. Spatial extent of the four lidar collections used in the analysis of terrain accuracy.

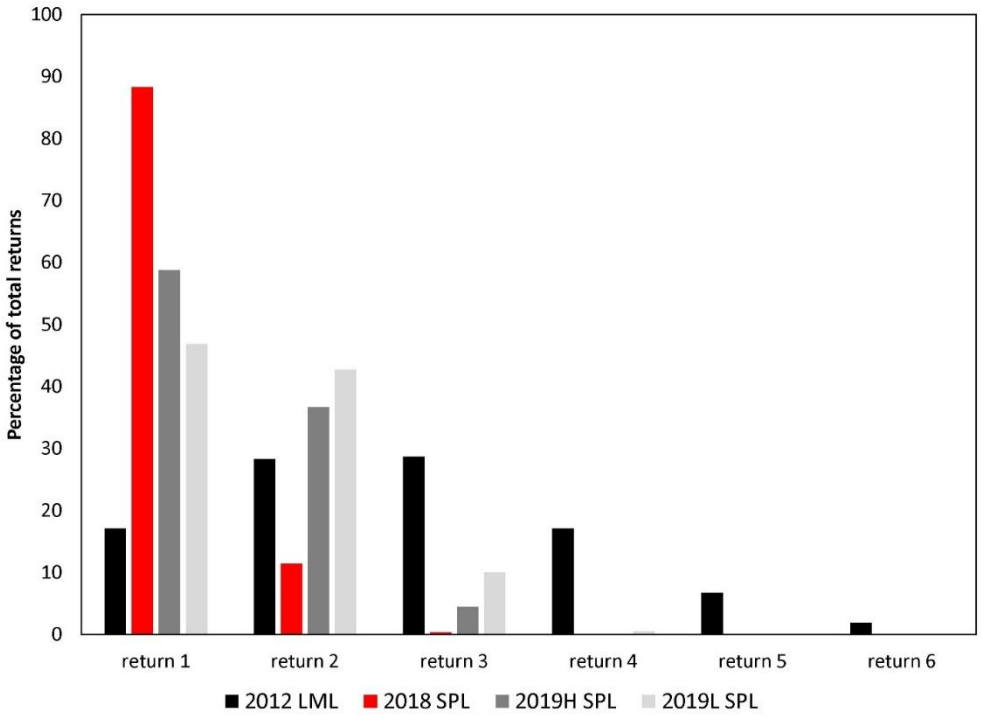

Figure 12. Distribution of returns for each lidar acquisition, by return number.

5.2 Real-Time Kinematic (RTK) survey data

Horizontal and vertical control data were acquired for a total of 327 checkpoints using a Sokkia FX 105 total station on June 17, 2019. The control network consisted of three published control locations maintained by the Ontario Ministry of Natural Resources and Forestry Control Survey Information Exchange (COSINE) database, as well as eight additional control points, established as inter-visible pairs distributed within the project study area. Three dual frequency Sokkia GSR2700 ISX receivers were stationed on the COSINE control monument locations and a fourth was used as a roving unit to provide coordinates for six of the new project control points. Due to the long baselines between COSINE monuments, the project control points were occupied for three hours with the roving unit. For the remaining two control points, a two-receiver method was used based on the calculated horizontal position of the Deep Bench Mark published control in Chalk River.

RTK checkpoints represented a range of vegetated and non-vegetated conditions. A total of 85 checkpoints were acquired in non-vegetated conditions (i.e. asphalt, gravel) and 242 checkpoints in vegetated conditions, that were characterized by the dominant tree species and or vegetation present (i.e. black spruce, coniferous plantation, intolerant hardwood, jack pine, low vegetation, mixedwood, red and white pine, and tolerant hardwood; Figure 13). Checkpoints were acquired along 50 or 100 m transects within each cover type group, with checkpoints located at 10 m intervals along the transects.

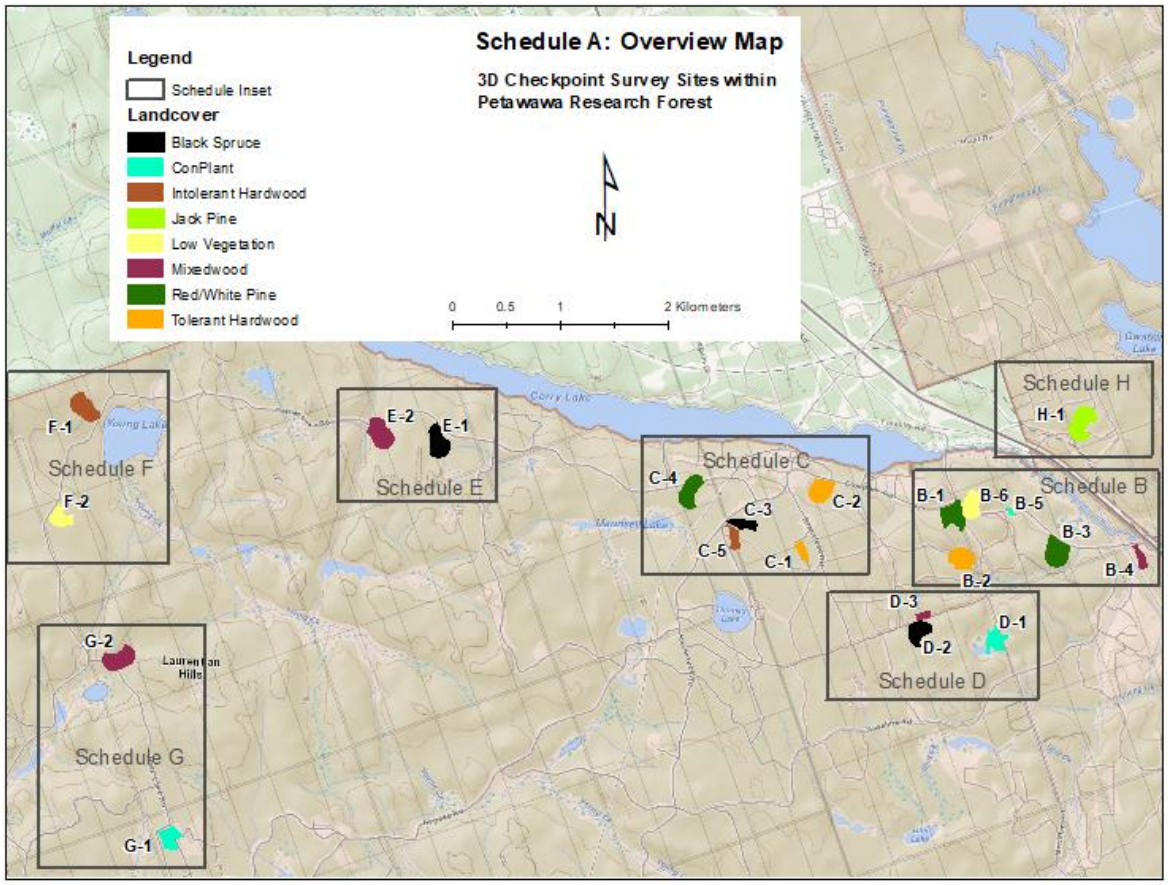

Figure 13. Location of RTK survey locations within the PRF.

5.3 Lidar Penetration Index (LPI)

To assess the impact of varying canopy cover conditions on the penetration of lidar pulses, and in turn, the accuracy of the DTM, the Lidar Penetration Index (LPI) was calculated for each of the four lidar acquisitions. This index provides a measure of the percentage of total returns that are found within ± 15 cm of the ground surface, regardless of whether those returns are classified as ground or not. The LPI provides a consistent measure of how the terrain surface is being represented, irrespective of whether the acquisition is leaf-on or leaf-off. From these continuous LPI values, four LPI classes were generated: LPI < 10%, LPI ≥ 10% and LPI < 20%, LPI ≥ 20% and LPI < 30%, and LPI ≥ 30%. We then calculated the 95th percentile of the difference between the RTK elevation and the lidar elevation for the RTK check points within each of these LPI classes. Theoretically, we would expect that the RTK survey results would be more accurate when the value of the LPI is greater; in other words, we would expect that the 95th percentile of the differences between the RTK survey elevations and the lidar elevations would decrease as the LPI increases.

5.4 Accuracy measures and qualitative assessment

Vertical accuracy statistics were generated following the Ontario Elevation Accuracy Guidelines Version 1.0 (OMNR, 2016), which is intended to be consistent with the American Society for Photogrammetry and Remote Sensing (ASPRS) Positional Accuracy Standards for Digital Geospatial Data (ASPRS, 2014). Horizontal accuracy and relative (swath-to-swath accuracy) were not calculated as part of this

analysis. The target accuracy for the SPL acquisition was lidar Quality Level 2 or 10 cm Vertical Accuracy Class (ASPRS, 2014), analogous to the quality level of the 3D Elevation Program (3DEP) of the USGS. More details on the collection and interpretation of the RTK survey data are provided in the detailed report prepared by the Ontario Ministry of Natural Resources and Forestry's Provincial Mapping Unit, included in Appendix H (Provincial Mapping Unit, 2019).

For the analysis conducted herein, the elevation of each RTK check point is compared to the corresponding elevation value from each of the lidar datasets. The difference between the check point elevation and the lidar elevation is the vertical error for that checkpoint. Errors for all checkpoints are then summarized via various statistical measures to report overall error, as well as error by different cover types. In the Ontario guidelines, there are two methods used to determine the vertical accuracy of a given elevation dataset: non-vegetated vertical accuracy (NVA) and vegetated vertical accuracy (VVA).

NVA is assessed using the RMSE of the elevation differences between the checkpoints and the lidar data; however, the RMSE-based NVA calculation is a parametric test, meaning that it is expected that the distribution of vertical errors exhibits a normal distribution. To check for a normal distribution, the Mean Vertical Error (MVE) is calculated as the arithmetic average of the check point errors (Eq. 7). If the MVE does not equal 0, then the normal distribution assumption does not apply to the RMSE calculation, and the use of the RMSE as an accuracy measure is not supported. Moreover, the ASPRS recommends that if MVE exceeds 25% of the target accuracy (which was10 cm for this project), Non-zero values for MVE can be caused by gross errors or blunders, systematic errors associated with the process of the check point data or the lidar data itself, and the presence of vegetation at control points. However it must be noted that, errors for lidar data are rarely normally distributed (Höhle and Höhle, 2009). In the event that the RMSE is deemed to not be an appropriate accuracy measure, Ontario's guidelines recommend that the VVA approach be used as an alternative.

MVE is calculated as follows:

$$MVE = \frac{1}{N}\sum_{i=1}^{n}(z_i - z_i') \qquad \text{(Eq. 8)}$$

Where: i is the index of points,

N is the number of points,

z_i are the elevations measured from the lidar data,

z_i' are the elevations from the checkpoint data.

NVA is typically assessed using a 95% confidence level of the RMSE of the check point errors and is calculated as follows:

$$NVA_{95\%} = 1.96 \times RMSE_Z \qquad \text{(Eq. 9)}$$

where $RMSE_Z = \sqrt{\frac{1}{N}\sum_{i=1}^{n}(z_i - z_i')^2}$

i, N , z_i, z_i' are as for Eq. 7

In contrast to NVA, the assessment of vertical accuracy for vegetated checkpoints does not make an assumption of a normal distribution for the elevation differences between the checkpoints and the lidar. VVA is computed as the 95th percentile of the absolute value of vertical errors in all vegetated land cover categories combined. VVA is calculated as follows:

$$VVA\ 95 = (1 - k) \times d_j + k \times d_{j+1} \quad \text{(Eq. 10)}$$

where $d_i = |z_i' - z_i|$

for i = 1 to N, reorderd from smallest to largest,

r = 1 + ((N-1) * 0.95)

(the 95th percentile rank), and

j = *integer (r)*,

$k = r - j$,

i, N , z_i, z_i' are as for Eq. 7

According to the ASPRS guidelines, a lidar dataset that is deemed to meet a 10-cm Vertical Accuracy Class (the target accuracy class for this project's assessment) would have an RMSE for non-vegetated checkpoints that was < 10 cm and an NVA that was < 19.6 cm (ASPRS, 2014). The VVA must be < 29.4 cm for the lidar data to meet the 10-cm Vertical Accuracy Class standard.

A point based assessment using the RTK data provides one approach to quantify the accuracy of the lidar data, however we were also interested in how the characteristics of the lidar impacted the derived digital terrain model (DTM). To this end, the Provincial Mapping Unit undertook a qualitative assessment of the DTMs to determine any issues in terrain characterization stemming from differences in the density and distribution of ground returns. The qualitative assessment was undertaken in seven selected sub-areas of the PRF, as detailed in the report included in Appendix H. For each area and each lidar dataset, a grey scale hillshade of the DTM was generated with an light source azimuth angle of 320 degrees, and a z-factor of 5.

5.5 Results

5.5.1 RTK survey results

The MVE calculations indicate that the assumptions supporting the use of $RMSE_Z$ to assess absolute accuracy are not valid (i.e. the mean of the vertical error values were not zero; Table 26). In addition, all four lidar datasets have MVE values in excess of the limit recommended by the ASPRS, that being 25% of specified $RMSE_Z$ for the project or 2.5 cm (Table 27).

Table 27. Mean Vertical Error (MVE) and $RMSE_z$ for non-vegetated checkpoints.

Non-vegetated check points (N = 79 / 85)	**2012 LML**	**2018 SPL**	**2019H SPL**	**2019L SPL**
MVE (cm)	-11 / -11.2	- 6.0 / -6.1	-8.6	-8.3
RMSEz (cm)	12 / 12.1	7.4 / 7.4	9.5	9.2

In the absence of gross errors or blunders in the RTK data that may influence the MVE, the Ontario guidelines recommend using the non-parametric test for NVA, as is used for the VVA Calculation (OMNR, 2016). The non-parametric test uses the 95th percentile to assess accuracy (as per the VVA calculation in Eq. 9). For the 10 cm Vertical Accuracy Class, the parametric NVA cut-off value for the 95th percentile is 19.6 cm, whereas the non-parametric VVA cut-off value for the 95th percentile is 29.4 cm. As indicated in Table 28, the 95th percentiles for all four lidar datasets were within the specified limits for the 10 cm Vertical Accuracy Class for both non-vegetated and vegetated check points. Accuracies varied by cover type, with low vegetation, mixedwood forests, and black spruce stands having the largest errors for the 2018 SPL data. Based on the results reported in Table 28, it was concluded that the four lidar datasets tested met the accuracy standards for Ontario Digital Geospatial Data for a 10 cm Vertical Accuracy Class. Actual Non-vegetated Vertical Accuracy (NVA) was found to be +/- 19.6 cm at the 95% percentile. Actual Vegetated Vertical Accuracy (VVA) was found to be +/- 29.4 cm at the 95% percentile.

Table 28. 95th percentile of errors between RTK check points and lidar data elevations, by cover type.

Category	**95th Percentile (sample size)***	**2012 LML**	**2018 SPL**	**2019H SPL**	**2019L SPL**
Non-Vegetated	**NVA (79/85)**	17.4 / 17.3	14.2 / 13.8	16.3	14.1
Vegetated	**VVA (220/235)**	18.5 / 18.7	23.4 / 24.0	16.9	14.5
Road	**Gravel Road (47/53)**	18.3 / 18.7	10.8 / 11.0	18.6	14.8
	Asphalt Road (32)	16.2	15.1	12.4	13.7
Conifer	**Black Spruce (37)**	18.8	29.5	15.0	13.8
	Jack Pine (15)	7.7	7.4	15.1	7.0
	Conifer Plantation (21/36)	20.1 / 20.1	9.8 / 15.8	14.5	11.9
	Red / White Pine (27)	17.4	16.2	20.8	13.6
Hardwood	**Intolerant Hardwood (37)**	19.7	17.6	15.6	14.9
	Tolerant Hardwood (35)	18.1	15.6	14.0	13.6
Other	**Mixedwood (34)**	16.3	26.5	19.3	17.6
	Low Vegetation (14)	13.0	24.7	5.0	8.7

Note that some of the RTK checkpoints did not fall within the boundaries of the 2019 SPL collection, therefore statistics are shown for both the intersecting footprint sample size (i.e. the smaller N) and the entire dataset (i.e. the larger N) where applicable.

5.5.2 Assessment under different canopy cover densities

The number of RTK checkpoints in each of the LPI classes varied (Figure 14), with the leaf-on acquisitions (2012 LML and 2018 SPL) having markedly more RTK check points with < 10% of returns within ± 15 cm of the ground surface. Conversely, the leaf-off acquisitions (2019H SPL and 2019L SPL) had more checkpoints with ≥ 30% of returns within ± 15 cm of the ground surface. Of note, the SPL data acquired at the higher altitude in 2019 (~3800 m) had more near-ground returns than the lower altitude acquisition (~1800 m). The median LPI for each of the lidar dataset, by checkpoint cover class, is shown in Figure 15; all 3 SPL datasets have a greater LPI for the non-vegetated classes (asphalt and gravel). Conversely, the LPI for the 2018 SPL is lower than the 2012 LML for all vegetated categories, with the exception of check points that were dominated by jack pine and low vegetation. Also of note, the median LPI for the 2019 SPL leaf-off data acquired at the higher altitude (3800 m) is greater than the median LPI for the 2019 SPL leaf-off data acquired at the lower altitude (2000 m). This contrasts with the expectation that a lower acquisition altitude would translate into a greater percentage of returns from near the ground surface.

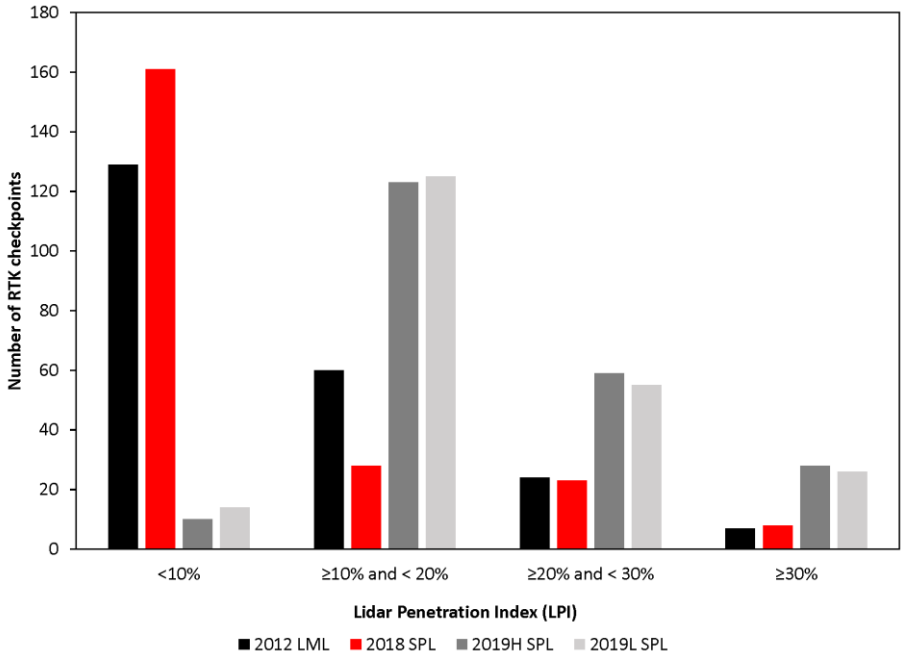

Figure 14. Distribution of RTK checkpoints within each of the LPI classes.

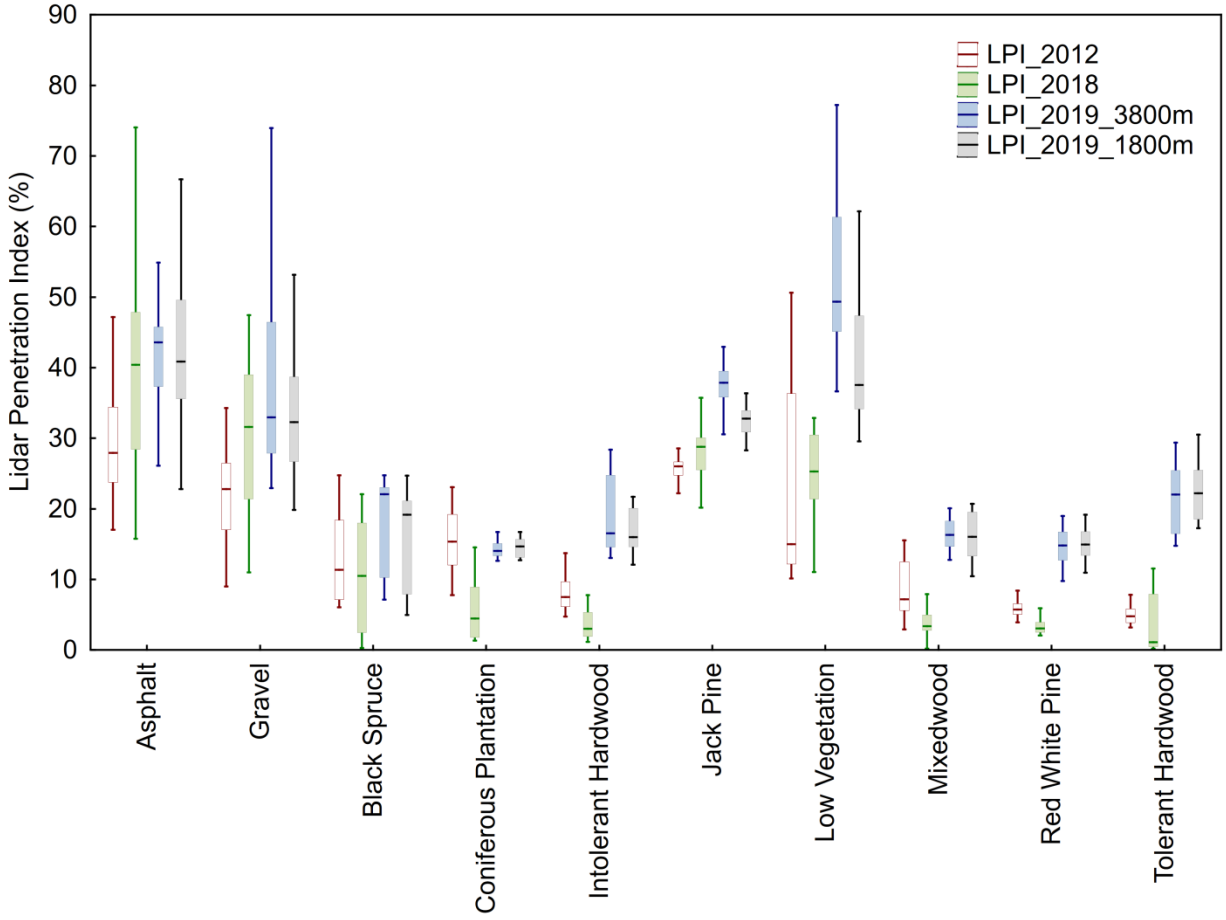

Figure 15. The median LPI value for each lidar dataset, by cover type. Boxes represent 25%-75% and whiskers indicate non-outlier range.

In terms of accuracy, the 95th percentile of differences between the RTK check points and lidar elevations indicates no particular relationship between the LPI (i.e. degree of penetration of the lidar pulses) and the accuracy of the captured elevation (Figure 16), except for the 2012 LML lidar, whereby the 95th percentile decreased with an increasing percentage of near-ground returns.

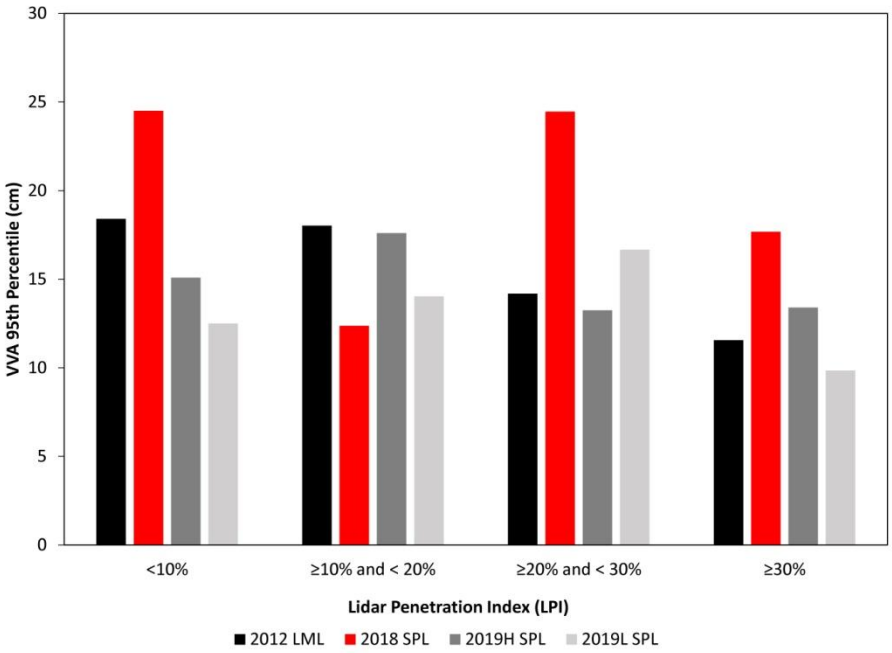

Figure 16. 95th percentile of difference between RTK Vegetation Vertical Accuracy (VVA), by Lidar Penetration Index (LPI) class.

5.5.3 Qualitative assessment of derived DTM

The different characteristics of the 2018 SPL data (i.e. more first returns, fewer ground returns) translate into artifacts in the derived digital terrain model (DTM) as well. Overall, the qualitative assessment concluded that all of the lidar DTMs were of good quality, with some minor issues, which included anomalies such as divots, spikes, and tinning artifacts. Artifacts in the triangular irregular network (TIN) used to generate the DTM are caused by a lower density of ground returns, and the greater the spacing the more interpolation and the larger the TIN facets. Similar issues were identified by CCMEO in their preliminary assessment of the 2018 SPL data for the PRF (CCMEO, 2019). Not surprisingly, the leaf-off SPL acquisitions produced better quality DTMs (Figure 17); however any difference in quality between the leaf-off SPL acquired at 3800 m versus 2000 m was marginal. Larger TIN facets are particularly evident in the 2018 SPL data at this particular site (Figure 18), which is located within tolerant hardwood and mixedwood forest types. These tinning artefacts are also influenced the complexity of the terrain, with areas of steeper slopes under denser cover being particularly problematic.

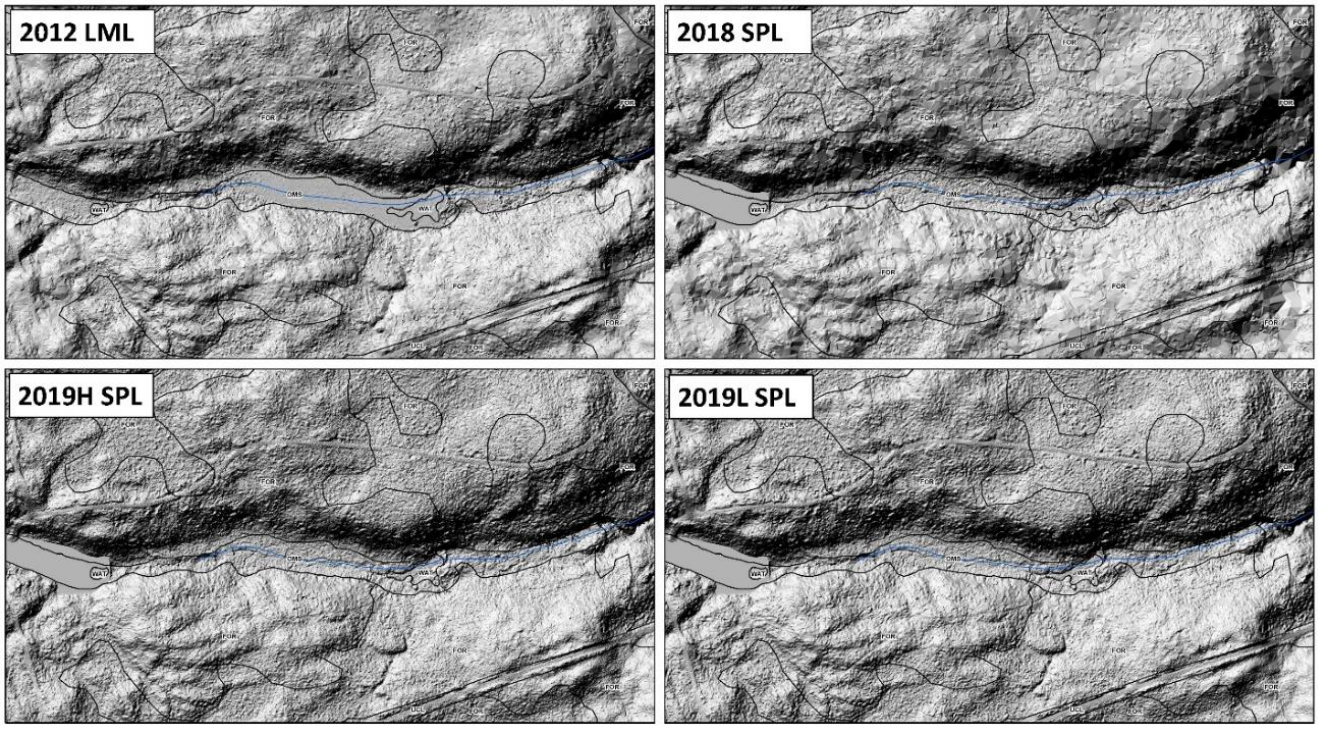

Figure 17. Hillshade of digital terrain model (DTM) generated for each of the four lidar acquisitions. The 2012 linear mode lidar (LML) and the 2018 single photon lidar (SPL) were acquired in leaf-on conditions. The 2019 SPL data were acquired in leaf-off conditions from an altitude of 3800 m (2019H SPL) and 2000 m (2019L SPL).

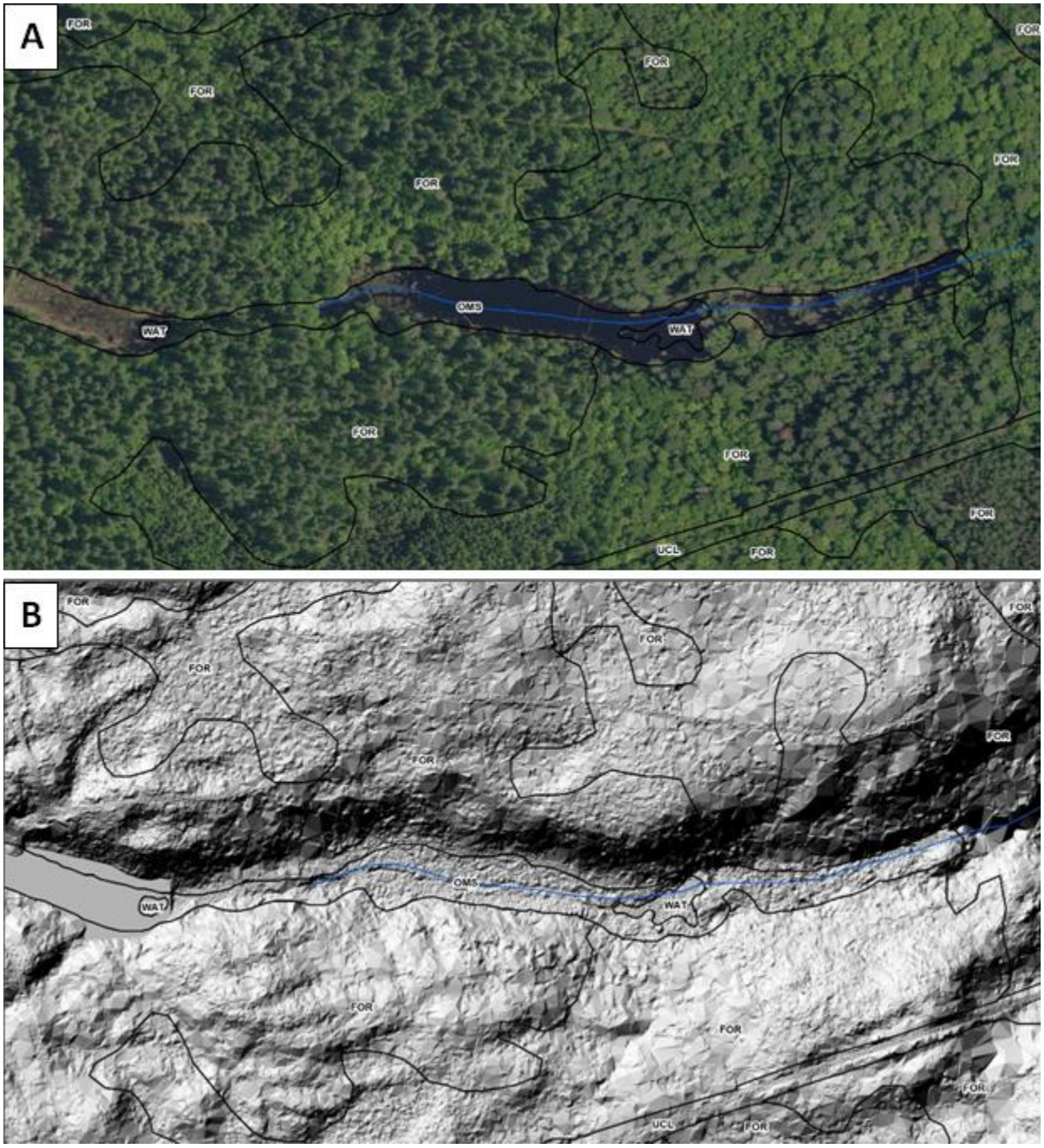

Figure 18. An area with dense tolerant hardwood and mixedwood forest types (A). Large TIN facets are visible in the SPL 2018 hillshade (B).

5.6 Summary

To quantify the comparative performance of SPL in characterizing terrain under varying forest types and canopy densities, RTK survey data was used to investigate the vertical accuracy of four different lidar acquisitions: 1 leaf-on SPL (2018); 2 leaf-off SPL (2019 at 3800 m and 2000 m); and 1 leaf-on LML

(2012). We explored and quantified the characteristics of the different datasets and examined how those characteristics impacted the derived DTM. Overall, all four lidar lidar datasets that were tested met the vertical accuracy standards for Ontario Digital Geospatial Data for a 10 cm Vertical Accuracy Class. The leaf-off SPL data acquired at an altitude of 2000 m was generally the most accurate for both non-vegetated and vegetated cover types. For the majority of cover types, the leaf-on SPL data acquired in 2018 had greater accuracy than the 2012 LML data, with the exception of the black spruce, mixedwood, and low vegetation categories.

6. Objective 3: Identify and explore incremental advantages or innovations for the eFRI program resulting from unique SPL data characteristics

The third and final objective of this project was to determine if the characteristics of the SPL data, particularly the increased point density, provided any advantages over LML data for the eFRI program. Two specific applications were investigated: tree species identification and detection and characterization of small trees underneath the main canopy.

6.1 Individual tree detection and species classification

In this analysis, species identification at the individual tree crown (ITC) level was investigated for 2012 LML and 2018 SPL data (Figure 19), representing a subset of the work of Prieur et al. (In review).

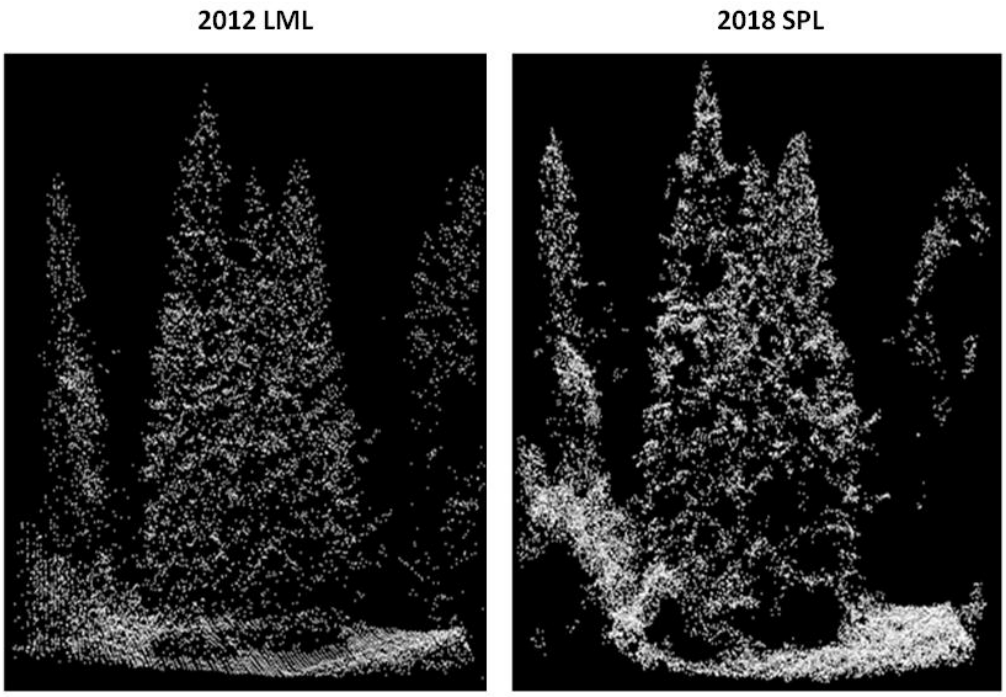

Figure 19. Comparison of the 2012 linear-mode lidar (LML) and 2018 single-photon lidar (SPL).

Figure 20 provides an overview of the workflow used to process the lidar data, generate the classification and compare the species classification outcomes. An important precursor to species mapping at the individual tree level is the identification and accurate delineation of individual tree crowns. The 2012 ALS data was used for individual tree crown ITC delineation using a software package developed at Université du Québec à Montréal (SEGMA 0.3). A 50 cm canopy height model (CHM) was extracted from the classified 2012 LML point cloud. SEGMA finds the local maximum (treetop) within a certain neighbourhood then uses an inverse watershed algorithm and region-growing approach to define the crown. These individual crowns (as well as calculated attributes such as diameter, area, height, etcetera) are saved as polygons in a shapefile. These polygons, representing individual tree crowns, are then identified in the field (using a GPS and a tablet) to accurately locate and record the crown location and

identify the species. These field data are then used as training data for the random forest classifier. Of note, it is known that there will be errors of omission and commission in the delineation of the individual tree crowns, as well as in the field identification of crowns, especially in dense hardwood forests. Delineation challenges, combined with challenges in obtaining accurate GPS locations under dense hardwood canopies, further complicate accurate and automated species identification approaches. In order to mitigate these effects, only the 2012 LML was used for segmentation, and the same crowns were carried forward for classification of the 2018 SPL data. In this way, the same features (crowns) are used throughout the analysis, and allow for classification accuracy to be assessed independent of delineation accuracy.

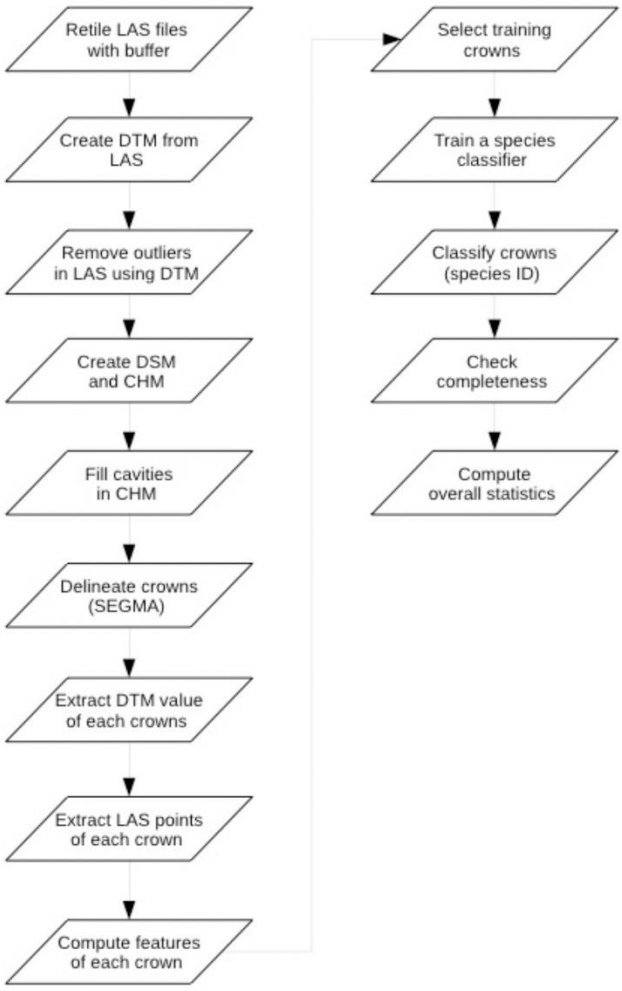

Figure 20. Overview of approach used in automated species mapping.

The number of tree crowns available for training each of the different levels of species groupings, ranging from the very general level of forest type (i.e. hardwood and softwood), to more detailed groupings of individual species, are summarized in Table 29. A spatial join is used to link these crown polygons to the lidar point cloud to extract individual lidar returns associated with each crown. A subset of the lidar point cloud features, both structural (based on X, Y, Z information only) and spectral (intensity) were calculated for each crown, as described in Budei et al. (2018). Feature selection was used to develop

parsimonious classification models. First, correlated features (i.e. $r \geq 0.9$) were identified and the feature with the highest random forest mean decrease in accuracy (MDA) was removed in order to keep the more robust feature of the pair. Second, the R package VSURF (Variable Selection Using Random Forest; Genuer et al. 2015) was used to select the desired number of features. Classifications using all features, a subset of 25 features, and a subset of 15 features were tested.

Table 29. Sample size (number of individual tree crowns) available for training each of the different groupings (i.e. forest type, functional group, 12 species groups, and 4 species groups).

Forest Type	**2012 LML**	**2018 SPL**
Hardwood	683	596
Softwood	673	546
Functional Group	**2012 LML**	**2018 SPL**
Hardwood	308	262
Intolerant hardwood	375	334
Other softwood	157	114
Pine	345	302
Spruce	171	130
12 Species	**2012 LML**	**2018 SPL**
Ash (Black/White)	81	66
Basswood	56	48
American Beech	67	59
Birch (White/Yellow)	89	77
Eastern White Cedar	44	36
Balsam Fir	69	43
Eastern Larch	44	35
Maple (Red/Sugar)	185	155
Red Oak	70	52
Pine (Red/White)	345	302
Trembling Aspen	135	139
Spruce (Black/White)	171	130
4 Species	**2012 LML**	**2018 SPL**
Maple	185	155
Pine	345	302
Poplar	135	139
Spruce	171	130

Table 30 shows random forest Out-Of-Bag (OOB) accuracy for the average of 25 independent classification runs (using the features selected as described above) for the various species configurations shown in Table 29. The *randomForest* package in *R* (Liaw and Weiner, was used to perform the classifications. Down sampling of minority classes was used to balance the class counts for the random forest models, as unbalanced sample counts can lead to biased results towards the majority class. Overall, a combination of 3D and intensity features resulted in the highest accuracy for both the 2012 LML and 2018 SPL data for all levels of species groupings. In general, accuracy results are comparable for both sensors, with 2018 SPL results lower than those of the 2012 LML, particularly in the case where only intensity values are used in the classification. Hardwood species identification at the individual tree crown level remains challenging as shown by the results in the 12 species case, whereby the best overall accuracy was ~51%. Improved results were obtained for both 2012 LML and 2018 SPL data for the higher level classifications of functional groups and forest types. While it is possible that the 2018 SPL

results are lower in part because the individual tree crowns from 2012 were carried forward for the 2018 classifications, thereby resulting in a temporal decorrelation between the structural and spectral features used for the classification and the morphology of the crowns themselves, results for a multispectral lidar acquisition in 2016 are similar to those of 2012 LML (results not shown).

Table 30. OOB accuracy for species classifications, averaged over 25 independent classification iterations. Results are shown for different feature combinations: structural metrics only (3D only), intensity metrics only (I only), and both spectral and intensity metrics combined (3D + I).

	2012 LML 3D ONLY	2012 LML I ONLY	2012 LML 3D + I		SPL 2018 3D ONLY	SPL 2018 I ONLY	SPL 2018 3D + I
	Forest Type						
All features (N)	84.0 (24)	76.2 (8)	86.4 (31)		80.1 (17)	59.1 (6)	82.9 (23)
25 features			86.1				
15 features	84.1		86.3		80.1		82.7
	Functional Groups						
All features (N)	55.7 (24)	52.5 (8)	68.9 (31)		50.4 (17)	43.3 (6)	63.6 (23)
25 features			67.4				
15 features	55.3		66.2		50.0		64.4
	12 Species						
All features (N)	38.9 (24)	33.2 (8)	50.7 (31)		37.8 (17)	25.8 (6)	44.5 (23)
25 features			51.3				
15 features	38.3		48.7		38.4		44.8
	4 Species						
All features (N)	65.4 (28)	64.7 (8)	75.1 (35)		64.5 (19)	50.1 (6)	68.3 (24)
25 features	65.5		74.3				
15 features	63.6		74.2		63.5		68.1

These results suggest that the nature and/or distribution of SPL returns may influence the accuracy of the classification approach presented. As shown in Table 30, after removing correlated features, 31–35 features were remaining for the ALS 2012 dataset, whereas only 23–24 features remain for the SPL 2018 dataset, indicating that the features in the SPL 2018 case are more correlated with each other. This results in fewer features available for use in the classifier, as well as in lower accuracy for the SPL 2018 data. This effect increases when features used in classification are further separated into structural and intensity metrics. The average difference in accuracy between classifications using structure-only features and intensity-only feature classification is 4% for the 2012 LML data, compared to 14% for the SPL 2018 data.

Lidar intensity, even in airborne linear systems, is a black-box value calculated by each instrument manufacturer's proprietary methods, confounding meaningful interpretations of these values. Currently, even less is known about the intensity values associated with the SPL data (e.g., how they are calculated, what they represent). Given this, it is difficult to provide a meaningful interpretation of the species classification results using the intensity features exclusively. Other differences were observed in the distribution of 1st and 2nd returns between the 2012 LML and 2018 SPL data, with SPL having a markedly greater proportion of first returns as compared to the 2012 LML (Table 26; Figure 21). One of the most

important features in the 15 feature classification scenarios (Table 30) for the 2012 LML data is a feature that characterizes the mean height difference between the 1st and 2nd returns. No analogous feature is available for the 2018 SPL data.

The results presented here indicate that for the ITC species identification methodology applied herein, certain characteristics (namely intensity and return distribution) of the SPL point cloud may result in lower species classification accuracies when compared to linear mode lidar.

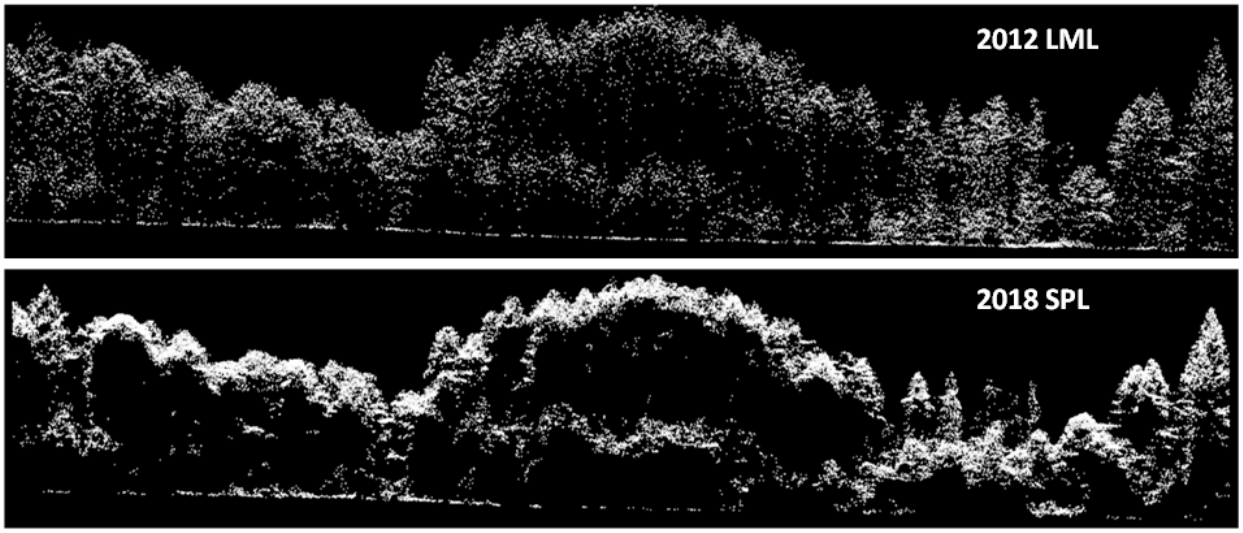

Figure 21. Profiles of the three lidar acquisitions in the Petawawa Research Forest.

6.2 Small tree detection and characterization

6.2.1 Small tree plot data

A total of eight small tree plots were established in four of the forest types within PRF (Table 31). These plots had a radius of 3.99 m and were designed to measure all commercial species with a DBH ≥ 2.5cm and < 9.1 cm (Appendix C). A random height sample was conducted for a subset of 5 trees in each small tree plot. The objective of establishing these small tree plots was to determine the capacity of SPL data to detect and characterize small trees in different forest types and overstorey conditions.

Table 31. Summary of small tree plot data.

Forest type	Plot	Number of small trees	DBH (cm)		Height (m)		Small tree species
			Mean	Std. Dev.	Mean	Std.Dev.	
Natural pine	PRF185	11	4.35	2.07	8.56	5.92	Red maple, balsam fir, striped maple
Plantation	PRF010	12	4.61	2.44	13.05	2.75	White birch, red maple, trembling aspen, alder, larch
	PRF209	3	1.73	0.25	3.00	1.05	Balsam fir, red maple
Natural hardwood	PRF101	8	2.16	0.68	4.36	1.25	Ironwood, beech, yellow birch, white pine
	PRF040	2	2.40	1.50	2.30	0.00	Sugar maple, white spruce
	PRF161	10	4.67	1.68	7.9	3.39	Yellow birch, red maple, balsam fir
Mixedwood	PRF176	5	4.41	0.68	5.65	0.7	Hemlock, beech
	PRF124	15	4.10	2.71	8.3	4.24	Red maple

6.2.2 Natural pine stands

PRF185 is dominated by a white pine overstorey of large mature trees with relatively open canopy conditions (Figure 22). In this natural pine stand, separation of the overstorey and understorey layer was clearly evident when visually examining the SPL data (Figure 22B). Of note, although the top of the secondary layer is well captured, there are insufficient returns between the top of the secondary layer (~9m) and the ground to enable characterization of the small trees in this secondary layer with any detail, or to compare the number of small trees measured in the ground plots. Only 39.68% of 1 m cells within PRF185 had ground returns (Table 32). A total of 11 trees were recorded in the small tree subplot PRF 185, with a mean DBH of 4.35 cm (σ = 2.07 cm) and a mean height of 8.56 m (σ = 5.92 m).

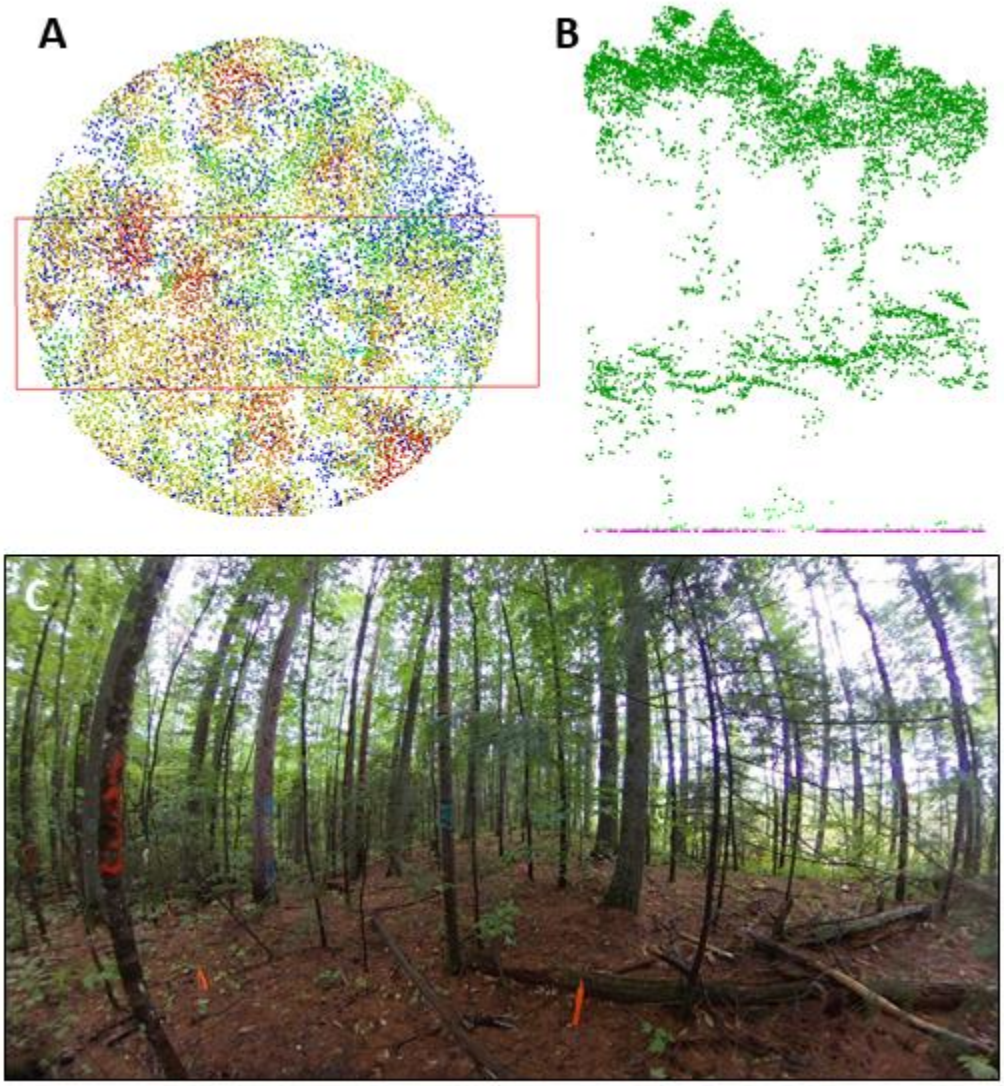

Figure 22. The full PRF185 plot (A; 14.1 m radius; blue = lower canopy heights, red = higher canopy heights) with a 10 m wide profile (red box and B) with SPL returns classified as ground (pink) and low (light green) and high (dark green) vegetation. Photo taken at plot centre (C).

Table 32. Characterization of penetration capacity of SPL data in plots sampled for small trees.

Calibration Plot	COUNT of 1 m cells in plot with returns (all)	COUNT of 1 m cells in plot with ground returns	% of 1 m cells in the plot with ground returns
PRF185	625	248	39.68
PRF010	618	530	85.76
PRF209	618	370	59.87
PRF101	622	149	23.95
PRF040	624	314	50.32
PRF161	620	113	18.23
PRF176	617	65	10.53
PRF124	619	144	23.26

6.2.3 Plantations

PRF010 is located within a red pine plantation and had a top height of 16.5 m and a stocking of 2656 trees per hectare. A total of 12 small trees (primarily deciduous) were measured on the subplot, with an average DBH of 4.61 cm and an average height of 13.05 m. Small trees in this plot were therefore proximal to the upper canopy layer. The foliage of these small trees likely contributed to the intermediary returns evident in the SPL point cloud (Figure 23B). PRF010 is characterized by a high density of returns in the upper canopy; however the red pines have relatively narrow crowns so the canopy itself is relatively open. In this plot, the sparse distribution of SPL returns through the canopy is indicative of the absence of a well organized or dense secondary layer or understorey. As a result, and in contrast to the natural pine stand of PRF185, 85.76% of 1 m grid cells within PRF010 had ground returns.

PRF209 is located in a spruce plantation with a top height of 17.8 m and a stocking of 1376 trees per ha (Figure 24). This plot had more understorey vegetation than its red pine counterpart (PRF010), but no secondary layer. Only 3 small trees were measured in PRF209 subplot, which are not captured in the SPL data and the canopy in this plot was fairly open, with 59.87% of 1 m grid cells in the plot having ground returns.

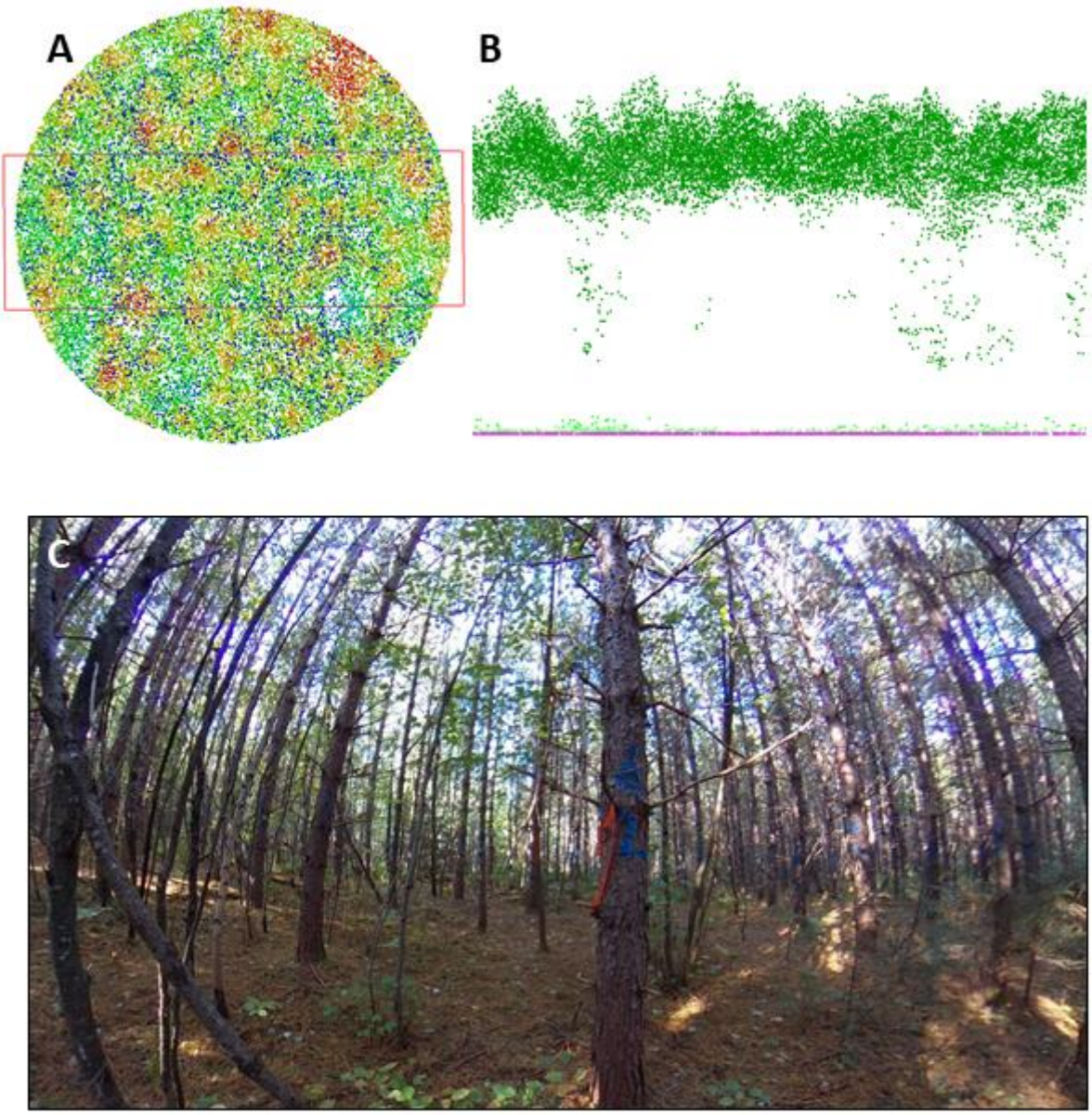

Figure 23. The full PRF010 plot (A; 14.1 m radius; blue = lower canopy heights, red = higher canopy heights) with a 10 m wide profile (red box and B) with SPL returns classified as ground (pink) and low (light green) and high (dark green) vegetation. Photo taken at plot centre (C).

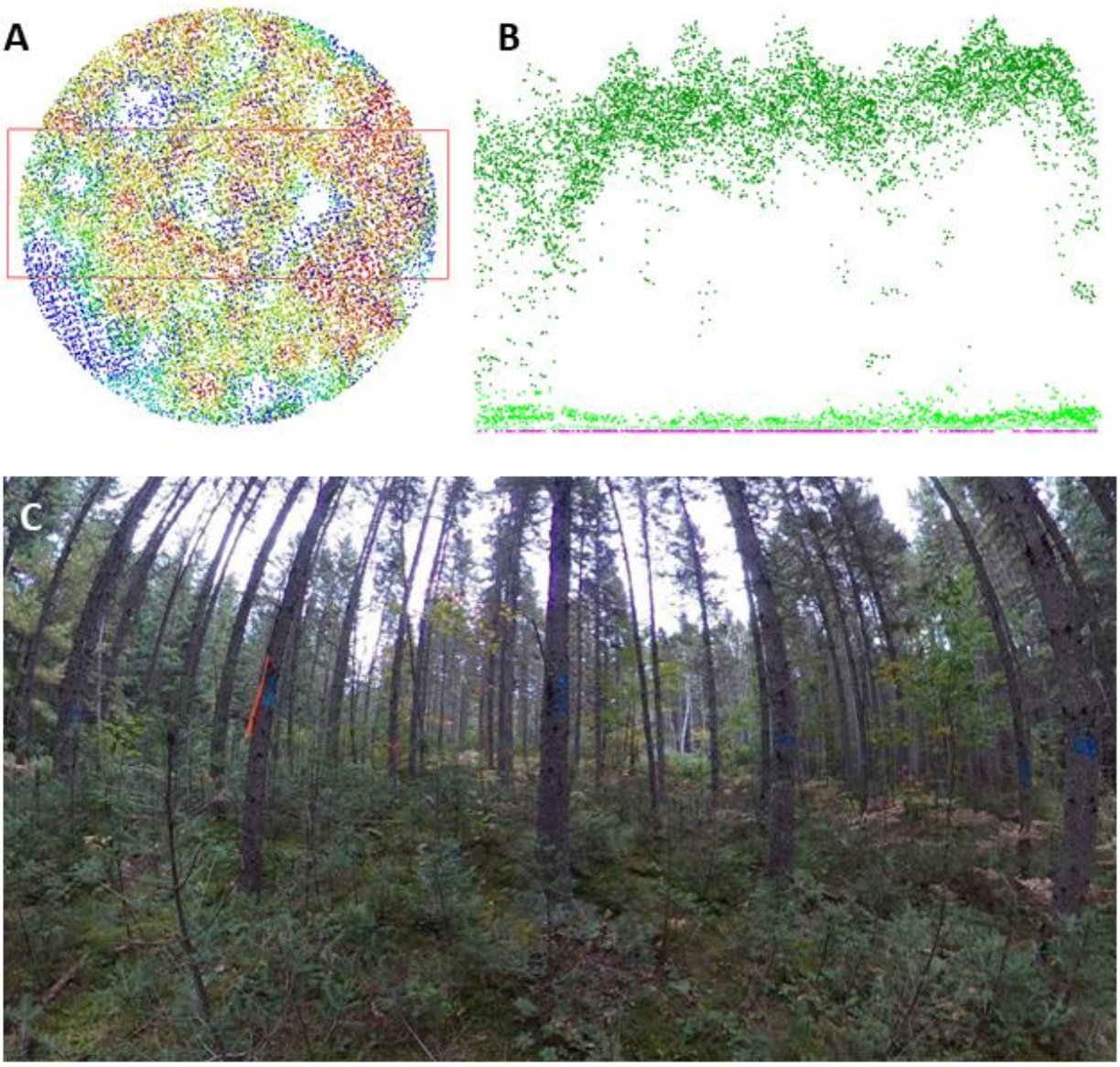

Figure 24. The full PRF209 plot (A; 14.1 m radius; blue = lower canopy heights, red = higher canopy heights) with a 10 m wide profile (red box and B) with SPL returns classified as ground (pink) and low (light green) and high (dark green) vegetation. Photo taken at plot centre (C).

6.2.4 Natural hardwood stands

Small tree subplots were established in three natural hardwood stands. These stands are characterized by more open spaces in the canopy between mature hardwood trees, potentially allowing for increased penetration of the SPL returns into the canopy. PRF101and PRF040 (Figure 25) are very similar. PRF101 had 8 small trees with an average DBH of 2.16 cm and an average height of 4.36 m. Top height was 23.9 m in PRF101 and 20.8 m in PRF040. Penetration of SPL to the ground was different between these two plots however. PRF101 had 23.95% of 1 m grid cells with ground returns, whereas PRF040 had 50.32%

of 1 m grid cells with ground returns. PRF161 had a similar top height (21.02 m) to the other natural hardwood stand, but a higher stocking (2440 trees per ha). This represented a younger, more even-aged cohort with a more uniform, denser canopy. A total of 10 small trees were measured in this plot with an average DBH of 4.67 m and an average height of 7.9 m. As a result of the dense overstorey and general lack of gapiness between crowns (when compared to PRF101 and PRF040), only 18.23% of 1 m grid cells in this plot had ground returns.

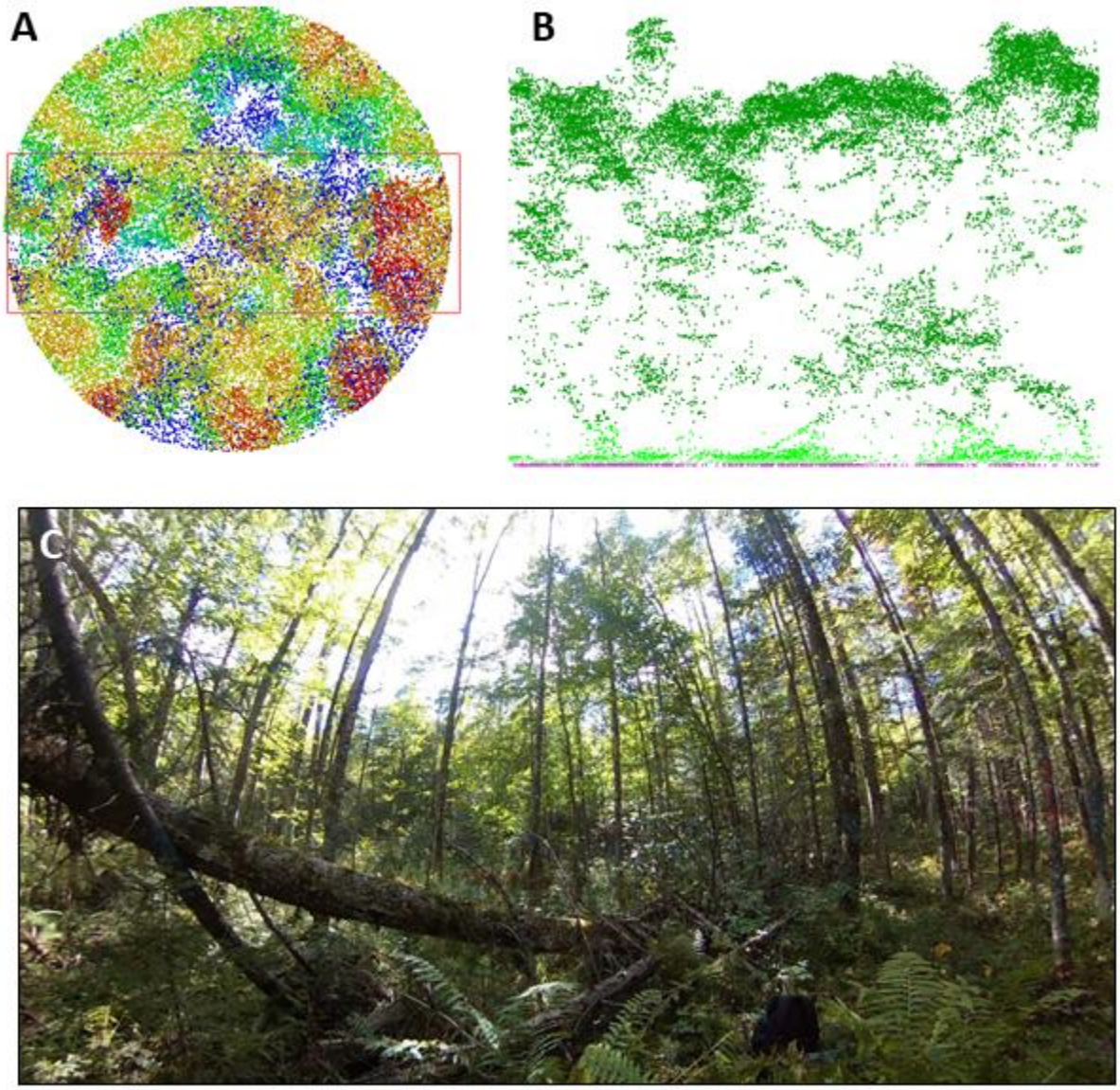

Figure 25. The full PRF040 plot (A; 14.1 m radius; blue = lower canopy heights, red = higher canopy heights) with a 10 m wide profile (red box and B) with SPL returns classified as ground (pink) and low (light green) and high (dark green) vegetation. Photo taken at plot centre (C).

6.2.5 Mixedwood stands

For mixedwood stands canopy conditions are complex. PRF124 is dominated by tall spruces, with many small red leaf maple trees in the second layer, with an average height of 8.3 m (Figure 26). The canopy is fairly open, allowing for a vertical distribution of SPL pulses through the canopy (Figure 26B). In contrast, the canopy in PRF 176 (not shown) is dominated by eastern hemlock, beech, and maple, with fewer small trees below the main canopy.

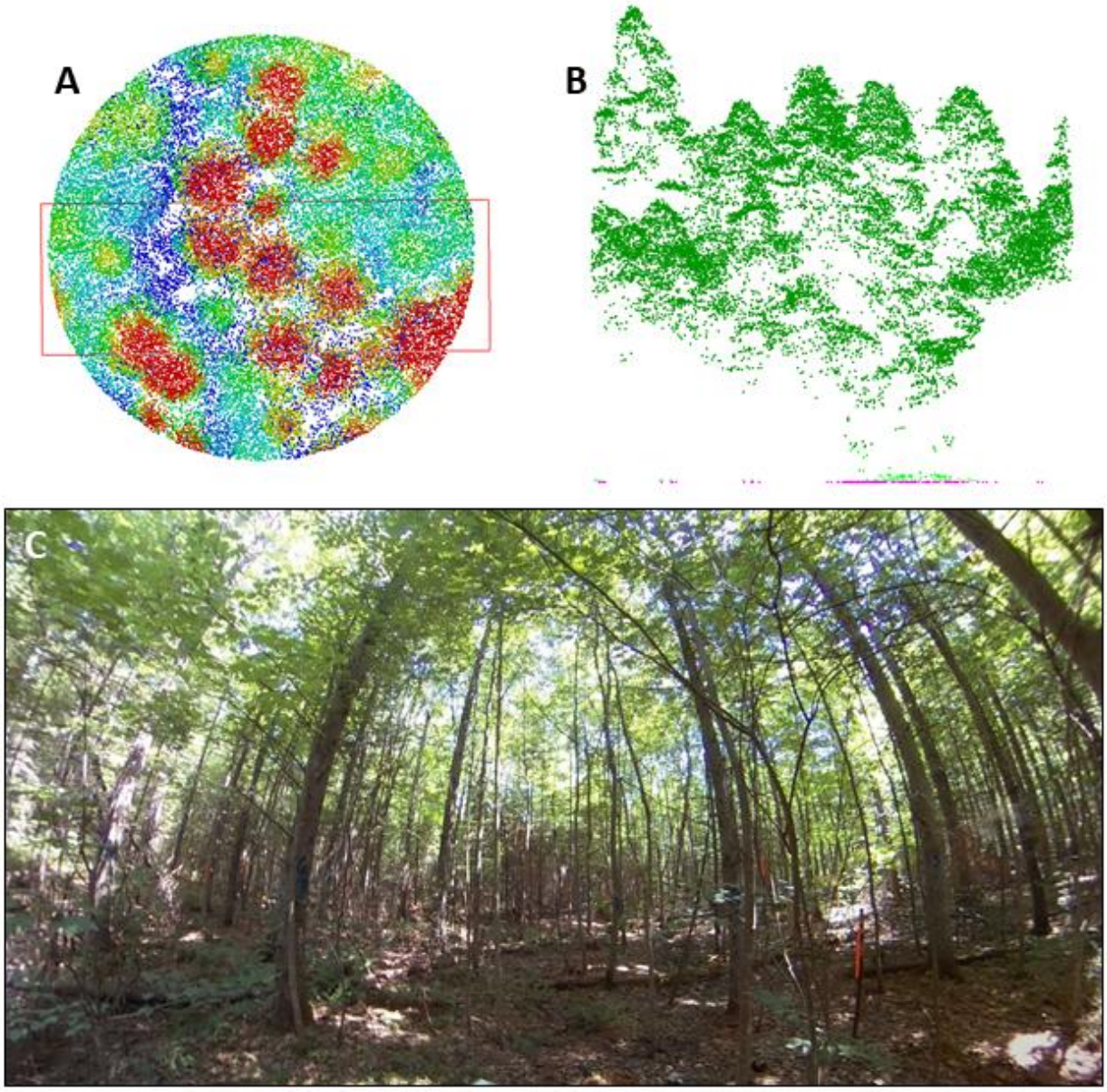

Figure 26. The full PRF124 plot (A; 14.1 m radius; blue = lower canopy heights, red = higher canopy heights) with a 10 m wide profile (red box and B) with SPL returns classified as ground (pink) and low (light green) and high (dark green) vegetation. Photo taken at plot centre (C).

6.2.6 Small tree detection

Regardless of forest type, we found that SPL data had significantly increased point density at the top of canopy; however, returns from secondary canopy layers and understorey depended on the canopy density, type, and configuration of trees in the overstorey. In dense, closed canopies, such as those found in red and white pine plantations, returns were primarily from the top of canopy, with sparse returns through the vertical profile of the canopy. In contrast, canopies of natural pine stands were more open, allowing for identification of emerging secondary layer in the stand. Direct extraction of small understorey trees within the subplots using the SPL data was not possible, due to a lack of returns through the full vertical profile of the canopy. Of note, we found that the amount of SPL returns in the lower canopy was not directly related to the number of small trees or amount of understorey measured in the field subplots, because the density and configuration of the overstorey directly impacted the amount of returns from the secondary layer/understorey. In other words, a dearth of returns through the vertical canopy profile was not necessarily indicative of the presence or amount of vegetation found underneath the main canopy. The percentage of SPL returns within designated height strata of 0–2 m, 2–5 m, 5–10 m, and 10–20 m were plotted against the number of small trees recorded in each small tree subplot and against basal area (Figure 27). No clear relationship was observed. Likewise, similar issues impact the number of ground returns found in the plots and non-vegetated surface objects such as rocks and stumps were not visible from SPL data.

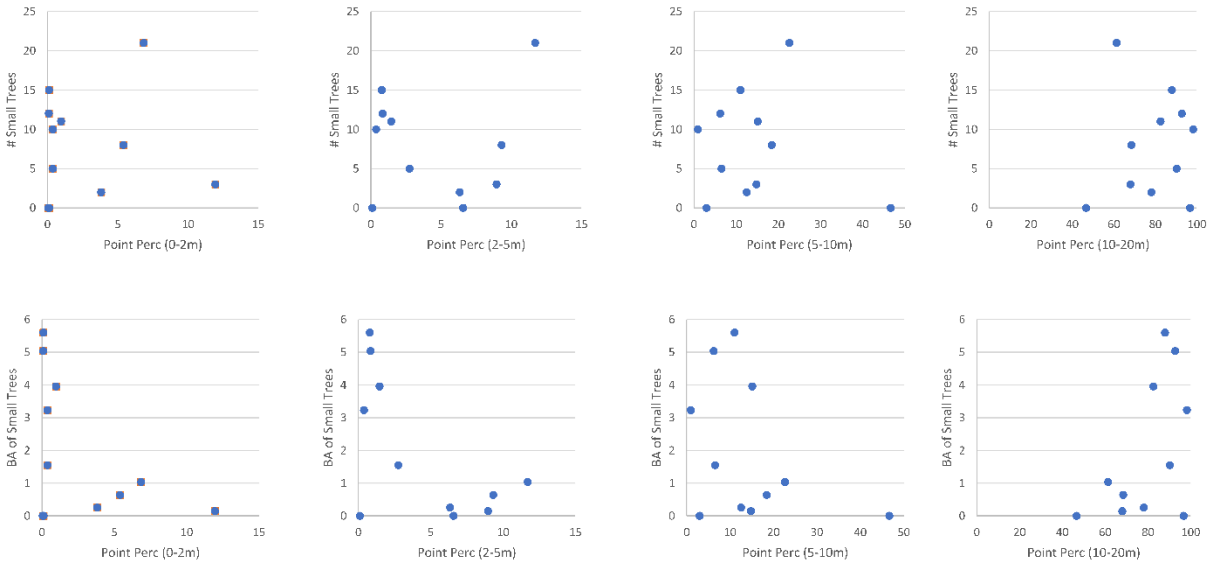

Figure 27. Number of small trees plotted against proportion of SPL returns found in specific height strata (0–2 m, 2–5 m, 5–10 m, 10–20 m).

6.3 Summary

For the final objective of this project, we explored any advantages that SPL data might offer for Ontario's eFRI program, specifically examining the use of SPL data for species classification and the identification of small trees. For species classification at the individual tree level, we found that the SPL data provided

results that were inferior to those generated using LML data, and attribute this result to specific characteristics of the SPL data, including the dominance of first returns at the top of canopy, and the lack of returns distributed through the full vertical profile of the canopy. Detection of small trees was likewise hampered by the limited distribution of returns through the full vertical profile of the canopy. In some of the plots examined, a secondary layer under the main canopy could be readily identified, but not individual trees and the capacity to identify a second layer depended on the density and configuration of the overstorey canopy, which varied by forest type.

7. Conclusion

The objective of this project was to explore the innovation potential and assess the capacity of SPL technology to support enhanced forest inventories and terrain characterization in forest conditions. The test site for this project was located at the Petawawa Research Forest and adjacent forest lands of the Canadian Nuclear Laboratories, representing a total area of approximately 15,000 ha. Forests in the study area include complex multi-layer stands of varying canopy densities, assemblages of various deciduous and coniferous tree species, and varying silvicultural and management histories. As such, these forests represent a challenging target for enhanced forest inventories and are an ideal location at which to benchmark new technologies. Extensive ground data were acquired for this project in order to enable the development of robust models for the forest attributes of interest, as well as for validating model estimates at the stand level, and for assessing the accuracy of the terrain elevations under varying vegetation conditions.

Overall, we found that the use of SPL data in an area-based approach provided reasonably accurate estimates of forest inventory attributes of interest and that the results achieved were comparable to those achieved using LML data in the same study site. Likewise, we found that the 2018 SPL data, acquired during leaf-on conditions, met the vertical accuracy standards for Ontario Digital Geospatial Data for a 10 cm Vertical Accuracy Class. However, the lower number of ground returns in the 2018 SPL data under some dense canopy configurations resulted in artifacts in the derived DTM, which were less evident in the 2019 leaf-off SPL acquisitions. The high point density of the SPL data acquired under leaf-on conditions did not translate into a high density of ground points under dense vegetation and as a result, there may be impacts on the level of spatial detail that can be captured in the derived digital terrain model. Lastly, there are notable differences in the SPL point clouds, primarily the lack of returns distributed through the full vertical profile of the canopy, which may impact applications that require that distributions of points (e.g. species identification, detection of small trees under the canopy). Further research should continue to explore issues and opportunities associated with the use of SPL point clouds for a range of forest management information needs, such as fire fuels mapping and habitat characterization, in a variety of forest environments.

8. References

American Society for Photogrammetry and Remote Sensing (ASPRS). 2014. *Positional Accuracy Standards for Digital Geospatial Data*. Version 1.0. November 2014. http://www.asprs.org/wp-content/uploads/2015/01/ASPRS_Positional_Accuracy_Standards_Edition1_Version100_November2014.pdf

Breiman, L. 2001. Random Forests. *Machine Learning*, 45: 5–32.

Budei, B.C., St-Onge, B., Hopkinson, C., Audet, F.-A. 2018. Identifying the genus or species of individual trees using a three-wavelength airborne lidar system. *Remote Sensing of Environment*, 204, 632–647.

Canada Centre for Mapping and Earth Observation (CCMEO). 2019. *Single-photon LiDAR assessment over the Petawawa Research Forest*. Natural Resources Canada, Internal Report. April, 2019

Eitel, J.U.H., Hoffle, B., Vierling, L.A., Abellan, A., Asner, G.P., Deems, J.S., Glennie, C.L., et al. 2016. Beyond 3-D: The new spectrum of lidar applications for earth and ecological sciences. *Remote Sensing of Environment*, 186: 372–392.

Genuer, R., Poggi, J.M., Tuleau-Malot, C., 2015. VSURF: An R package for variable selection using random forests. *The R Journal*, 7, 19–33.

Hyyppä, J., Yu, X., Hyyppä, H., Vastaranta, M., Holopainen, M., Kukko, A., Kaartinen, H., et al. 2012. Advances in forest inventory using airborne laser scanning. *Remote Sensing*, 4: 1190–1207.

Höhle, J., Höhle, M. 2009. Accuracy assessment of digital elevation models by means of robust statistical methods. *ISPRS Journal of Photogrammetry and Remote Sensing*, 64: 398–496.

Isenburg, M. 2020. LAStools, Efficient LiDAR Processing Software (version 190604). Obtained from: http://lastools.org.

Kuhn, M. 2018. Caret: *Classification and Regression Training*, R package version 6.0-80; R Core Team: Vienna, Austria.

Lambert, M.-C., Ung, C.-H and Raulier, F. 2005. Canadian national tree aboveground biomass equations. *Canadian Journal of Forest Research*, 35: 1996–2018.

Liaw, A., Wiener, M. 2002. Classification and Regression by randomForest. *R News*, 2(3): 18–22.

Næsset, E. 2015. Area-based inventory in Norway - from innovations to operational reality. Chapter 11 in Maltamo, M., Næsset, E.,Vauhkonen, J. *Forestry Applications of Airborne Laser Scanning, Concepts and Case Studies*, New York, NY: Springer.

Ontario. Elevation Coordination and Consultation Committee. 2016. *Elevation Accuracy Guidelines*. Version 1.0. Peterborough: Queens Printer for Ontario. 24 October 2016. Available online : https://www.sse.gov.on.ca/sites/MNR-PublicDocs/EN/CMID/Elevation%20Accuracy%20Guidelines%20-%20User%20Guide.pdf.

Penner, M., D.G. Pitt, Woods, M.E. 2013. Parametric vs nonparametric LiDAR models for operational forest inventory in boreal Ontario. *Canadian Journal of Remote Sensing*, 39(5): 426–443.

Penner, M., Woods, M.E., Pitt, D.G. 2015. A comparison of airborne laser scanning and image point cloud derived tree size class distribution models in boreal Ontario. *Forests*, 2015, 6: 4034–4054.

Prieur, J.-F., St-Onge, B., Rana, P., Woods, M., Kneeshaw, D., Fournier, R.A. In Review. A comparison of three airborne lidar types for individual tree species identification using random forest and feature selection.

Sharma, M. 2016. Comparing height-diameter relationships of boreal tree species grown in plantations and natural stands. *Forest Science*, 62: 70–77.

Sharma, M., Parton, J. 2009. Modeling stand density effects on taper for jack pine and black spruce plantations using dimensional analysis. *Forest Science*, 55: 268–282.

Stoker, J.M., Abdullah, Q.A., Nayegandhi, A., Winehouse, J. 2016. Evaluation of Single Photon and Geiger Mode Lidar for the 3D Elevation Program. *Remote Sensing*, 8: 767

Swatantran, A., Tang, H., Barrett, T., DeCola, P., Dubayah, R. 2016. Rapid, high-resolution forest structure and terrain mapping over large areas using single photon lidar. *Scientific Reports*, 6:28277.

Thomas, V., Treitz, P., McCaughey, J.H.,, Morrison, I. 2006. Mapping stand-level forest biophysical variables for a mixedwood boreal forest using LiDAR: An examination of scanning density. *Canadian Journal of Forest Research*, 36: 34–47.

Treitz. P., K. Lim, M. Woods, D. Pitt, D. Nesbit, Etheridge, D. 2012. LiDAR sampling density for forest resource inventories in Ontario. *Remote Sensing*, 2012, 4, 830–848.

Wästlund, A., Holmgren, J., Lindberg, E., Olsson, H. 2018. Forest variable estimation using a high altitude single photon lidar system. *Remote Sensing*, 10, 1422.

White, J.C., Wulder, M.A., Varhola, A., Vastaranta, M., Coops, N.C., Cook, B.D., Pitt, D.G., Woods, M. 2013. *A best practices guide for generating forest inventory attributes from airborne laser scanning data using the area-based approach*. Information Report FI-X-010. Canadian Forest Service. Canadian Wood Fibre Centre. http://cfs.nrcan.gc.ca/pubwarehouse/pdfs/34887.pdf

White, J.C., Coops, N.C., Wulder, M.A., Vastaranta, M., Hilker, T., Tompalski, P. 2016. Remote sensing for enhancing forest inventories: A review. *Canadian Journal of Remote Sensing*, 42(5): 619–641.

White, J.C., Tompalski, P., Vastaranta, M., Wulder, M.A., Saarinen, S., Stepper, C., Coops, N.C. 2017. *A model development and application guide for generating an enhanced forest inventory using airborne laser scanning data and an area-based approach*. Information Report FI-X-018, Canadian Forest Service, Canadian Wood Fibre Centre. https://cfs.nrcan.gc.ca/publications?id=38945

Woods, M., Pitt, D., Penner, M., Lim, K., Nesbitt, D., Etheridge, D.,Treitz, P. 2011. Operational implementation of a LiDAR inventory in boreal Ontario. *The Forestry Chronicle*, 87(4): 512–528.

Woods, M, MacMillan, J., Arbour, P., White, J.C. 2018. *AFRIT SPL field plot remeasurement protocols for the Petawawa Research Forest 2018*. Canadian Forest Service Internal Report, 23 pp (See Appendix C).

Wulder, M.A., Bater, C.W., Coops, N.C., Hilker, T., White, J.C. 2008. The role of LiDAR in sustainable forest management. *The Forestry Chronicle*, 84: 6: 807–826.

Zakrzewski, W.T and M. Penner. 2013. *A comparison of tree stem taper models for use in Ontario*. Ontario Forest Research Institute, Queen's Printer for Ontario. Forest Research Report No. 176. 26p.

Acknowledgements

We are grateful to our project partners, who provided financial and technical support to this project:

- Canadian Institute of Forestry
- Canadian Nuclear Laboratories
- Canada Centre for Mapping and Earth Observation
- Canadian Wood Fibre Centre

Many individuals have contributed to the results presented in this report. We acknowledge and appreciate their contributions and collaborations on this project:

- Jordan MacMillan and Brian Batchelor, Canadian Institute of Forestry
- Melissa Vekeman, Peter Arbour, and Kyle Harbin, Canadian Wood Fibre Centre
- Annie Morin, Canadian Nuclear Laboratories
- David Bélanger and Charles Papasodoro, Canada Centre for Mapping and Earth Observation
- Thomas Krahn, Craig Onafrychuk, Ian Sinclair, Roger Grose, Dennis Gertridge, Junlin Zhao, Morgan Goadsby, and Scott Charboneneau, Ontario Ministry of Natural Resources and Forestry
- Dr. Jili Li, FPInnovations
- Jean-Francois Prieur, Université de Sherbrooke

Appendix A: Technology Transfer and Knowledge Exchange Activities

DATE	LOCATION	DESCRIPTION
February 6, 2019	**Online (national; recorded)**	**Canadian Institute of Forestry (CIF) e-Lecture** *Exploration of the innovation potential of single-photon LiDAR for Ontario's eFRI* (Murray Woods) PDF: http://www.cif-ifc.org/wp-content/uploads/2018/12/Woods_Sinclair-CIF_electure_Feb6_2019_-Exploration-of-SPL_Feb6_FINAL.pdf Video: http://cif-ifc.adobeconnect.com/ptu6q4capftm/
October 4, 2019	**Canmore, AB**	**Annual National Forest Inventory Collaborator's Meeting** *Exploration of the innovation potential of single-photon LiDAR for Ontario's eFRI* (Joanne White)
October 6, 2019	**Pembroke, ONT**	**Canadian Institute of Forestry (CIF) Annual General Meeting** *Exploration of the innovation potential of single-photon LiDAR for Ontario's eFRI* (Murray Woods)
October 16, 2019	**Online (national; recorded)**	**Canadian Institute of Forestry (CIF) e-Lecture** *New LiDAR technologies on the horizon: SPL and Multi-spectral LiDAR* (Joanne White) PDF: http://www.cif-ifc.org/wp-content/uploads/2019/10/AWARE_CIF_eLecture_New_LIDAR_Technologies_on_the_Horizon.pdf Video: http://cif-ifc.adobeconnect.com/pivbgfusx8is/
November 26, 2019	**Kenora, ONT**	**FPInnovations-CIF Workshops: Innovations in LiDAR Acquisition and Implementation to Improve Operational Efficiency and Fibre Supply Precision** *Seeing the forest floor through the trees: An evaluation of SPL's ability to measure ground elevation* (Murray Woods) *Exploring the innovation potential of Single Photon LiDAR for enhancing Ontario's forest inventories* (Murray Woods)
November 28, 2019	**Thunder Bay, ONT**	
January 21, 2020	**Mattawa, ONT**	
January 23, 2020	**Sudbury, ONT**	

Appendix B: Cross-walk for calibration and validation forest types and species codes

Forest types in calibration and validation data do not use exactly the same nomenclature in all cases. Table B1 outlines the relative correspondence between forest types in these two data sources.

Table B1. Cross-walk of forest types between calibration and validation data.

Calibration Plots	Calibration Plots (Abbreviation)	→ Validation Stands	Validation Stands (Abbreviation)
Intolerant Hardwood	Intolerant Hwd	Poplar	Poplar
Lowland Conifer	Lowland Con	Lowland Conifer	LowlandConifer
Mid-tolerant Hardwood	Mid tolerant Hwd	Oak	Oak
Mixed Deciduous	MIXED deciduous	Mixedwood	Mixedwood
Mixed Conifer	MIXED conifer	Mixedwood	Mixedwood
Pine-Oak	Pine Oak	White Pine Managed	PwManaged
Jack Pine Plantation	Pj Plant	Jack Pine	JackPine
Red Pine Plantation	Pr Plant	Red Pine Plantation	PrPlantation
White Pine Plantation	Pw Plant	N/A	N/A
White pine-Red pine	Pw Pr	White Pine Natural	PwNatural
Spruce	Sb	Black Spruce	BlackSpruce
Spruce Plantation	Spruce Plant	N/A	N/A
Tolerant Hardwood	Tolerant Hwd	Tolerant Hardwood	TolerantHwd

Table B2. Common tree species in Ontario.

Species Common Name	Species Code	Species Common Name	Species Code
American elm	EW	Red pine	PR
American beech	BE	Hard/Sugar Maple	MH/MS
Balsam fir	BF	Tamarack	TA
Balsam poplar	PB	White ash	AW
Basswood	BD	White Oak	OW
Black cherry	CB	White pine	PW
Largetooth aspen	PG	White birch	BW
Black ash	AB	White spruce	SW
Black spruce	SB	Willow	WI
Eastern hemlock	HE	Yellow birch	BY
Ironwood	IW	Norway Spruce	SN
Eastern red cedar	CR	Poplar	PO
Jack pine	PJ	Unknown Species	
Northern white cedar	CE		
Pin cherry	CP		
Trembling Aspen	PT		
Red (soft) maple	MR		
Red oak	OR		

Appendix C: Field plot measurement protocols

Copies of the following field sampling protocols are available by request (joanne.white@canada.ca).

Part 1: General field measurement protocols for calibration data

Woods, M, MacMillan, J., Arbour, P., White, J.C. (2018). *AFRIT SPL field plot remeasurement protocols for the Petawawa Research Forest 2018*. Canadian Forest Service Internal Report, 23 pp.

Part 2: Field measurement protocols for small tree plots

Li, J. (2018). *AFRIT SPL Small Tree Project*. FPInnovations Internal Report, 8 pp.

Part 3: Field measurement protocols for validation data

Woods, M. (2019). *2019 Validation Data Collection Protocols for the Petawawa Research Forest.* Canadian Forest Service Internal Report, 12 pp.

Appendix D: Detailed report on area-based modelling and predictor selection

Penner, M., Woods, M. 2020. Single Photon LiDAR: Petawawa Research Forest Implementation. Final Report (March 18, 2020), 46 pp.

Copy of report available upon request (joanne.white@canada.ca).

Appendix E: 2018 Enhanced Forest Inventory (EFI) layers for the PRF

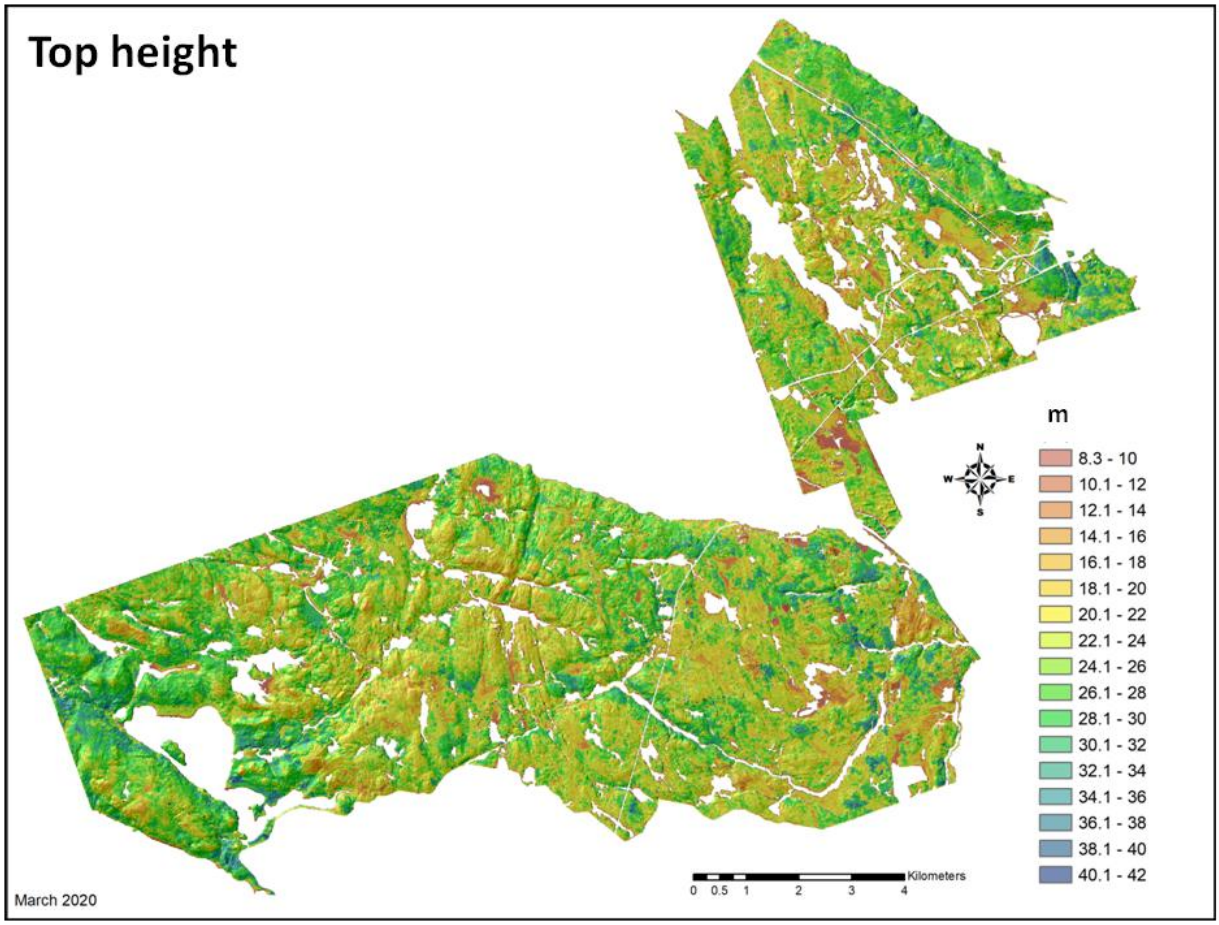

Figure E1. Area-based prediction of top height for PRF and CNL lands derived using SPL 2018 and ground plot data.

Appendix E (continued)

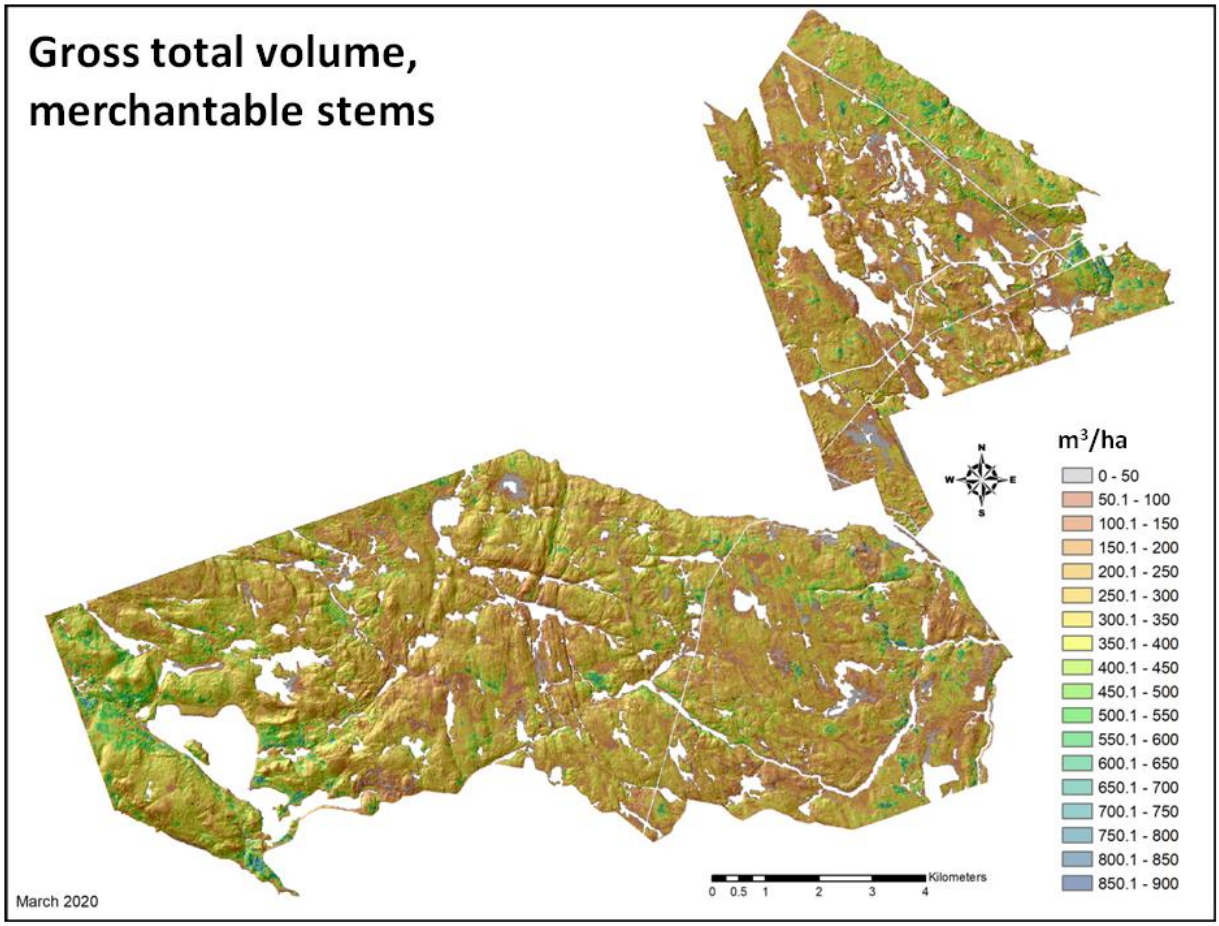

Figure E2. Area-based prediction of gross total volume, merchantable stems, for PRF and CNL lands derived using SPL 2018 and ground plot data.

Appendix E (continued)

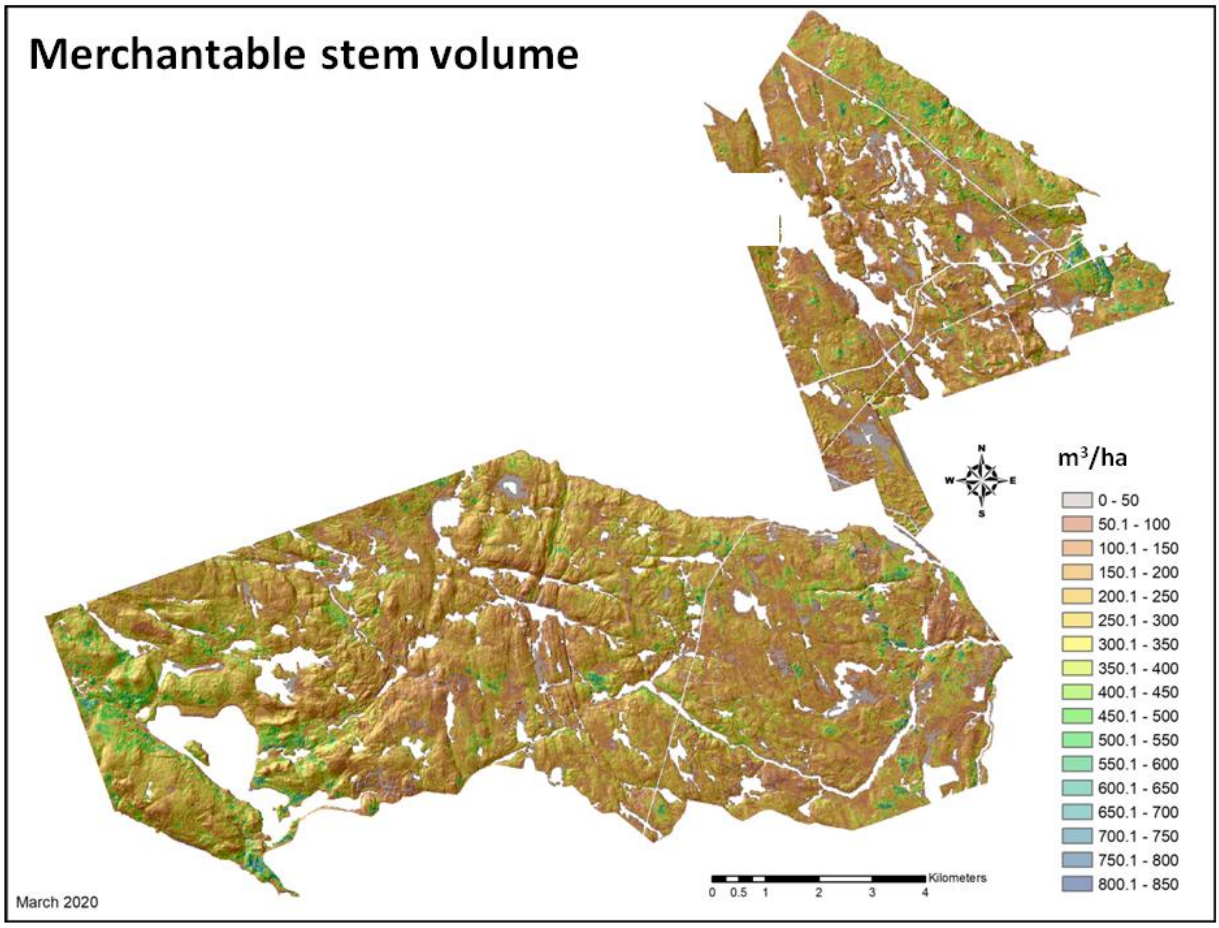

Figure E3. Area-based prediction of merchantable stem volume for PRF and CNL lands derived using SPL 2018 and ground plot data.

Appendix E (continued)

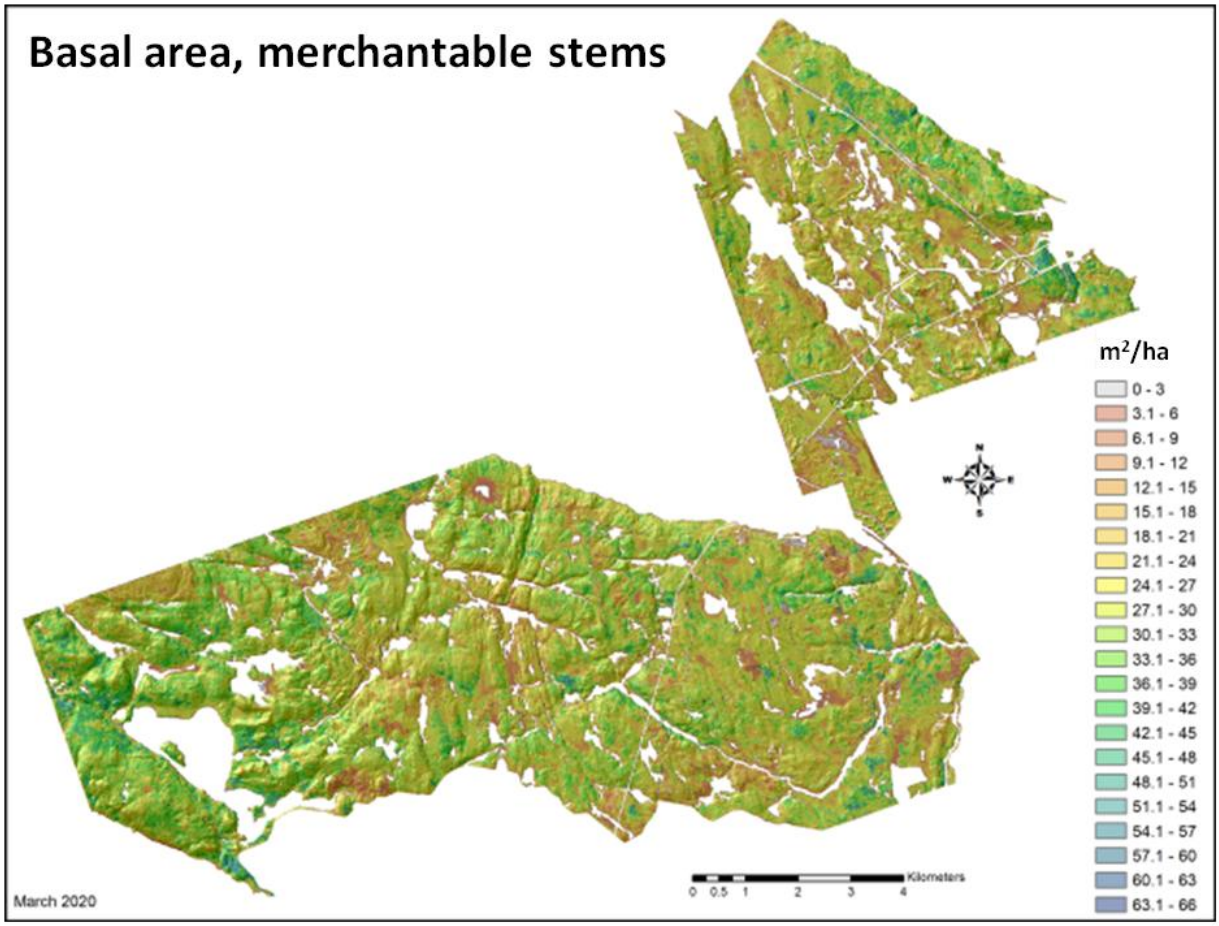

Figure E4. Area-based prediction of basal area, merchantable stems for PRF and CNL lands derived using SPL 2018 and ground plot data.

Appendix E (continued)

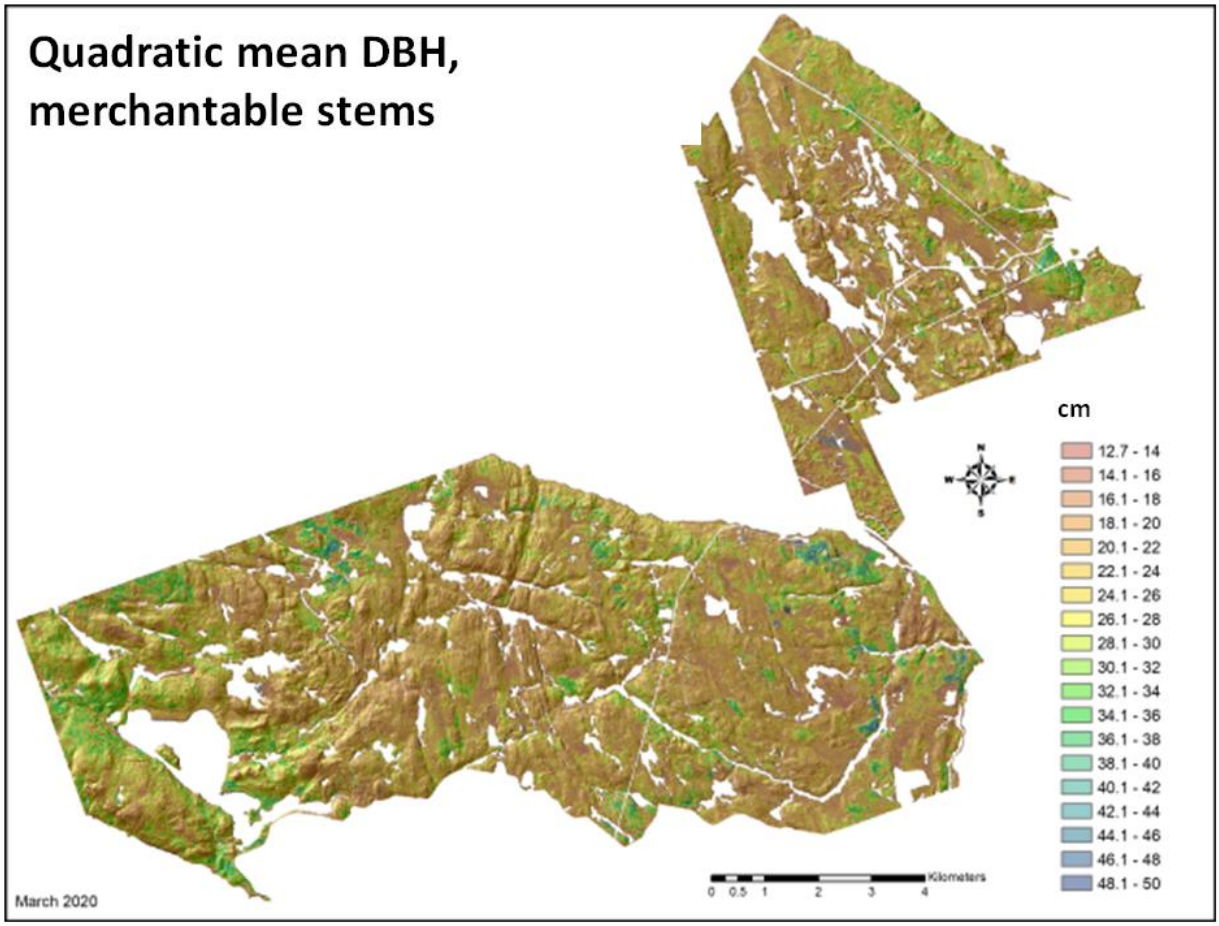

Figure E5. Area-based prediction of merchantable stem volume for PRF and CNL lands derived using SPL 2018 and ground plot data.

Appendix F: Full list of predictors used in 2012 area-based models

Table F1. Predictors used in 2012 area-based model development. The full point-cloud was used (regardless of return classification).

Attribute	Threshold (m)	Description
MEAN	0.0	Mean height (m)
STD_DEV95	0.0	Standard Deviation trimmed @95%
ABS_DEV95	0.0	Absolute Standard Deviation trimmed @95%
SKEW95	0.0	Skewness trimmed @95%
KURTOSIS95	0.0	Kurtosis trimmed @95%
P10	0.0	First Decile LiDAR Height (m)
⋮		
P90	0.0	Ninth Decile LiDAR Height (m)
D1	0.0	Cumulative percentage of the number of returns found in Bin 1 of 10
⋮		
D9	0.0	Cumulative percentage of the number of returns found in Bin 9 of 10
DA	0.0	First returns/ All Returns
DV	0.0	First Vegetation Returns/All Returns
DB	0.0	First and only return / All Returns
VDR	0.0	Vertical Distribution Ratio = [Max−Median]/Max
Covar	0.0	Std Dev (all Returns)/ mean(All Returns)
CanCovar	0.0	Std Dev (First Returns Only)/ mean(First Returns Only)
VCI	0.0	Vertical Complexity Index
CCR	0.0	Canopy Relief Ratio (mean-Min)/(Max-Min)
MEANT2	2.0	Mean height (m)
STD_DEV95T2	2.0	Standard Deviation trimmed @95%
ABS_DEV95T2	2.0	Absolute Standard Deviation trimmed @95%
SKEW95T2	2.0	Skewness trimmed @95%
KURTOSIS95T2	2.0	Kurtosis timed @95%
P10T2	2.0	First Decile LiDAR Height (m)
⋮		
P90T2	2.0	Ninth Decile LiDAR Height (m)
D1T2	2.0	Cumulative percentage of the number of returns found in Bin 1 of 10
⋮		
D9T2	2.0	Cumulative percentage of the number of returns found in Bin 9 of 10
DAT2	2.0	First returns/ All Returns
DVT2	2.0	First Vegetation Returns/All Returns
DBT2	2.0	First and only return / All Returns
VDRT2	2.0	Vertical Distribution Ratio = [Max−Median]/Max
CovarT2	2.0	Std Dev (all Returns)/ mean(All Returns)
CanCovar T2	2.0	Std Dev (First Returns Only)/ mean(First Returns Only)
VCIT2	2.0	Vertical Complexity Index
CRRT2	2.0	Canopy Relief Ratio (mean-Min)/(Max-Min)

Table F1 (continued). Predictors used in 2012 area-based model development. The full point-cloud was used (regardless of return classification).

Attribute	Threshold (m)	Description
RuggedMean		SAGA Ruggedness Mean from a 50cm LiDAR CHM
RuggedSTD		SAGA Ruggedness STD from a 50cm LiDAR CHM
RoughMean		SAGA Roughness Mean from a 50cm LiDAR CHM
RoughSTD		SAGA Roughness STD from a 50cm LiDAR CHM
TexMn5Mean		PCI Texture Mean for a 5x5 window
TexMn5STD		PCI Texture Mean STD for a 5x5 window
TexMn11Mean		PCI Texture Mean for a 11x11 window
TexMn11STD		PCI Texture Mean STD for a 11x11 window
TexMn25Mean		PCI Texture Mean for a 25x25 window
TexMn25STD		PCI Texture Mean STD for a 25x25 window
Var5Mean		PCI Texture Variance Mean for a 5x5 window
Var5STD		PCI Texture Variance STD for a 5x5 window
Var11Mean		PCI Texture Variance Mean for a 11x11 window
Var11STD		PCI Texture Variance STD for a 11x11 window
Var25Mean		PCI Texture Variance Mean for a 25x25 window
Var25STD		PCI Texture Variance STD for a 25x25 window
CB2	0.0	Cumulative percentage of Vegetation returns 0-2
⋮		
CB46	0.0	Cumulative percentage of Vegetation returns 0-46m
S2	0.0	% of vegetation returns in slice 0-2m
⋮		
S46	0.0	% of vegetation returns in slice 44 - 46m
CC2		Crown closure (%) based on percentage of 2m raster cells containing vegetation returns >2m
⋮		
CC46		Crown closure (%) based on percentage of 2m raster cells containing vegetation returns >46m

Appendix G: Random forest variable importance for 2012 and 2018 area-based model

Top predictors for key forest inventory attributes in 2012 area-based models.

Table G1. Variable importance scores for 2012 EFI area-based models. For variable descriptions, see Appendix F, Table F-1.

Merchantable Basal Area (Ba_merch)	Merchantable DBHq (DBHq_merch)	Merchantable stem volume (MVOL)	Gross Total Merchantable Volume (TVOL)
CB6	P70T2	RoughMean	Mean
CCR	P80T2	P70	P70
CB8	CB22	RuggedMean	P60
RuggedSTD	CB24	P60	RoughMean
P40	VCI	Mean	TexMn11Mean
P60	P80	CC22	CC20
D1	S24	CB20	RuggedMean
RoughStd	P60	CC20	TexMn5Mean
CANCOVAR	S16	CC26	P50
CC6	CB20	CC14	CC22

As noted in Section 4.4, forest inventory attributes in the 2018 EFI were either predicted directly (e.g. DBHq_merch, BA_all), or were derived from other attributes that were predicted directly (constrained by VBAR ratios (i.e. BA_merch, TVOL_merch, and MVOL). Dependencies between predicted and derived (target) attributes are listed in Table G2. The top 10 predictors (based on Random Forests variable importance scores) are listed in Table G3.

Table G2. Relationship between predicted and derived (target) attributes.

Target Attribute	Predicted Attribute	Dependencies
DBHq_merch	DBHq_merch	None
TVOL_all	TVOL_all	None
BA_all	BA_all	None
BA_merch	BA_merch_ratio	BA_all
TVOL_merch	VBAR_tvol_ratio	TVOL_all, BA_merch_ratio
MVOL	VBAR_mvol_ratio	pred_TVOL_merch, VBAR_MVOL_ratio

Table G3. Top 10 lidar predictors for the 2018 area-based models. For variable descriptions, refer to Table 5.

Merchantable DBHq (DBHq_merch)	Gross Total Volume All (TVOL_all)	Basal Area All (BA_all)	Basal Area Merch ratio	VBAR_TVOL_ratio	VBAR_MVOL_ratio
a_d10-12	a_p70	a_p50	a_d4_6	a_d4_6	a_std_95
a_d14-16	a_p60	a_p40	a_d2_4	a_d2_4	a_p99
a_d12-14	a_p50	a_LPI_15	a_d6_8	a_d6_8	a_dns_25m
a_std_95	a_qav	a_b70	a_d8_10	a_b10	a_d14-16
a_p80	a_dns_25m	a_p05	a_b10	a_b50	a_p90
a_dns_25m	a_p80	a_p60	a_d10_12	a_b30	a_b10
a_dns_20m	a_p90	a_avg	a_std_95	a_d8_10	a_d28-30
a_p90	a_p95	a_qav	a_qav	a_b40	a_dns_15m
a_p60	a_avg	a_b50	a_ske_95	a_kur_95	a_p95
a_p99	a_dns_15m	a_dns_8m	a_LPI_15	a_dns_2m	a_p80

Appendix H: Detailed report on accuracy of SPL for terrain characterization

Ontario Ministry of Natural Resources and Forestry. (2020). *Petawawa Research Forest Single Photon Lidar 2018–2019 Accuracy Assessment*. Provincial Mapping Unit, Mapping & Geomatics Services Section, Mapping and Information Resources Branch, Corporate Management and Information Division. Internal Report.

Copy of report available upon request (joanne.white@canada.ca).